CHAPTER 1

INTRODUCTION

Early Forward Genetic Screens

Investigation of genetics to understand biologic systems has been a long-standing and time-tested method to understand organismal development and behavior. Early studies commonly relied on mutants arising from spontaneous mutation within a population or random mutagenesis. The early mutagenesis screens in invertebrates paved the way to a new era of biology targeted at understanding the roles of large groups of genes in specific biologic phenomena. The first large-scale mutagenesis screen was performed in the early 1970's using the model system *Caenorhabditis elegans* (Brenner, 1974). By chemically inducing genetic mutation, approximately 300 individual mutant lines were isolated affecting either development or behavior. This study demonstrated that large groups of mutants with assayable phenotypes could be generated and mapped to specific genetic targets via random mutagenesis (Brenner, 1974).

Several years later, Nὺsselein-Volhard and Wesichaus performed a mutagenesis screen in Drosophila hoping to discover all genes necessary for patterning and segmentation (Nusslein-Volhard and Wieschaus, 1980), a novel concept exploiting the unique power of large-scale screens to theoretically reach genome saturation. These early large-scale screens demonstrated that random mutagenesis could provide identifiable mutations in genes that result in phenotypes influencing early development,

cellular function, or behavior. These pioneering studies illustrated multiple advantages of forward genetic screens. The application of forward genetic approach facilitates the discovery of novel genes or known genes functioning in a novel way since the generated mutations are completely unbiased. In other words, since mutants are identified by an observable morphologic or functional defect, the underlying mutation is pre-selected to be functionally significant.

The work performed in invertebrates yielded revolutionary studies expanding countless areas of biology. Indeed, the mutants from the initial invertebrate screens contributed significantly to the understanding of vertebrate development and behavior, since a central dogma of genetics is that the molecular mechanisms are conserved through evolution However, the utility of invertebrates for understanding vertebrate biology is limited. For example, invertebrates lack neural crest cells, an early migratory cell layer responsible for development of craniofacial structure and the peripheral nervous system. Additionally, complex organs such as the brain are organized differently between invertebrate and vertebrates and are significantly more structurally and genetically complex (Detrich et al., 1999).

Forward Genetics in Zebrafish

In the late 1960's work from the lab of George Streisinger began to demonstrate that zebrafish (*Danio rerio*) are a viable vertebrate model system for genetic manipulation and mutagenesis (Chakrabarti et al., 1983; Streisinger, 1983; Streisinger et al., 1986; Walker and Streisinger, 1983). These studies from the Streisinger lab established, among other things, that induced mutations could be generated in

zebrafish by using mutagens such as irradiation or chemical agents. Zebrafish rapidly began to be recognized as a powerful model organism due to various desirable traits including external fertilization, large clutch numbers, ease of care, and optical clarity allowing ease of observation and manipulation of target organs (Detrich et al., 1999). Before long, many laboratories began to take advantage of the strengths of the new zebrafish model.

Despite the appearance of zebrafish as a new vertebrate model system, no large-scale mutagenesis screens were performed. A pilot study from the Nùsslein-Volhard lab developed methods necessary to perform saturation level mutagenesis screens (Mullins et al., 1994). These new methods prompted large scale projects comparable to previous invertebrate screens. One key discovery was that ethylnitrosourea (ENU), a chemical mutagen first used to induce point mutations mutations in mice (Russell et al., 1979), was found to induce germ-line mutations an order of magnitude more often than EMS (Mullins et al., 1994). This pilot study was the precursor to numerous large-scale screens in zebrafish exploring multiple developmental and behavioral processes. In 1996, an entire issue of the journal Development was dedicated to the zebrafish mutagenesis studies from the Nùsslein-Volhard and Driever/Fishman labs. Over a thousand germ-line mutant strains were created and classified into groups emphasizing embryogenesis, organogenesis, patterning, and locomotor behavior (Driever et al., 1996; Haffter et al., 1996). This colossal undertaking from the Nùsslein-Volhard lab proved that numerous mutant lines could be generated in a vertebrate, exploring groups of genes within discrete developmental and functional phenotypes.

From the Nùsslein-Volhard lab and others, many zebrafish mutants were being generated. However, the plethora of mutants highlighted the need for efficient methods for the molecular identification of the underlying genetic mutation. Initially, zebrafish, unlike their invertebrate model system counterparts, did not possess fine-tuned positional cloning techniques. Therefore, early mutational analysis was performed via comparative biology. The first published example was the molecular identification of the zebrafish mutant *no tail (ntl)*. A candidate gene approach was applied to identify *ntl*, because of similarity of the zebrafish phenotype to the mouse knockout of T *(brachyury)* (Schulte-Merker et al., 1994a; Schulte-Merker et al., 1994b). The mouse T (*brachyury*) gene, is required for normal mesoderm development and body axis extension. The similarity in mutant phenotypes between mouse and zebrafish gene homologues allowed successful identification of the genetic basis of zebrafish *ntl*. However, a candidate gene approach would not be sufficient for mass identification of randomly generated mutants, and a more globally applicable molecular system was required.

The initial resources for positional cloning in zebrafish were based on a collection of polymorphic meiotic markers (Johnson et al., 1994). These markers typically were microsatellite repeats that could be rapidly screened by PCR. Furthermore, by observing the segregation pattern of meiotic markers in haploid genome zebrafish, a linkage group map was established to allow finer positional mapping (Postlethwait et al., 1994). Many more meiotic markers and linkage databases were rapidly generated offering greater range of gene identification (Shimoda et al., 1999). In addition, physical maps of the

zebrafish genome were generated by hybridizing pieces of zebrafish chromosomes to mouse cell lines (Ekker et al., 1996; Geisler et al., 1999; Hukriede et al., 1999; Kwok et al., 1998). The continued growth of these databases provided an increasingly efficient tool for the positional cloning and molecular identification of zebrafish mutants. Currently, the majority of the zebrafish genome is sequenced and annotated with large databases containing sequence information and reference markers. However, only approximately 90% of the zebrafish genome is currently assembled (http://www.sanger.ac.uk/Projects/D_rerio/). This means investigators can still find genomic regions poorly assembled or genes mapping to loci without available sequence or genetic markers.

Collectively, large groups of zebrafish mutants are available from forward mutagenesis screens exploring various developmental and functional aspects of biology. Considering the status of genomic tools the identification of the precise genetic aberration of any forward mutation can be reliable and efficiently performed, typically within a year's time. To date, characterized zebrafish mutants from screens have provided new insight into key biological mechanisms and to several human diseases. For example, the zebrafish *accordion (acc)* mutant with a missense mutation in SERCA2a in skeletal muscle is a new model for Brody's Syndrome, a rare genetic disease in humans (Hirata et al., 2004). The *shocked (sho)* zebrafish mutant has a missense mutation in a glycine transporter (GlyT1) expressed within the CNS. In humans, the function of this transporter protein is considered a component of the startle response (Cui et al., 2005). In the rest of this thesis, I will illustrate how a forward genetic screen

in zebrafish has added in the understanding of skeletal muscle function and a human congenital myopathy.

Skeletal Muscle: Excitation-Contraction Coupling

The function of muscle is to receive input from the nervous system, and generate a contractile force, the foundation of all movement. Striated skeletal muscle is structurally and functionally different from two other muscle types, smooth muscle and cardiac muscle, which are responsible for autonomous contraction or heart contraction, respectively. Muscle fibers are capable of contracting because each fiber contains specialized myofibrils. A myofibril is composed of a series of repeating contractile units known as sarcomeres. Each sarcomere contains cross-bridged actin-myosin protein chains that in the presence of calcium move and shorten the sarcomere. The shortening sarcomeres causes the entire muscle tissue to shorten thereby generating movement. Within a muscle, the process of converting electrical input into a chemical signal necessary to produce movement is known as excitation-contraction (EC) coupling. EC coupling in striated skeletal muscle involves well-studied structures proteins (Germann and Stanfield, 2005).

EC coupling occurs within triads, which are junctions of the transverse tubule (t-tubule) and the sarcoplasmic reticulum (SR). T-tubules are invaginations of the sarcolemma (muscle plasma membrane) (Figure 1.1). Depolarization from the sarcolemma propagates through the t-tubules to allow calcium release from the sarcoplasmic reticulum (SR). Two primary proteins are involved in EC coupling. One is the dihydropyridine receptor (DHPR), an L-type calcium channel that serves as a voltage

sensor. The other is the ryanodine receptor (RYR) found in the SR membrane that upon activation allows calcium release from SR stores (Bannister, 2007; Tanabe et al., 1990; Tanabe et al., 1988). Triads were first observed when DHPR, RYR, and other EC coupling proteins were labeled with antibodies in myotubes. This showed that all EC coupling proteins were in targeted foci aligned in longitudinal order (Flucher et al., 1993a; Protasi et al., 1998). These foci represent individual triads. An important function of triads is to bring the EC coupling proteins in close proximity, because the DHPR activates the RYR by physical coupling (Paolini et al., 2004a; Protasi et al., 2002; Tanabe et al., 1988). Extensive work demonstrates that multiple intracellular regions of the DHPR directly or indirectly interact with the RYR1 (Fig1.2) (Block et al., 1988; Felder et al., 2002; Protasi, 2002; Protasi et al., 1998; Protasi et al., 2002; Takekura and Franzini-Armstrong, 1999).

DHPRs not only need to correctly target to triads, they also need to acquire a specialized spatial orientation in relation to the RYR homotetramer. Numerous studies demonstrated that four DHPRs align over a single RYR; this structure is known as a tetrad (Fig1.3). Tetrads cluster in highly organized orthogonal arrays distinguishable by using freeze fracture electron microscopy. The images from freeze fracture yield a direct picture of these calcium release units (CRU) in skeletal muscle (Block et al., 1988; Protasi et al., 1998; Protasi et al., 2002; Protasi et al., 2000; Takekura and Franzini-Armstrong, 1999). Indeed, ryanodine binding to RYR1 alters the inter-protein spacing of DHPRs within a tetrad, consistent with the hypothesis that DHPR and RYR directly interact in skeletal muscle (Paolini et al., 2004a). Ryanodine is an plant alkaloid that

strongly binds ryanodine receptors, and at micromolar concentrations irreversibly blocks calcium release from the SR (Hille, 1992)

Unique Properties of Skeletal Muscle EC coupling proteins

The evolutionary appearance of organized tetrad formations occurs in early craniata, when chordates developed defined heads with boney or cartilaginous internal structure. In the Chordata amphioxus (lancelet), the arrangement of DHPRs is random with no observable organization of DHPR particles (Di Biase and Franzini-Armstrong, 2005). A random arrangement of DHPRs is consistent throughout invertebrate muscle and vertebrate cardiac and smooth twitch muscle, suggesting no physical link between the DHPR and RYR isoforms in these muscle types (Moore et al., 2004; Protasi et al., 1996; Takekura and Franzini-Armstrong, 2002; Tijskens et al., 2003). An interesting hypothesis is that, at the point of origin of the early craniates, gene duplications generated isoforms of DHPR and RYR sufficient to physically couple, and the by-product was a different mechanism of EC coupling (Di Biase and Franzini-Armstrong, 2005).

Studies have demonstrated the properties of the primary EC coupling proteins in vertebrate skeletal muscle, which are necessary for normal function. These studies capitalized on the *dysgenic* mouse line that has a null mutation in the muscle specific DHPR α1S and a complete absence of EC coupling (Klaus et al., 1983; Knudson et al., 1989; Tanabe et al., 1988). The first studies clearly demonstrated that expressing wildtype DHPR α1S in dysgenic myotubes completely restored EC coupling (Knudson et al., 1989; Tanabe et al., 1988). However, when non L-type calcium channels (α1A P/Q Type and α1B N-type) were expressed in dysgenic myotubes, no punctate foci of calcium

channels were identified nor restoration of EC coupling. This indicates only L-type (α1S) have the proper signals for triad targeting (Flucher et al., 2000; Grabner et al., 1998; Wilkens and Beam, 2003). When the cardiac or neuronal isoforms of L-type HVA calcium channels (α1C and α1D) were expressed in *dysgenic* myotubes, the non-endogenous channels did localize to triads (Grabner et al., 1998; Kasielke et al., 2003; Kugler et al., 2004). However, non-endogenous L-type calcium channels could not restore skeletal muscle EC coupling. Triad targeting is then a conserved property among the L-type calcium channels, yet only the DHPR α1S is able to support the necessary interactions to allow skeletal muscle type EC coupling (Garcia and Beam, 1994; Kasielke et al., 2003; Nakai et al., 1998b; Tanabe et al., 1990). In teleosts, boney fish, such as zebrafish, the DHPRα is duplicated to slow and fast twitch fiber isoforms. In addition, the DHPR α1S of higher teleosts does not carry current in response to depolarization (Schredelseker et al., 2010). In mammals, the DHPR does pass Ca2+ but the L-type calcium current is too slow to account for EC coupling and is not required for EC coupling. Rather, the DHPR current may support contractions during prolonged depolarization or activity (Bannister et al., 2009). The variation between mammals and teleosts is worth noting because it raises the question of whether the requirements for EC coupling are different between organisms, or if the DHPRα L-type current is actually insignificant in muscle function.

Expression of non-endogenous forms of DHPR β subunits have been performed in zebrafish lacking the DHPR β1 subunit in muscle. The loss of the DHPR β1 subunit in zebrafish results in immobility and complete loss of EC coupling due to a significant

decrease of triadic DHPR α (Schredelseker et al., 2005; Zhou et al., 2006). Expression of either the β2a subunit, a cardiac and neuronal expressed gene (Hullin et al., 1992; Zhou et al., 2008), or the βm subunit, the ancestral housefly subunit (Grabner et al., 1994), could not restore tetrads nor EC coupling. However, non-endogenous L-type calcium channel β subunits can restore DHPRα localization to the triads. The Grabner lab study demonstrated that triad targeting of the DHPRα subunit is an intrinsic property of calcium channel beta subunits. However, supporting the proper interaction between the DHPR and RYR is a property of the muscle specific β1a subunit (Schredelseker et al., 2009).

The RYR1 isoform in skeletal muscle is also specialized in its ability to allow skeletal muscle type EC coupling. Studies were performed using the *dyspedic* mouse mutant, a knock-out of the RYR1 gene which completely abolishes EC coupling in skeletal muscle (Buck et al., 1997; Takekura et al., 1995). In addition, RYR3 is expressed in skeletal muscle. However, studies indicate that RYR3 is predominately non-junctional as observed by electron microscopy (Felder and Franzini-Armstrong, 2002). In *dyspedic* myotubes overexpressing the RYR3 isoform, freeze fracture indicated tetrads were no longer present, suggesting that RYR3 was incapable of supporting interactions with the DHPR and recovering EC coupling (Protasi et al., 2000). These studies show that the EC coupling proteins of the DHPRα, RYR1, and β1 are expressed specifically in skeletal muscle and are necessary for the assembly of functional calcium release units.

Structure of the L-type calcium channel Complex in Skeletal Muscle

Early studies of calcium currents from various tissues clearly demonstrated a wide range of functional and pharmacological responses (Bean, 1989; Llinas et al., 1992; Nowycky et al., 1985b; Tsien et al., 1988). However, within different types of muscles and neurons, studies defined a new type of calcium current. This current is high voltage activated (HVA), slow inactivating, long lasting, and inhibited most notably by dihydropyridines (Reuter, 1983). These currents were named L-type for long lasting because substituting barium for calcium or treating with the agonist Bay K8644 significantly prolong the current response, which did not occur for other identified calcium current types (Nowycky et al., 1985a, b).

Analysis of the skeletal muscle complex producing L-type calcium current from isolated t-tubules revealed a combination of proteins including an α, β,γ, α2, and δ subunit (Curtis and Catterall, 1984; Hosey et al., 1987; Takahashi et al., 1987). The pore forming α subunit is approximately 2000 amino acids in length with a structure similar to voltage gated sodium channels that are composed of four repeating domains each containing six transmembrane segments (Takahashi et al., 1987; Tanabe et al., 1987). The β subunit is a cytoplasmic protein containing predominately alpha helices (Ruth et al., 1989). The gamma subunit is a membrane protein containing four transmembrane domains (Jay et al., 1990). The α2 and δ subunits form a single transmembrane protein complex. These subunits are generated from one peptide that is cleaved and reattached by disulfide bonds (Jay et al., 1991). When the mammalian DHPR α1S is heterologously expressed in Xenopus oocytes, no current is detectable. Expression of the α1S and β1b subunits together are necessary to produce current in oocytes. In

addition, the inclusion of the α2δ1 subunit increases the amount of observable current (Ren and Hall, 1997). This heterologous expression study provides a basic illustration of the importance of the protein subunits, especially the β, associated with the DHPRα.

In mammals, there are four DHPR β genes (CACNB1-4), and most have multiple isoforms (Birnbaumer et al., 1998). However, only the β1a isoform is expressed in skeletal muscle (Ruth et al., 1989; Takahashi et al., 1987). The β1a and β1b isoforms are identical except for an additional exon in β1a (Dolphin, 2003; Zhou et al., 2008). β1 proteins all contain a SH3 domain, a guanylate kinase (GK) domain, and a beta interacting domain (BID). The GK domain is similar to the MAGUK (membrane associated guanylate kinase) family of proteins, yet does not possess the ATP binding domain or the P-loop necessary for kinase activity (Hanlon et al., 1999). It is via the β subunit's GK domain that crystal structure studies predict interacts with the I-II intracellular loop of the DHPRα subunit (Chen et al., 2004; Opatowsky et al., 2004; Van Petegem et al., 2004).

Regulation of Skeletal Muscle Dihydropyridine Receptor

The DHPR α subunit is the pore forming subunit of L-type calcium channel complexes (Catterall et al., 2005). The loss of the DHPR α1S in skeletal muscle results in a complete loss of EC coupling (Klaus et al., 1983; Knudson et al., 1989; Tanabe et al., 1988). *The tottering (tg)* mouse has a mutation in the neural HVA calcium channel 1A, resulting in ataxia and paroxysmal dystonia (Campbell and Hess, 1999; Campbell et al., 1999; Fureman et al., 1999). Calcium channel α subunit mutants show that the pore

subunits are critical for normal function. Here I will discuss two prominent mechanisms that regulate the activity of the channel, interaction with calmodulin (CaM) and the RYR.

One widely studied regulatory mechanism is the impact of CaM on the L-type calcium channels α1C (cardiac) and α1S (skeletal muscle). Both apo-CaM (calcium unbound) and calcium bound CaM (Ca-CaM) bind to the IQ domain within the HVA calcium channel carboxyl termini (Erickson et al., 2003; Pate et al., 2000; Peterson et al., 1999; Tang et al., 2003; Zuhlke et al., 1999). Both α1C and α1S undergo a Ca-CaM dependent inhibition of channel activity (Stroffekova, 2008; Zuhlke et al., 1999). However, current data suggests only the α1C possesses a Ca-CaM mechanism for facilitation of activity, showing a varied and complex role of CaM dependent regulation (Zuhlke et al., 1999). The variation of CaM influence on different calcium channel types, α1C and α1S, could be in part due to amino acid variations within the IQ domain between channel types that impact the affinity of CaM binding (Halling et al., 2009; Ohrtman et al., 2008).

The proper interaction between the DHPR and RYR in skeletal muscle is critical for normal function (Garcia et al., 1994; Nakai et al., 1998a; Tanabe et al., 1990). Chimera experiments were performed substituting α1S intracellular loops with the cardiac α1C L-type calcium channel which does not support EC coupling when expressed in *dysgenic* muscle (Grabner et al., 1998; Kasielke et al., 2003). Chimera experiments demonstrated that switching the α1S II-III intracellular loop with the α1C II-III loop significantly impaired depolarization-induced calcium release (Nakai et al., 1998b). Likewise, manipulation of the DHPR II-III loop significantly impaired RYR1 dependent

potentiation of L-type current, known as retrograde regulation (Avila and Dirksen, 2000; Grabner et al., 1999; Nakai et al., 1998b). Indeed, the II-III loop of the DHPR α1S binds part of the amino terminus of the RYR1 (Leong and MacLennan, 1998; Proenza et al., 2002). These studies illustrate a form of bi-directional regulation of the skeletal muscle DHPR and RYR that is dependent on the proper spatial interactions of each channel. In addition to RYR regulation of the activity of the DHPR, the associated subunits of the DHPR channel complex modulate localization and activity. The following sections will explore the functional impact of each subunit of the DHPR complex.

Regulation of the Dihydropyridine Receptor by the β Subunit

The interaction of the β1a and DHPR α1S is necessary as demonstrated by the β1 knockout mouse that has no EC coupling or localization of the DHPRα to triads (Gregg et al., 1996). In addition, two different functionally null alleles of the zebrafish *relaxed* mutant (*red*), *CACNB1* nonsense mutants, exhibit no EC coupling and significantly reduced or absent DHPRα localization to triads (Schredelseker et al., 2005; Zhou et al., 2008). Indeed, the association of β1a/DHPRα appears to be necessary for triadic targeting of β1a since fluorescently tagged β1a subunits do not localized in *dysgenic* myotubes (Leuranguer et al., 2006; Papadopoulos et al., 2004). In *relaxed* zebrafish mutants, a structural defect is apparent in the EC complex as observed by freeze fracture EM. *Relaxed* mutants show that a loss of the β1a subunit completely abolishes tetrad formation, suggesting that β1a is necessary for proper interaction with RYR1 (Schredelseker et al., 2005). The finding that a cluster of positive residues in the foot region of RYR1, a large cytoplasmic portion of the protein, can directly bind β1a

supports a DHPRα/RYR1 interaction mediated by β1a (Cheng et al., 2005). The findings from both zebrafish and mouse mutants of the β1 gene indicatethat the β1a/DHPRα interaction functions to enhance targeting of the DHPRα to the triadic junction (Schredelseker et al., 2005; Strube et al., 1996; Zhou et al., 2006). Thus, the presence or absence of the β subunit has a significant impact on the regulation of the DHPR complex. The important biologic questions are: by what mechanisms do the β subunit, and other proteins, influence DHPRα regulation. Two β subunit-directed mechanisms that will be discussed are β interactions with small G-proteins and ER export regulation of the DHPRα.

Small G-proteins of the RGK (Rem, Rem2, Rad, and Gem/Kir) family can inhibit L-type calcium channels through interactions with the β subunit (Finlin et al., 2006; Finlin et al., 2003; Sasaki et al., 2005). RGKs bind β subunits within the guanlyate kinase domain, but in a region distinct from where the DHPRα interacts (Beguin et al., 2007; Finlin et al., 2006). Overexpression studies in numerous preparations, including skeletal muscle myotubes (Bannister et al., 2008a), have shown that RGKs can drastically reduce L-type calcium currents (Crump et al., 2006; Finlin et al., 2005; Seu and Pitt, 2006; Yada et al., 2007). Consequently, RGK overexpression significantly reduces gating currents of L-type calcium channels, suggesting less surface expression or voltage responsiveness (Bannister et al., 2008a; Murata et al., 2004). However, some heterologous expression studies have indicated that RGK overexpression has no impact on surface expression of calcium channels (Chen et al., 2005; Finlin et al., 2005). Collectively, these studies

support a role of a RGK- β subunit interaction that negatively regulates L-type calcium channel activation.

A recent study investigating RGK based regulation of calcium channels suggests a more complex mechanism. The work from the Colecraft lab suggests RGKs possess multiple mechanisms to regulate cardiac calcium channels encompassing reduction of surface expression, decreasing open probability, and immobilization of the voltage sensor (Yang et al., 2010). In addition, specific domains of the RGK and the small G-protein's phosphorylation state dictate which type of influence the RGK-β interaction will have on the calcium channel (Yang et al., 2010). The work from Yang et al also demonstrated that co-expression of a dominant negative version of dynamin inhibited RGK overexpression based suppression of L-type calcium currents. The dynamin protein family is important in clathrin-mediated endocytosis (McMahon and Boucrot, 2011; Takei et al., 2005). Other studies have shown that homodimerization of the SH3 domain of the L-type calcium channel β subunit mediates recruitment of dynamin to the channel complex (Gonzalez-Gutierrez et al., 2007; Miranda-Laferte et al., 2011).

Another mechanisms of RGK regulation of L-type channels has been proposed. RGK binding of 14-3-3 and calmodulin (CaM) can sequester the calcium channel β subunit in the cell nucleus. Sequestering the β subunit results in reducing L-type calcium channel expression (Beguin et al., 2006; Beguin et al., 2005a; Beguin et al., 2005b). A RGK/β mechanism for dynamin directed endocytosis of L-type calcium channels is a potentially interesting hypothesis for future investigation.

In cardiac myotubes, β subunit-free L-type calcium channels are targeted to proteasomes for degradation within the ER. Normally, the β subunit prevents degradation by blocking a RFP2 mediated ubiquitination sequence on the DHPRα. Controlled protein removal is part of the quality control mechanism of the endoplasmic reticulum (ER) (Altier et al., 2011). Despite the lack of a unifying mechanism, it is apparent that calcium channel regulation via the β subunit is important to cellular function. Whether every cell type with L-type calcium channels employs all these varied modes of regulation is unknown. However, continuing studies will shed light on the specific details of β directed regulation of calcium channels.

Regulation of the Dihydropyridine Receptor by the α2δ1 Subunit

α2δ (1-4) subunits are expressed in various tissues and are part of all L-type calcium channel complexes (Catterall et al., 2005). Several spontaneous mouse mutant alleles exist for the α2δ2 subunit, (*ducky, ducky*(*2J*), and *entla*) which are expressed in the nervous system. Homozygous α2δ2 mutant mice exhibit ataxia, susceptibility to seizure, and reduced spontaneous firing of Purkinje cells (Barclay et al., 2001; Brill et al., 2004; Brodbeck et al., 2002; Donato et al., 2006). However, knockout of the isoform expressed in muscle (α2δ1) is embryonic lethal. A targeted knockout of α2δ1 for heart alone is viable, and shows reduced cardiac contractility and a muscle relaxation phenotype (Fuller-Bicer et al., 2009). Yet, these studies do not determine the precise skeletal muscle role of the α2δ1.

In order to study the role of α2δ1 in skeletal muscle, siRNA was employed to knockdown α2δ1 in cultured myotubes. Significant siRNA-mediated reduction of α2δ1 (down to approximately 2% original levels) did not perturb DHPRα triadic or tetradic targeting or the amplitude of depolarization or agonist-induced calcium release (Gach et al., 2008; Obermair et al., 2005). However, extracellular calcium did influence calcium release properties from α2δ1 knockdown myotubes. In the presence of normal levels of extracellular calcium (2 mM), myotubes could not maintain calcium release during sustained depolarization or high frequency stimulation. This result suggests that the α2δ1 in skeletal muscle is important for shaping and maintaining calcium transients. Interestingly, α2δ1 knockdown myotubes in nominal extracellular calcium (7μM) show no difference from wildtype myotubes in sustained calcium release kinetics. These experiments indicate that the α2δ1 subunit is important for modulating prolonged but not acute activity (Gach et al., 2008).

Regulation of the Dihydropyridine Receptor by the γ Subunit

The γ subunit of the DHPRα complex is comprised of a family of four proteins (Catterall et al., 2005). The γ1 subunit is predominately expressed in skeletal muscle (Biel et al., 1991). Two different knockout lines of the γ1 subunit were independently generated and neither demonstrated any gross impact on calcium release in skeletal muscle (Ahern et al., 2001; Freise et al., 2000). Only subtle kinetic properties of the macroscopic L-type current were altered in the γ1 knockout lines (Ahern et al., 2001; Freise et al., 2000; Ursu et al., 2001). Even expression of the DHPRα in heterologous

oocytes studies demonstrated that the inclusion of the gamma subunit had no significant impact on functional surface expression (Ren and Hall, 1997). Despite the seemingly minor role of γ1, studies have shown that the neural γ2 subunit of calcium channels would not associate with the muscle calcium channel complex. This suggests functional and structural heterogeneity amount the gamma subunits (Arikkath et al., 2003). Unlike the γ1, mutation of the neuronal γ2 subunit results in multiple phenotypes. A hypomorphic allele of γ2 is the molecular basis of the *stargazer* mutant mouse, which displays ataxic gate and elevated head positioning (Letts et al., 1998; Letts et al., 1997; Noebels et al., 1990; Sharp et al., 2001). Indeed, analysis of cerebellar synapses in stargazer mutants show a reduction of presynaptic L-type calcium channels, but not P/Q-type calcium channels, showing a selective interference in calcium channel trafficking or regulation (Leitch et al., 2009). The work with neuronal gamma subunits suggests this subunit has a significant functional role. Further study may be required to determine a significant functional role of the gamma subunit in skeletal muscle.

Structure of Skeletal Muscle Ryanodine Receptor

Ryanodine receptors (RYR) form homotetramers and are the largest known ion channel complex with a combined mass of >2MDa (Inui et al., 1987a; Lai et al., 1988; Zorzato et al., 1990). RYRs are located in either the ER or SR, the major calcium storage compartments of cells (Imagawa et al., 1987; Smith et al., 1988). RYRs are named after the plant alkaloid ryanodine that specifically and irreversibly binds open-state RYRs (Chu et al., 1990; Inui et al., 1987b). In mammals, three isoforms, RYR1, 2, and 3, have been identified and were found originally to be expressed in skeletal muscle, heart, and brain

respectively (Hakamata et al., 1992; Nakai et al., 1990; Takeshima et al., 1989). RYR3 is also found in skeletal muscle. In chicken and frog skeletal muscle two RYR1 isoforms were identified, RYR a and b (Ottini et al., 1996; Oyamada et al., 1994). Experiments looking at zebrafish skeletal muscle show that the two isoforms of RYR1 are specifically expressed in either slow or fast twitch muscle fiber types (Hirata et al., 2007). Interestingly, slow and fast twitch fibers in zebrafish are independently responsible for specific motor behaviors during early development (Naganawa and Hirata, 2011).

Due to the large size of RYRs, detailed structural information is not available. However, the N-terminal cytoplasmic "foot" region is well described since it can be observed by electron microscopy (Block et al., 1988; Franzini-Armstrong, 1970; Saito et al., 1984). This foot region is estimated to account for approximately 80% of the RYR protein, and contain numerous micro-structures that support protein interactions (Serysheva et al., 2008).

Regulation of Skeletal Muscle Ryanodine Receptor

The RYR is an essential component of the EC coupling complex. Proteins such as calmodulin, FKBPs, and calsequestrin are all known to regulate the activity of RYR channels. Calmodulin (CaM) binds directly to all RYR isoforms in a ratio of four CaM to each homotetramer (Tang et al., 2002). CaM is a small ubiquitously expressed calcium binding protein (Lanner et al., 2010). Both apo-CaM and Ca-CaM bind RYR at the same location within the foot region (Moore et al., 1999). However, apo-CaM acts as an agonist whereas Ca-CaM acts as an inhibitor of RYR-mediated calcium release (Rodney et al., 2000; Tripathy et al., 1995). Interestingly, the sensitivity to calcium can be

drastically different between isoforms, as has been demonstrated between skeletal muscle RYR1 and cardiac RYR2 (Fruen et al., 2000; Fruen et al., 2003). Cryo-EM mapping of RYR shows that CaM binding results in structural changes. The CaM binding domain, depending on whether apo-CaM or Ca-CaM is present is displaced by approximately 33 angstroms, potentially influencing channel properties (Samso and Wagenknecht, 2002; Wagenknecht et al., 1994; Wagenknecht et al., 1997). Another calcium binding protein, S100A1, binds to the same location on RYR as CaM. Knockdown of S100A1 results in decreased activity-induced calcium release in skeletal muscle. However, the full extent of the competitive interaction of S100A1 and CaM *in vivo* is not well understood (Prosser et al., 2008; Wright et al., 2008).

FKBPs are a group of proteins belonging to the immunophilin family and named for their molecular weight. All FKBPs bind immunosuppressive drugs such as FK506 and rapamycin. The FKBP protein families have been implicated in protein trafficking, signaling, and transcriptional regulation (Lanner et al., 2010; Ozawa, 2010). FKBPs are expressed in most tissues, and FKBP12 and FKBP12.6 interact directly with all the isoforms of mammalian RYR (Chelu et al., 2004). Structural studies demonstrated that the RYR binding FKBPs associate with a stoichiometry of four FKBPs per RYR homotetramer (Jayaraman et al., 1992; Timerman et al., 1993). However, binding affinity and expression levels of FKBP relative to RYR vary dramatically between different tissues. Studies show high affinity physical interaction between FKBP12 and RYR1 (Jayaraman et al., 1992) and FKBP12.6 with RYR2 (Lam et al., 1995).

The primary role of FKBP binding to RYR is thought to be stabilization of the closed state of the channel (Brillantes et al., 1994; Marx et al., 2001; McCall et al., 1996; Ondrias et al., 1998). Indeed, inhibition of FKBP12 binding to RYR1, using immunosuppressive drugs, in skeletal muscle leads to more frequent channel opening and longer open times (Ahern et al., 1997; Marx et al., 1998). In mice with a specific skeletal muscle FKBP12 deficiency, impaired EC coupling is observed in a manner consistent with abnormal communication between the RYR and DHPR, suggesting that in skeletal muscle, FKBP12 may influence the physical DHPR/RYR interaction (Tang et al., 2004). Similarly, in cardiac muscle manipulating FKBP binding or expression produces phenotypes similar to cardiomyopathy (McCall et al., 1996; Shou et al., 1998). A particularly interesting hypothesis regarding FKBPs is their potential role in muscle aging phenotypes. Aging muscle displays phenotypes similar to FKBP binding interference phenotypes. Indeed, studies have demonstrated that aging muscle shows progressively less FKBP expression despite similar levels of RYR in aged matched controls, indicating FKBP regulation may be a partial factor in understanding muscle aging (Russ et al., 2011).

Calsequestrin (CSQ) is a SR luminal protein that interacts with the RYR via binding to junctin or traidin. Junctin and traidin are transmembrane proteins that form a quartenary structure with the RYR and CSQ (Zhang et al., 1997). CSQ is a major calcium binding protein in the SR important for maintaining calcium homeostasis and regulating RYR mediated calcium release. However, the precise mechanisms of CSQ interaction with triadin or junctin, or the latter proteins role in calcium release are still poorly

understood (Beard et al., 2009; Lanner et al., 2010). Two CSQ genes (CSQ1 and CSQ2) exist and are expressed in different striated muscle types (Fliegel et al., 1990; Scott et al., 1988). CSQ1 is exclusively expressed in skeletal muscle fiber types, whereas CSQ2 is found predominately in cardiac muscle with low levels found in slow twitch fiber types (Biral et al., 1992; Damiani and Margreth, 1994). In both cardiac and skeletal muscle, CSQ has similar physical properties and serves as a high capacity calcium storage protein. CSQs ability to store calcium is highest when calcium concentrations exceed approximately 1mM when CSQ aggregates in polymers in the SR lumen (Fryer and Stephenson, 1996; Wang et al., 1998). Upon calcium binding CSQ undergoes structural changes (Ikemoto et al., 1972), as well as during EC coupling implicating conformational changes of CSQ may be modifying RYR function (Ikemoto et al., 1991).

Despite similarities in CSQ1 and CSQ2 physical properties, they have inversely functional roles at physiological conditions in skeletal muscle or cardiac muscle. CSQ1 in skeletal muscle reduces RYR1 activity and CSQ2 increases opening of RYR2 (Wei et al., 2009). Knockout of CSQ1 in mice resulted in multiple muscle phenotypes in homozygous mutants including atrophy, reduced peak calcium release, slower calcium kinetics, increased RYR expression, and SR swelling (Paolini et al., 2007). Conversely, overexpression of CSQ1 in skeletal muscle myotubes enhanced voltage dependent calcium release (Shin et al., 2003). Interestingly, CSQ2 null mice showed no visible cardiac phenotype under basal conditions. Yet exposure to catecholamines enhanced SR leak and spontaneous release leading to arrhythmia (Knollmann et al., 2006). Whereas, mice overexpressing CSQ2 showed dramatic heart failure with significant

reductions in SR calcium release and spontaneous calcium release events (Jones et al., 1998; Sato et al., 1998). The studies exploring CSQ impact on RYR regulation demonstrate a complex mechanism with some results, especially in skeletal muscle, to be seemingly contradictory. Despite CSQ clearly being important for modulating RYR mediated calcium release many details of the mechanism still, remain to be resolved.

Ryanodine Receptor in Human Skeletal Muscle Disease

Null RYR1 mouse mutants are immediately post-natal lethal (Takekura et al., 1995). However, hypomorphic or partial loss of function mutations in RYR1 account for numerous human muscle diseases. Mutations in RYR1 account for many serious disorders including malignant hyperthermia (MH) (MacLennan et al., 1990), multiminicore disease (MmD) (Ferreiro et al., 2002), and central core disease (CCD) (Zhang et al., 1993). To date, approximately 300 different mutations in RYR1 alone have been identified as the molecular basis of human myopathy (Lanner et al., 2010).

MH episodes are most commonly induced while a susceptible individual is exposed to volatile anesthetics or muscle relaxants. Without the proper external trigger, MH susceptible individuals are typically unaware of the underlying condition. During a MH episode, patients experience rises in body temperature (1^0C per 5 minutes) and muscle rigidity. Subsequently this leads to rhabdomyolysis (muscle break down) and potentially death. The molecular cause of MH symptoms is the increased calcium release during an attack that results in the muscle rigidity. Furthermore, the removal of the excess calcium consumes large amounts of ATP producing heat, which leads to many of the other symptoms. To date, the only FDA approved treatment for a MH attack is

the administration of dantrolene, a RYR calcium release blocker. MH episodes typically occur approximately 1 in every 40,000 individuals under general anesthesia, however, some individuals may not have an episode until multiple anesthetic treatments (Lanner et al., 2010; Mickelson and Louis, 1996).

Six different genetic loci are correlated to MH susceptibility (MHS 1-6). The most common is MHS1 representing RYR1 in skeletal muscle. Of the 300 identified human disease causing mutations in RYR1, approximately half are responsible for MH. Numerous other RYR1 centric myopathies have MH susceptibility as a related symptom (Lanner et al., 2010). In the late 1960's a porcine line was identified with pale and lean muscle which exhibited MH like symptoms when exposed to halothane, a volatile anesthetic (Nelson et al., 1975). The porcine MH model was used to develop halothane testing on muscle biopsies as a potential method for identifying MH susceptibility in human patients (Zhang et al., 1992). Genetic analysis showed the porcine MH resulted from a single point mutation in RYR1 (Fujii et al., 1991). From the original porcine MH model, modeling of other MH correlated mutations in mouse RYR1 has been performed using the *dyspedic* line. Analysis of the six most common MH susceptibility RYR1 mutations show grossly normal EC coupling, but with consistent trends in activity such as increased sensitivity to calcium release agonists and depolarization, with decreased sensitivity to inhibition (Yang et al., 2003). These changes in RYR1 function are consistent with many MH mutations explored so far (Du et al., 2001; Tong et al., 1997; Wehner et al., 2002). MH susceptibility is well studied in numerous myotube culture

investigations, however, development of further animal models is still required to develop novel therapeutic agents and susceptibility detection systems.

Multiminicore (MmD) is a rare autosomal recessive congenital myopathy displaying multiple phenotypes, but commonly axial muscle weakness and hypoxia. MmD causing mutations exist in selenoprotein N, yet the most common genetic locus to date is RYR1. Biopsies from afflicted patients show numerous small cores (disorganized sarcomere lesions) throughout the muscle associated with diminished oxidative enzyme activity (Jungbluth et al., 2000; Jungbluth et al., 2005; Zorzato et al., 2007). Interestingly, MmD not only displays a wide range of clinical phenotypes, but also allelic heterogeneity, as both missense and splicing mutations have been identified as genetic causes (Ferreiro et al., 2002; Monnier et al., 2003). Currently, MmD is a poorly understood myopathy and the presentation of muscle cores is still not recognized as a cause or side effect of the disease.

Central core disease (CCD) is a rare autosomal dominant myopathy correlated to mutations in RYR1 in over ninety percent of patients (Wu et al., 2006). The occurrence of CCD is approximately 1 in every 100,000 live births (Jungbluth, 2007) Patients affected by CCD display lower extremity weakness and delayed development of motor skills with impaired calcium homeostasis in skeletal muscle (Robinson et al., 2006). Many CCD cases have symptoms that include MH susceptibility (Robinson et al., 2002; Tong et al., 1997). Transverse electron microscopy sections of CCD muscle show large centrally located cores, or amorphous regions, lacking mitochondria or oxidative activity (Magee and Shy, 1956; Shuaib et al., 1987). Currently, identified CCD mutations are

point mutations most commonly within the pore-forming domain of RYR1 resulting in elevated resting cytosolic calcium and increased RYR calcium leak in muscle cells (Lynch et al., 1999; Monnier et al., 2000; Tilgen et al., 2001; Tong et al., 1997).

Dihydropyridine Receptor in Human Skeletal Muscle Disease

Mutations in the DHPR α1S can cause human disease. One previously identified DHPR α1S based disease is hypokalemic periodic paralysis (hypoPP) (Fontaine et al., 1994; Ptacek et al., 1994). HypoPP is part of a pair of periodic paralysis conditions including hyperkalemic periodic paralysis (hyperPP). Both disease types show dominant inheritance and exhibit reversible periods of muscle weakness, lasting from hours to days, triggered by a wide range of environmental or physiological cues. During an attack of muscle weakness, blood potassium levels either increase or decrease depending on the specific condition, hyperPP or hypoPP, respectively (Lapie et al., 1997). Mutations in the skeletal muscle voltage gated sodium channel, Nav1.4, have also been identified as causing hypoPP (Fontaine et al., 1990; McClatchey et al., 1992; Ptacek et al., 1992). The prevalence of either sodium or calcium channel based HypoPP is about 1 in 100,000 individuals. Despite hypoPP or hyperPP rarely being lethal (Lapie et al., 1997), older patients, in their 40-50's, may develop constant and permanent muscle weakness due to the development of vacuolar myopathy (Bradley et al., 1990; Dyken et al., 1969).

Analysis of HypoPP causing mutations in DHPR α1S revealed that the majority of disease alleles are caused by missense mutations within the S4 voltage sensor of the channel (Jurkat-Rott et al., 1994; Matthews et al., 2009; Ptacek et al., 1992; Ptacek et al., 1994). Consequently, the identified hypoPP causing mutations within the skeletal

muscle voltage gated sodium channel also predominately occur within the voltage-sensor (Cannon, 2010; Struyk and Cannon, 2007). Electrophysiological investigation of two of the most common hypoPP-causing DHPR mutations demonstrated distinct alterations of L-type current. One mutation, R528H, showed a 40 mV hyperpolarizing shift in L-type current inactivation (Sipos et al., 1995). Another mutant, R1239H, showed no alterations in kinetics, yet a 30% decrease in peak L-type current (Lehmann-Horn et al., 1995; Sipos et al., 1995). Both studies from dissociated human patient myotubes showed subtle defects in L-type current, without any gross EC coupling abnormalities. In addition, both human hypoPP alleles had no impact on expression of the DHPR α1S (Lehmann-Horn et al., 1995; Sipos et al., 1995). The investigation of myotubes from patients with two different hypoPP alleles has shown that EC coupling is grossly normal, yet subtle and variable alterations to L-type current occur. One model of how these hypoPP alleles result in disease is that when incorporated into a tetrad they result in a loss of tetrad function. Therefore, a tetrad composed of one or more DHPRs with hypoPP causing mutations cannot induce calcium release (Lehmann-Horn et al., 1995; Sipos et al., 1995).

Heterologous systems have been used to explore the functional impact of the human hypoPP allele R528H. The analogous mutation was generated in the rabbit DHPR α1S and transfected into either *dysgenic* myotubes (Jurkat-Rott et al., 1998), or L-cells (Lapie et al., 1996). L-cells are a mouse fibroblast like line with no endogenous calcium currents (Perez-Reyes et al., 1989). The analogous DHPR R528H mutation in L-cells yielded L-type currents suggesting the channel were expressed and not voltage

insensitive. Interestingly, no kinetic shifts of activation or inactivation were observed, only a small yet significant decrease in current density compared to wildtype DHPR (Lapie et al., 1996). In dysgenic myotubes expressing the hypoPP R528H mutation, only a subtle hyperpolarizing shift in L-type current inactivation was observed (Jurkat-Rott et al., 1998). Heterologous system results varied depending on the system used and were not closely comparable to the large hyperpolarizing shift in inactivation observed in human myotubes from hypoPP R528H patients (Sipos et al., 1995). Understanding DHPR mutations causing hypoPP still requires much investigation. However, the studies performed thus far would suggest hypoPP mutations in DHPR α1S are highly sensitive to the presence or absence of associated subunits, which are not present in L-cells, and the cellular environment. Therefore, future investigation into the pathophysiology of hypoPP requires detailed understanding of the mechanisms involved in DHPR regulation in skeletal muscle.

Mutations in human DHPR α1S are also known to cause MH susceptibility, the pathology of which has been discussed previously. Unlike RYR1 where extensive number of MH susceptibility causing mutations have been identified (Lanner et al., 2010), very few are known for DHPR α1S. One human mutation, T1354S is located within an extracellular loop of the channel close to the pore domain. Expressing the analogous DHPR mutation in *dysgenic* myotubes demonstrated faster activation kinetics of the L-type currents and increased sensitivity to caffeine and voltage mediated calcium release (Pirone et al., 2010). Similarly, another MH mutation studied in *dysgenic* myotubes, human mutation R1086H located within the intracellular III-IV loop, yielded

increased activation kinetics and calcium release sensitivity (Weiss et al., 2004). The impact of known DHPR-based MH mutations result in similar defects compared to common RYR based MH mutations (Yang et al., 2003). Interestingly, human DHPR α1S amino acid residue 1086 is mutated in several independent ethnic backgrounds with MH susceptibility (Monnier et al., 1997; Stewart et al., 2001). Studies of the DHPR α1S III-IV loop show this region is important for proper gating and calcium release kinetics, but not for supporting EC coupling (Bannister et al., 2008b). Studies exploring currently un-mapped MH susceptibility loci implicate other DHPR subunits as putative targets, in addition, to the pore forming alpha subunit (Sudbrak et al., 1993). One currently unidentified MH causing genetic locus is mapped to the human chromosome location containing the α2δ1 subunit (Iles et al., 1994). Further investigation of DHPR and RYR mutations leading to MH susceptibility will hopefully lead to better detection methods for a potentially lethal human condition, and to the understanding the complex regulation between the two primary EC coupling protein complexes.

Native American Myopathy

Native American myopathy (NAM)(OMIM#255995) is an autosomal recessive disease (Stamm et al., 2008a) first described in the Lumbee Native Americans (Bailey and Bloch, 1987). The Lumbee tribe is located in south-central North Carolina (Stewart et al., 1988). This tribe is the largest Native American group east of the Mississippi River and has been culturally isolated for approximately the past two centuries (Bryant and LaFromboise, 2005). NAM is clinically described as a congenital disease displaying cleft

palate, micrognathia, ptosis, muscle weakness, and susceptibility to malignant hyperthermia (Bailey and Bloch, 1987; Meluch et al., 1989; Stewart et al., 1988).

Individuals with NAM have a 36% mortality rate by the age eighteen. Among the Lumbee population the incidence of NAM is approximately 1 in every 5,000. Despite NAM patients having delayed motor development, there are no identified psychological or neural defects. Muscle biopsies from a 2 month old patient displayed small muscle fiber diameters with non-descript myopathic features (Stamm et al., 2008a). The myopathic nature of NAM, including the susceptibility to MH, led early investigators to believe NAM was a form of King Syndrome (Stewart et al., 1988). King Syndrome is a rare disease described as exhibiting symptoms of general skeletal muscle myopathy and MH susceptibility, and typically caused by mutations in RYR1 (Dowling et al., 2011). However, NAM patients have no mutations in RYR1 (Stamm et al., 2008a). Homozygosity mapping revealed that the region of the NAM mutation mapped to the human chromosome location 12q13.13-14.1. Four candidate genes previously implicated in various myopathies were sequenced (Integrin α-7, MLCsa, PIP5K2C, and PDE1B), but no non-conserved genetic variations were identified (Stamm et al., 2008b).

STAC Protein Family

In vertebrates, three different *STAC* genes are present *Stac1*, *Stac2*, and *Stac3*. The Stac proteins are characterized by a high degree of amino acid homology and contain an amino-terminal C1 domain and two carboxyl-terminal SH3 domains (Fig 1.4) (Chapter 2). SH3 domains are prototypical protein-protein interaction domains (Agrawal and Kishan, 2002). C1 domains are cysteine rich sequences that typically bind

diacylglycerol (DAG) found in the cell membrane. However, atypical C1 domains are known which do not bind DAG and whose precise function is unclear (Colon-Gonzalez and Kazanietz, 2006). Stac1 was first identified and published as a novel protein expressed in neural tissue and found in both humans and mice (Kawai et al., 1998; Suzuki et al., 1996). Later studies demonstrated that unique expression patterns of stac1 and stac2 occurs in discreet groups of dorsal root ganglion (DRG) neurons. This implied potential subgroups within the DRG population (Legha et al., 2010). To date, no functional studies exist for either stac1 or stac2. A study from the Kuwada lab described in this thesis demonstrates that stac3, a skeletal muscle specific gene, is essential for normal EC coupling and motor behavior, and is the basis of the congenital human disease NAM (Chapter 2 and 3). This work on stac3 is the first functional investigation into the role of a STAC protein. Understanding STAC3 may help pave the way for understanding the other STAC proteins and potentially lead to understanding further human diseases or lead to new understanding of cellular regulation, signaling, and behavior.

Figure 1.1

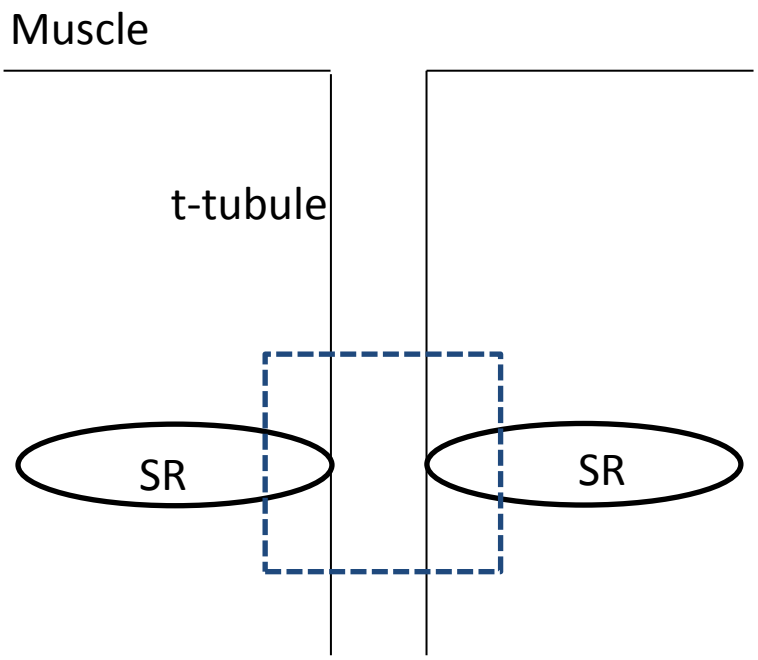

Figure 1.1: Diagram of a Skeletal Muscle Triad. Diagram showing a t-tubule invaginating from the muscle membrane. A triad (area within blue dotted square) is where the t-tubule membrane junctions with the SR.

Figure 1.2

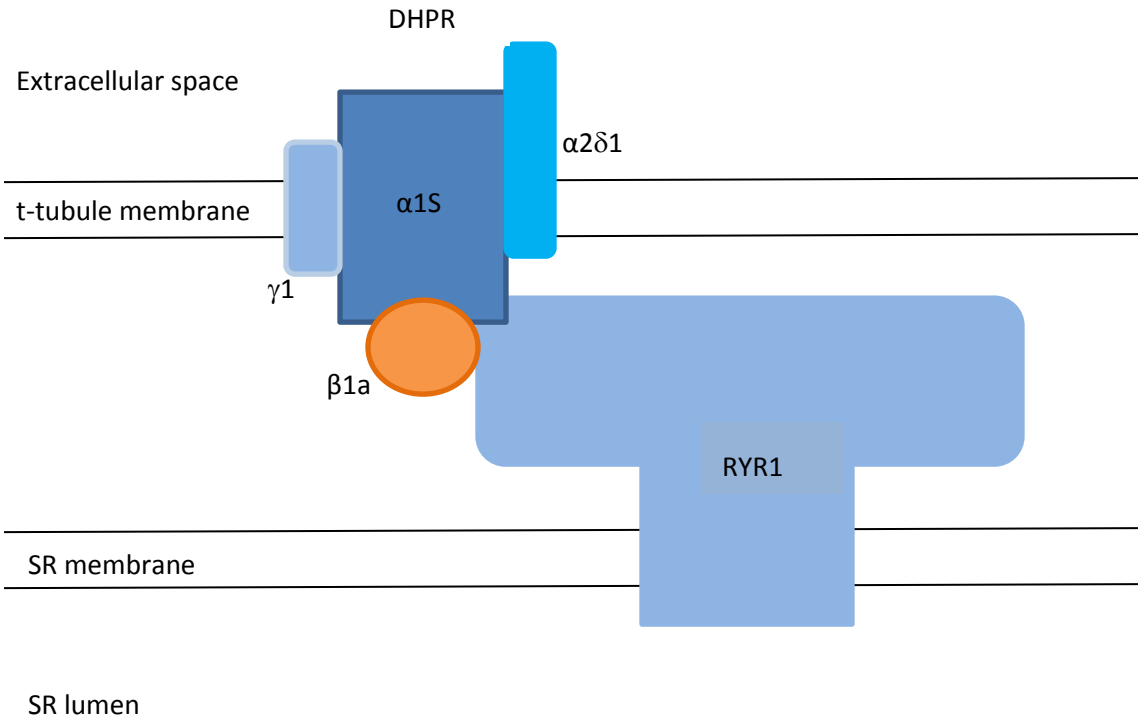

Figure 1.2: Diagram of EC coupling complex found in triads: The DHPR is pictured in the t-tubule membrane showing all subunits identified in-vivo. The RYR1 is pictured in the SR membrane. Note that the DHPR and RYR are shown to be closely if not directly interacting.

Figure 1.3

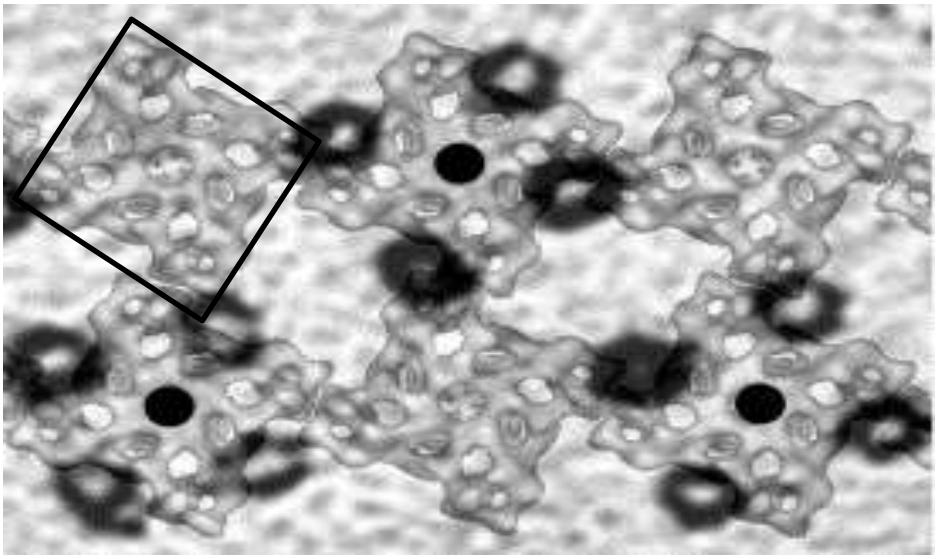

Figure 1.3: Representation of the Tetrad: Superimposition of RYR foot and tetrad arrays. Black box shows a single RYR foot within an RYR array in a 3D reconstruction from EM imaging. Overlaid on the RYR array is an EM image showing tetrads, where the DHPR is seen as a black outlined circle. The center of a tetrad is denoted by a solid black circle. Modified from (Paolini et al., 2004b).

Figure 1.4

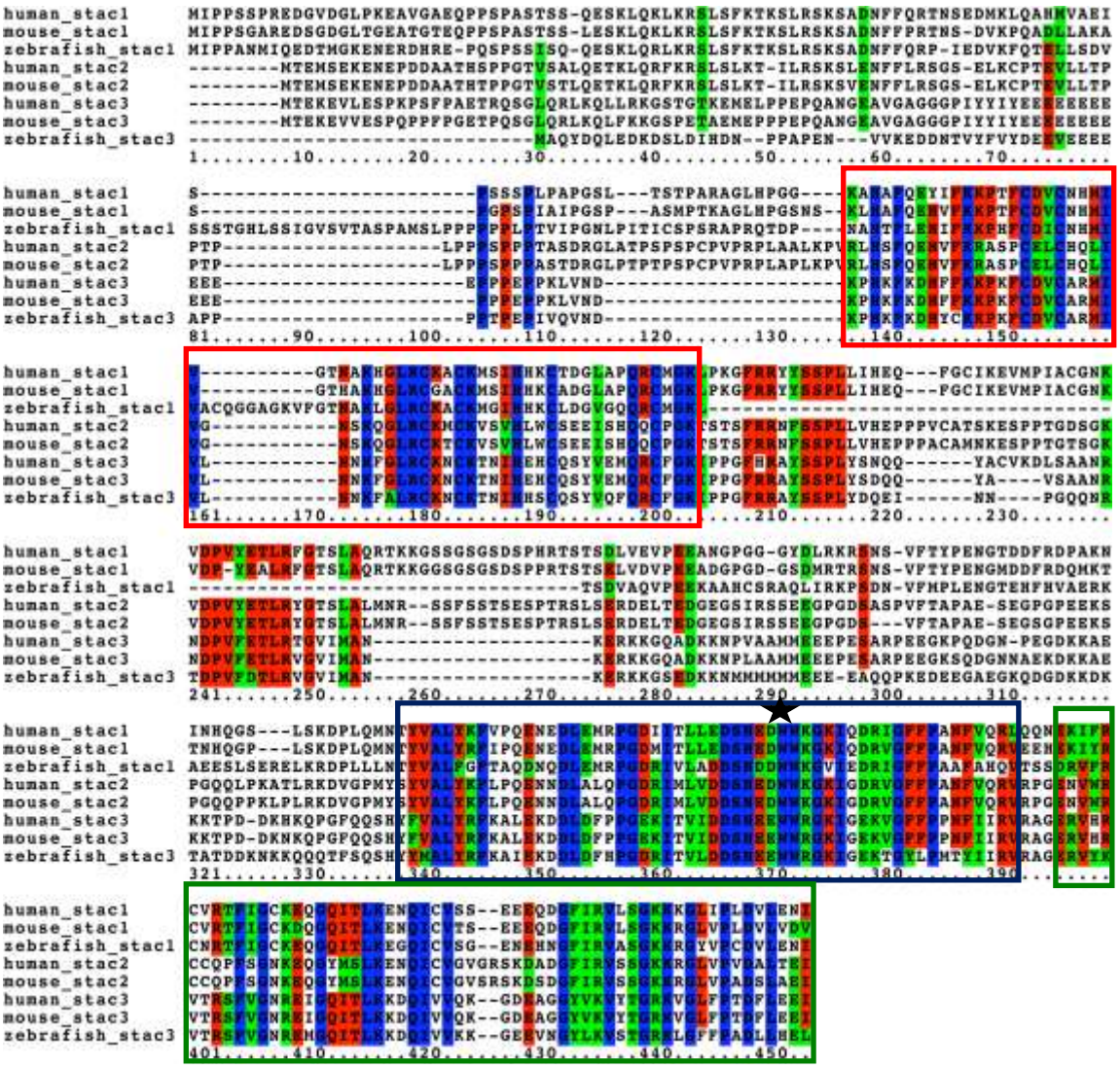

Figure 1.4: Alignment of mammalian and zebrafish STAC proteins. Blue represents completely conserved residues, red is identical residues, and green is similar residues. The residues within the red box are the C1 domain. The residues within either the blue or the green boxes are the SH3 domains. The alignment was generated using Biology Workbench software. Location of the W mutation to S in NAM noted by a black star.

CHAPTER 2

STAC3, A NOVEL REGULATOR OF MUSCLE EXCITATION-CONTRACTION COUPLING, IS THE BASIS FOR CONGENITAL MYOPATHY

[Manuscript in preparation to be published as: Eric J. Horstick, Jeremy W. Linsley, James J. Dowling, Kristin K. McDonald, Allison Ashley-Koch, Michael A. Hauser, Louis Saint-Amant, Akhila Satish, Wilson W. Cui, Weibin Zhou, Shawn M. Sprague, Hiromi Hirata and John Y. Kuwada]

Abstract

Defects in excitation-contraction (EC) coupling, the process that regulates contractions by skeletal muscles, are associated with human muscle diseases. EC coupling transduces changes in membrane voltage to release of Ca^{2+} from an internal store to activate muscle contraction. Although some components of EC coupling are well studied, relatively little is known about how EC coupling is regulated. A forward genetic screen performed in zebrafish and *in vivo* physiological analyses identified the *stac3* gene that encodes a novel regulator of EC coupling in skeletal muscles. EC coupling is defective in mutants due to a decrease in the dihydropyridine receptors (DHPRs) that sense voltage shifts in muscle. Furthermore, pedigree analysis demonstrated that mutation of *STAC3* is responsbile for Native American myopathy (NAM), a debilitating congenital myopathy that results in significant mortality by adulthood. Finally, expression of the NAM allele in stac3 null zebrafish demonstrates that the NAM allele leads to defective EC coupling, suggesting that the basis for the myopathy is a decrease in EC coupling. The identification of STAC3 as a key regulator of EC coupling and a causative gene for myopathy enhances our understanding of both EC coupling and the biology of

myopathies. This discovery could aid in the development of therapeutic agents for congenital myopathies.

Introduction

Muscle contractions are initiated by depolarization of the voltage across the plasma membrane resulting from synaptic release at the neuromuscular junction (NMJ), the synapse between the motor neuron and skeletal muscle. EC coupling is responsible for transducing the depolarizing shift in the membrane voltage to increase cytosolic levels of Ca^{2+} that leads to contraction. Genetic defects in EC coupling components are associated with numerous congenital myopathies that appear in infancy and are characterized by a variety of symptoms that may include muscle weakness, hypotonia, atrophy and susceptibility to malignant hyperthermia, a condition in which individuals experience adverse reactions to general anesthesia that can be fatal. Despite the debilitating nature of congenital myopathies, their biology is poorly understood. Furthermore, many individuals exist that are afflicted by congenital myopathies of unknown origin.

In skeletal muscles, EC coupling occurs at triads. Triads are junctions of the transverse tubules that are infoldings of the plasma membrane and the sarcoplasmic reticulum (SR), an internal Ca^{2+} store. Changes in the membrane voltage of the transverse tubules are detected by the dihydropyridine receptor (DHPR), an L-type Ca^{2+} channel located in the transverse tubule membrane at triads (Bannister, 2007; Tanabe et al., 1990; Tanabe et al., 1988). DHPR is composed of the principal □1s subunit that contains the pore and several accessory subunits. Activated DHPR, in turn, is thought to

directly activate ryanodine receptor 1 (RyR1), which is a Ca^{2+} release channel in the SR membrane side of the triadic junctions (Paolini et al., 2004a). In mammalian skeletal muscles the DHPR also conducts Ca^{2+} from the external solution to the cytosol but this is not required for EC coupling (Dirksen and Beam, 1999; Tanabe et al., 1990). Interestingly in teleost skeletal muscles EC coupling is similarly independent of Ca^{2+} influx from the exterior and the DHPR appears to have evolved so that it no longer conducts Ca^{2+} (Schredelseker et al., 2010). Activation of RyR1 leads to release of Ca^{2+} from the SR into the cytosol, and subsequently leads to contraction mediated by the contractile machinery.

Although DHPR and RyR1, the primary components of EC coupling, are well studied, how the regulation of EC coupling and establishment of the triadic molecular complex are poorly understood. EC coupling involves a complex of proteins localized to triads in addition to DHPR and RyR1, and the identity and roles of other components of the complex are largely unknown. Other components of the triadic complex include FKBP12, triadin, junctin and calsequestrin. Triadin, junctin and calsequestrin are SR proteins that regulate RyR1 from the luminal side of the SR (Beard et al., 2004; Chopra et al., 2009; Knollmann et al., 2006). FKBP12 is an immunophilin, an immunosuppressive drug binding protein, that co-purifies and co-immunoprecipitates with RyR1 in striated muscles (Jayaraman et al., 1992), and appears to stabilize RyRs in their open state *in vitro* (Brillantes et al., 1994). Two other cytosolic proteins that interact with EC components are SepN1 and calmodulin (CaM). SepN1 is a selenoprotein that co-immunoprecipitates with RyR1α and is associated with myopathy

(Moghadaszadeh et al., 2001) and is required for formation of slow twitch muscles in zebrafish (Jurynec et al., 2008). CaM can bind RyR and DHPR and modify EC coupling (Halling et al., 2006). Despite the identification of these factors, the mechanisms by which they regulate EC coupling are poorly understood. These analyses illustrate the complexity of the EC coupling complex and its regulation, and suggest that a genetic strategy might be useful for further understanding EC coupling.

Zebrafish have been useful for the analysis of a many of biological processes because they are amenable to forward genetic screens and *in vivo* manipulations (Driever et al., 1996; Haffter et al., 1996). Pertinent to a genetic analysis of EC coupling, zebrafish muscles can also be analyzed *in vivo* with electrophysiology and live imaging (Buss and Drapeau, 2000; Schredelseker et al., 2005). We took advantage of these features to identify a zebrafish mutation in which EC coupling was defective. The gene responsible for the mutant phenotype encoded for Stac3, a novel regulator of EC coupling. Finally we found that a missense mutation in human *STAC3* is responsible for the debilitating Native American myopathy (OMIM255995).

Materials and Methods

Animals, Behavioral Analysis and Statistical Analysis

Zebrafish were bred and maintained according to approved guidelines of the University Committee on Use and Care of Animals at the University of Michigan. The *stac3*^{mi34} mutation was isolated from a mutagenesis screen using procedures previously reported (Driever et al., 1996; Haffter et al., 1996). Embryonic behaviors were video-recorded

using a Point Grey Firefly MV USB camera mounted on a stereomicroscope and analyzed with ImageJ. In some cases the heads of embryos were embedded in low melting temp agar with the trunk and tail free to move. Where indicated data were analyzed by t-tests.

Electrophysiology

Previously published protocols were followed to electrophysiologically record from zebrafish embryonic muscles (Buss and Drapeau, 2000). Briefly embryos were anaesthetized, pinned on a Sylgard dish and the skin peeled off to allow access to the underlying muscles. For recordings embryos were partially curarized (5 µM d-tubocurarine) and muscles patched under visually guidance using Hoffman modulation optics. Recordings of muscle responses to tactile stimulation were made with patch electrodes (3-10 MΩ) filled with solution containing 105 mM K gluconate, 16 mM KCl, 2 mM $MgCl_2$, 10 mM Hepes, 10 mM EGTA and 4 mM Na_3ATP at 273 mOsm and pH 7.2 and extracellular Evans solution (134 mM NaCl, 2.9 mM KCl, 2.1 mM $CaCl_2$, 1.2 mM $MgCl_2$, 10 mM glucose and 10 mM Hepes at 290 mOsm and pH 7.8) using an Axopatch 200B amplifier (Axon Instruments), low-pass filtered at 5 kHz and sampled at 1 kHz. Data were collected with Clampex 8.2 and analyzed with Clampfit 9.0. Mechanosensory stimulation was delivered by ejecting bath solution from a pipette to the tail using a Picospritzer III to induce fictive swimming. Voltage dependence of contraction was performed in a similar fashion as above except embryos were exposed to 50 µM d-tubocurarine, voltage steps delivered to muscle via voltage clamp and muscle contractions video-recorded at 60Hz. Behavioral responses to 5mM caffeine from dissected embryos were

video-recorded and measured. Caffeine was applied by a Picospritzer III (10 psi, 1 seconds pulse).

Ca^{2+} Imaging

One cell stage embryos were injected with a plasmid using the skeletal muscle α-actin promoter (Higashijima et al., 1997) to drive GCaMP3 (*α-actin:GCaMP3*) (Tian et al., 2009). Following further development embryos mosaically expressed the injected construct within skeletal muscle. 48 hpf embryos were genotyped by behavior and dissected to expose skeletal muscles. Prior to imaging tricaine was removed and embryos allowed to recover in Evans for 10 minutes and then treated with 200 μM N-benzyl-p-toluene sulphonamide (bts) in Evans to inhibit contraction for 5 minutes. 100 μM NMDA was added to initiate the swimming motor network (Cui et al., 2005). GCaMP3 expressing cells were then frame scanned at 200Hz using the resonance scanner of a Leica SP5 confocal microscope. Confocal software was used to measure relative fluorescence intensity changes and kinetics of induced Ca^{2+} transients.

Immunolabeling

Wholemounted embryos were immunolabeled as described previously (Hirata et al., 2005). For labeling dissociated skeletal muscle fibers, 48 hpf embryos were incubated in collagenase type II (3.125 mg/ml in CO_2-independent medium (Gibco)) at 20°C for 1.5 h with the muscle fibers triturated every 30 min. Fibers were spun at 380*g* in a benchtop centrifuge for 5 min, supernatant removed and fibers resuspended in CO_2-independent medium and allowed to settle on polyornithine coated coverslips. Fibers were washed in

CO_2-independent medium then fixed. Dissociated muscles were labeled using 0.25% detergent in the incubation solutions containing the following primary antibodies/toxin: 1/200 dilution of anti-RyR (34C IgG1, Sigma); 1/200 anti-DHPRα1 (1A IgG1, Affinity BioReagents);1/10 bungarotoxin-Alexa594 (Invitrogen); 1/500 anti-SV2; 1/200 anti-α actinin; and 1/200 anti-dystrophin (all from Iowa Hybridoma Bank). Secondary antibodies were anti-mouse Alexa 488/568 and anti-rabbit Alexa 488/568 (Invitrogen). All immunolabeled embryos or fibers were imaged by confocal microscopy.

Positional Cloning of *stac3*

To identify the gene mutated in *stac3*^{mi34} mutants, the mutation was meiotically mapped to PCR-scorable, polymorphic CA repeats as described previously (Shimoda et al., 1999) by scoring 2009 mutant embryos derived from appropriate mapping crosses. Flanking markers were identified located on linkage group 9; z1830 that was 0.21 cM north of *stac3*^{mi34} and z1663 that was 1.24 cM south. Analysis of the zebrafish genome database (http://www.sanger.ac.uk/Projects/Drerio/clones.shtml) revealed that z1830 was located in a small contig of assembled sequence (Scaffold 450) from the zV5 assembly of the sequenced genome that contained the *pcbp2* gene. A new marker (zh1) located in *pcbp2* mapped 0.11 cM north of *stac3*^{mi34}. A sequenced 156 kb BAC (CR848672) that contained *pcbp2* was identified and analyzed for potential genes with the gene prediction program, GENSCAN (http://genes.mit.edu/GENSCAN.html), and BLASTing predicted genes against the NCBI database (http://www.ncbi.nlm.nih.gov/BLAST). These were *pcbp2, kif5a, arp5* and a gene similar to *stac*. New markers, zh34 located in *kif5a* (0.04 cM north), zh16 in *arp5* (0.04 cM

south) and zh31 in the *stac*-like gene (no recombinants), were identified. The *stac*-like cDNA from wildtype and mutant embryos were isolated and sequenced and the mutant cDNA contained an insertion that included an in frame stop codon. Sequencing of cDNAs for *kif5a* and *arp5* from wildtype and mutant embryos found no mutations suggesting that the *stac*-like gene was responsible for the *stac3*^{mi34} phenotype. Analysis of genomic sequences determined that the *stac3*^{mi34} allele contained a splice site mutation that transformed a splice donor site for the intron between exon 4 and exon 5 (GT to AT) that lead to incorrect splicing and inclusion of the intron in the cDNA.

Mutant Rescue

Rescue of *stac3*^{mi34} behavior was performed by subcloning zebrafish *stac3*^{wt}, *stac3*^{mi34}, *stac3*^{NAM} or human *STAC3* into *pHSP70-EGFP* (Halloran et al., 2000). Zebrafish *stac3*^{NAM} construct was generated by site-directed mutagenesis converting W254 into S. Constructs (10 ng/µl) were injected into one cell stage embryos from a cross between *stac3*^{mi34} carriers with a Nanoject II (Drummond Scientific Company). At 48 hpf *stac3*^{mi34} mutant embryos were behaviorally identified and heat induced by switching them from water at 28.5^{0}C to water at 37^{0}C for 1 h. After heat induction, embryos were switched back to 28.5^{0}C and assayed 3 and 24 h later. Embryos with approximately 10% or more skeletal muscle fibers expressing EGFP were used for behavioral assays. Responses of embryos to touch were video-recorded and measured. For Ca^{2+} imaging of Stac3^{wt} or Stac^{NAM} expressing muscle fibers *pHSP70:stac3*^{wt}*-mCherry* and *pHSP70:stac3*^{NAM}*-mCherry* were generated along with *α-actin:GCaMP3*. Embryos were injected with a 1:1 mixture of a *stac3* construct and *α-actin:GCaMP3* each at 10ng/µl. Following heat

induction embryos with skeletal muscle fibers expressing both constructs were selected for Ca^{2+} imaging.

Polyclonal Antiserum Production and Purification

Full length zebrafish Stac3 was expressed as a His-Sumo fusion protein in B21(DE3) cells (Invitrogen), and affinity-purified using Ni-NTA agarose (Qiagen). Protein was further purified by electrophoresis in a NuPAGE 4-12% SDS-PAGE Bis-Tris Gel (Invitrogen), Coomassie staining of the gel, and subsequent excision of appropriate band. Rabbits were immunized with gel slices of purified fusion proteins (ProSci). Antiserum was purified by passing through a Sulfolink column (Thermo) containing the immobilized fusion protein.

Western Blot Analysis and Immunoprecipitation

~50 *stac3*^{mi34} mutant and sibling embryos were collected, lysed using a Total Protein Extraction Kit (Biochain), and isolated protein loaded and separated by SDS/PAGE as described in Schredelseker et al., 2005. Anti-DHPRα1 was used for immunoblotting at 1:500 (Thermo), anti-pan-RyR at 1:2000 (DSHB 34C-c). Adult female fish were sacrificed using 0.1% tricaine (Sigma), skeletal muscle was dissected on dry ice, and total protein extracted using a Total Protein Extraction Kit (Biochain). Protein lysate from an individual fish was immunoprecipitated using anti-DHPRa1 (1:100), or anti-pan-RyR (1:200) crosslinked with BS^3 (Thermo) to Protein G Dynabeads (Invitrogen).

Quantification of Fluorescence

For all immuno-fluorescence quantification of Stac3, labeling between sibs and mutants was performed side by side to maintain conditions per experiment. All confocal setting were identical between sibs and mutants during imaging per experiment. To obtain a fluorescent measure a rectangular region of interest encompassing part of a band of labeling (band consistent with triadic localization) of muscle labeling was selected, roughly 3-4 micron square. In a single muscle fiber, 5 different fluorescent measures were taken at evenly spaced distances along a single fiber. All 5 measures were averaged to represent a single fiber fluorescent signal. Similar measures were taken over several embryos between sibs and mutants. Fluorescence was standardized to sibs for comparison with mutants.

Molecular Analysis of Native American Myopathy

The cohort of individuals with NAM was previously described (Stamm et al., 2008a). Initially, each exon and the surrounding splicing regions of *STAC3* were screened in 3 NAM patients and 3 related individuals through PCR amplification and automated Sanger sequencing. After identification of the NAM mutation in exon 10 of *STAC3*, the entire cohort of available samples from NAM pedigrees was screened by exon amplification and sequencing for the mutation. In all, a total of 21 individuals from 7 Lumbee families were sequenced. In addition, genomic DNA were screened from 2 neurologically normal control individuals (Coriell Institute NDPT006 and NDPT009) and from a collection of 111 adult subjects without evidence of neurological disease (Rainier et al., 2006).

Electron Microscopy

Electron microscopy was performed as previously described (Dowling et al., 2009). In brief, zebrafish larvae at the indicated ages were euthanized with tricaine and immersed in Karnovsky's fixative overnight at 4^0C. They were then dehydrated, stained with osmium and embedded in epon. Thin sections were cut and then samples analyzed on a Phillips Transmission electron microscope. A minimum of 3 larvae per condition were examined.

Results

The *mi34* Zebrafish Mutant is Defective in EC Coupling

In order to identify new genes involved in the regulation of EC coupling, a forward genetic screen in zebrafish was performed to isolate motor behavior mutants (Cui et al., 2005; Hirata et al., 2005; Hirata et al., 2004; Hirata et al., 2007; Zhou et al., 2006). One mutation, *mi34*, was autosomal recessive with mutants dying as larvae and exhibiting defective motor behaviors at early stages of development. Normally zebrafish embryos exhibited spontaneous slow coiling of the body starting at 17 h postfertilization (hpf), touch-induced escape contractions of the body at 22 hpf and touch-induced swimming by 28 hpf (Saint-Amant and Drapeau, 1998). Mutants were defective in all three motor behaviors with reduced amplitude of spontaneous coiling, decreased touch induced escape contractions and ineffective swimming (Figure 2.1; Figure 2.2A). Aberrant behavior in mutants could be due to defects in the nervous system and/or skeletal muscles. If signaling within the nervous system were abnormal in mutants, then one would expect the output of motor neurons to muscles to be aberrant. To determine this, the synaptic response of muscles to tactile stimulation of the embryo was

electrophysiologically recorded *in vivo*. Tactile stimulation initiated synaptic potentials in both slow and fast twitch muscles that were comparable between wildtype sibling and mutant embryos (Figure 2.2B). Furthermore the distribution of motor neuron terminals and muscle acetylcholine receptors (AChRs) were indistinguishable between wildtype sibs and mutants (Figure 2.3). Thus the nervous system and the NMJ were normal in mutants and the primary defect was in the muscle response to activation of the NMJ.

Activation of the NMJ leads to depolarization of the muscle membrane potential that in turn initiates muscle contraction. To examine how the mutation affects the relationship between muscle voltage and contraction, the membrane voltage of skeletal muscles were depolarized to various values and the amount muscles contracted was measured. Mutant muscles contracted much less than wildtype sib muscles at depolarized membrane potentials (Figure 2.4). The decreased contraction to depolarizations could be due to a defect in EC coupling or a defect in the contractile machinery. However, the fact that mutant and wildtype sib muscles contracted similarly when exposed to 5 mM caffeine, an agonist of RyRs, suggested that the contractile machinery was intact in mutants and that the store of Ca^{2+} in the SR was not grossly perturbed (Figure 2.5). Corroborating this finding, mutant muscles exhibited no obvious morphological defects early in development with apparent normal distribution of contractile proteins and other muscle proteins. These findings coupled with normal activation of the NMJ in mutants pointed to a defect in EC coupling in mutant muscles.

Since EC coupling takes place at triads, their anatomy was examined with TEM. Longitudinal sections showed that triads exhibited normal anatomy in mutant muscles (Figure 2.2C) suggesting that aberrant EC coupling was not due to a defect in triad anatomy but rather a defect in function. The hallmark of EC coupling is the release of Ca^{2+} from the SR to the cytosol. EC coupling was directly examined *in vivo* by imaging Ca^{2+} transients in skeletal myofibers expressing the GCaMP3 Ca^{2+} indicator (Tian et al., 2009) during swimming. Swimming was evoked by application of NMDA, which activated the swimming network in the CNS (Cui et al., 2005). Ca^{2+} transients were greatly reduced in both mutant slow and fast twitch fibers in mutant fast twitch fibers (Figure 2.2D, Figure 2.6). Thus the EC coupling in skeletal muscles was defective in the *mi34* mutants.

stac3, **a Novel Muscle Gene, is the Basis for the *mi34* Phenotype**

A combination of meiotic mapping and analysis of zebrafish genome resources identified the gene responsible for the *mi34* phenotype as *stac3* (Figure 2.7), a gene similar to murine *stac* that encodes an adaptor-like protein of unknown function (Suzuki et al., 1996). *stac3* encodes for a putative 334 residue soluble protein with an N-terminal cysteine rich domain (CRD) similar to the C1 domain found in Ca-dependent protein kinase and two SH3 domains (Figure 2.8 A). The mutant allele carried a splice site mutation that disrupted a splice donor site and led to the inclusion of intron 4 and a premature stop codon in the transcript. The mutation in *stac3* predicted a protein that was truncated within the N-terminal CRD suggesting that the $stac3^{mi34}$ mutation was functionally null. Western blotting with an antibody generated against Stac3 revealed an

approximately 49 kDa protein in wildtype embryos but no protein in mutants (Figure 2.8B). *In situ* hybridization showed that skeletal muscles selectively expressed *stac3* during embryogenesis (Figure 2.9), and labeling with anti-Stac3 revealed that Stac3 co-localized with the DHPRs and RyR1s at muscle triads in wildtype but not mutant embryos (Figure 2.8C). These findings suggested that a mutation in *stac3* was responsible for defective EC coupling and that Stac3 was a component of the triadic molecular complex.

The molecular identity of the mutation was confirmed by mutant rescue experiments. Induced expression of *hsp70:stac3*^{wt}*-egfp* in mutant muscles rescued the behavioral phenotype and triadic localization of Stac3 whereas induced expression of *hsp70:stac3*^{mi34}*-egfp* did not (Figure 2.10A). Furthermore Ca^{2+} imaging of mutant muscles co-expressing *stac3*^{wt}*-mCherry* and *GCaMP3* showed that wildtype Stac3 could restore normal muscle Ca^{2+} transients in mutant embryos (Figure 2.10B). Given that Stac3 co-localizes with DHPR and RyR1 at triads, we examined whether Stac3 may be part of the DHPR/RyR1 molecular complex. Indeed co-immunoprecipations with antibodies against RyR and DHPR both pulled down Stac3 from wildtype adult muscles (Figure 2.11) indicating that Stac3 is part of the DHPR/RyR1 complex found at triads. Thus Stac3 is a component of the triadic complex that is required for EC coupling in skeletal muscles.

A Loss of DHPR is the Basis for Decreased EC Coupling in Embryos Deficient for Stac3

To investigate how the loss of Stac3 leads to diminished EC coupling, the status of DHPR and RYR1 in mutant muscles was examined. First, dissociated skeletal muscles

were labeled with anti-DHPRβ1 and wildtype siblings showed striated bands along a muscle fiber. In *stac3*^{mi34} muscle fibers, a banded organization can still be observed, but fainter compared to siblings (Figure 2.12A, top). Quantification of the fluorescence intensity of β1 bands shows approximately a 40% reduction in mutants compared to siblings (Figure 2.12A, bottom). Whole embryo labeling with anti-RYR showed similar striated banded labeling in both sibling and *stac3*^{mi34} muscle (Figure 2.12B). Second, Western blotting demonstrated a dramatic decrease in DHPRα in mutants compared with wildtype siblings, whereas RYR protein was minimally reduced in *stac3*^{mi34} (Figure 2.12C). To see if the loss of Stac3 might decrease synthesis of DHPRs, the message levels of *dhprα1sa* and *dhprα1sb* that are expressed by the slow and fast twitch muscles, respectively, were assayed by qPCR. Message levels of both *dhprα1a* and *dhprα1sb* were comparable between wildtype siblings and mutants (Figure 2.13). These data suggest that the decrease in DHPRα1 in mutants cannot be due to decreased transcription of *dhprα1*. Third, the molecular anatomy of the DHPRs at triads was assayed in mutants and wildtype siblings by freeze-fracture analysis (Block et al., 1988; Schredelseker et al., 2005). In freeze fracture EM, intramembranous particles in the inner leaflet of the plasmamembrane at the triadic junctions are thought to represent individual DHPRs and in wildtype muscles these particles are arranged in geometrically arrange groups of four called tetrads. There was both a decrease in the number of particles and complete tetrads in the skeletal muscles of mutants compared with wildtype (Figure 2.14A, B). In sections of muscle fibers examined with transmission electron microscopy (TEM) one can see rows of electron dense material called triadic

feet that are thought to represent the large cytoplasmic portions of RyR1. The triadic feet were comparable between wildtype and mutants (Figure 2.14C). Thus *in vivo* labeling, Western blotting and freeze fracture analysis suggest a significant decrease in DHPRs in mutant muscles but not RYRs. Furthermore, the results are consistent with defective processing of DHPRs in the secretory pathway and/or decreased stability of DHPRs at the triadic junctions.

A Mutation in Human *STAC3* Causes a Congenital Myopathy

The loss of Stac3 resulted in a progressive breakdown of myofibers during larval stages with apparent swollen SR observed by 7 dpf (Figure 2.15). Given the myopathic features of mutants, we explored whether *stac3* mutations might cause congenital human myopathies. Human *STAC3* mapped to chromosome 12q13-14, and its specific location was within the previously defined genetic locus for a rare congenital myopathy called Native American myopathy (NAM) (Stamm et al., 2008a; Stamm et al., 2008b). NAM is an autosomal recessive disorder found within the Lumbee Native American population of North Carolina that is characterized by a constellation of clinical features including congenital onset of muscle weakness, susceptibility to malignant hyperthermia, multiple joint contractures, dysmorphic facial features including ptosis and 36% mortality by 18 years of age. Patient muscle biopsies revealed a non-specific myopathic pattern. The genetic basis of NAM remained unsolved, though the presence of susceptibility to malignant hyperthermia as a clinical feature suggested a defect in a component of the EC coupling apparatus. To see if *STAC3* was the basis for NAM, *STAC3* coding regions were sequenced in a cohort of 7 NAM families that included 5 affected

and 16 unaffected individuals. In all affected individuals, there was a G>C missense mutation of base pair 1046 in exon 10 of the *STAC3* gene (Ensembl transcript ID ENST00000332782). This mutation resulted in a tryptophan (W) to serine (S) substitution at amino acid 284 in the first SH3 domain (Figure 2.16A). The sequence change perfectly segregated with the NAM phenotype, and was not found in any unaffected family members nor in > 200 control individuals. In addition, *STAC3* has been sequenced as part of the 1000 genome project, and this mutation has not been detected. This pattern of inheritance suggested that *STAC3* was the basis for the congenital myopathy.

How the NAM mutation might affect the function of Stac3 was determined to confirm that the NAM allele of *STAC3* was the basis for the myopathy. To do this the analogous W>S substitution was encoded in zebrafish *stac3* (*hsp70:stac3*^{NAM}*-egfp*) and expressed in *stac3*^{mi34} null mutant muscles to assay for phenotypic rescue. Unlike *stac3*^{wt}*-egfp*, expression of *stac3*^{NAM}*-egfp* failed to rescue touch induced swimming although some Stac3^{NAM} localized to triads (Figure 2.16B). Furthermore, Ca^{2+} imaging of mutant fast twitch muscles expressing *stac3*^{NAM}*-mCherry* and *GCaMP3* exhibited Ca^{2+} transients that were decreased compared with mutant muscles expressing *stac3*^{wt}*-mCherry* and *GCaMP3* (Figure 2.10B, Figure 2.16C). Additionally, expression of wildtype human *STAC3* in mutant zebrafish muscles rescued the motor phenotype (Figure 2.17). Thus the NAM mutation significantly diminishes EC coupling in fast twitch muscles suggesting that the NAM phenotype is due to decreased EC coupling in the skeletal muscles of patients afflicted with NAM.

Discussion

This study identified Stac3 as a novel regulator of EC coupling in skeletal muscles. In principle Stac3 could regulate EC coupling by a variety of mechanisms. First, Stac3 might modulate the channel properties of DHPR and/or RyR1 or how DHPR and RyR1 interact. The triadic localization of Stac3 and biochemical demonstration that Stac3 is part of the DHPR/RyR1 complex are consistent with this possibility. Regulation of DHPR or RyR1 channel properties by other triadic components include modulation of the properties of DHPR by RyR1 and of RyR1 by FKBP12. In RyR1-deficient myotubes the complement of DHPR on the muscle membrane is normal, but the DHPRs pass much less Ca^{2+} than normal (Nakai et al., 1996). The immunophilin, FKBP12, copurifies with RyR and anti-FKBP12 can pull down RyR in striated muscles (Jayaraman et al., 1992). When RyR were examined with single channel recordings, FKBP12 was found to optimize channel function (Brillantes et al., 1994). The β1a subunit of DHPR also appears to be critical for interactions between DHPR and RyR1 since β1a is required for formation of DHPRs into tetrads (Schredelseker et al., 2005). Second, Stac3 might regulate the synthesis of DHPR. However, the finding that transcription of *dhprα1a* and *dhprα1b* are comparable between mutants and wildtype siblings argues against this possibility. Third, Stac3 might be involved in protein trafficking or stability of DHPR. An example of a factor that may be important for trafficking or stability of DHPRs is REM, a member of the RGK GTP-binding protein family. REM can bind β subunits of voltage-dependent Ca^{2+} channels when expressed heterologously and overexpression of REM inhibits L-type Ca^{2+} channels in C2C12 cells (Finlin et al., 2003) and in skeletal muscles due to a decrease of

DHPR in the muscle membrane (Bannister et al., 2008a) via dynamin dependent endocytosis (Yang et al., 2010). Although the loss-of-function phenotype for REM is not known, these results suggest that REM may inhibit localization of DHPRs in triads either by decreasing processing of the channels into triadic junctions or by increasing the removal of the channel from triads.

The fact that Stac3 localizes to triads and is part of the DHPR/RyR1 molecular complex is consistent with a role for Stac3 in protein trafficking of DHPRs to and/or stability at triads. This possibility is further supported by a decrease in DHPRs in *stac*^{mi34} mutants as assayed by triadic labeling in embryos, Western blotting and freeze fracture analysis. It should be possible to investigate this hypothesis further in future experiments in zebrafish by pharmacological and genetic manipulations to directly examine protein trafficking of DHPRs to the triads and endocytotic removal of DHPRs from the triads. Furthermore, the availability of mutants deficient for DHPR (Schredelseker et al., 2005; Zhou et al., 2006) and RyR1 (Hirata et al., 2007) in addition to the *stac3*^{mi34} mutant should be invaluable for analysis of how Stac3 regulates ER coupling.

These same approaches should also be useful for the generation of a transgenic line of *stac3*^{NAM} mutant zebrafish to delineate the biology of NAM and for identifying potential therapeutic agents. This is particularly relevant given the increasing recognition of mutations in genes associated with EC coupling in a growing range of human muscle diseases. In addition, *STAC3* is an attractive candidate for the genetic basis of currently undefined congenital myopathies, particularly those associated with

susceptibility to malignant hyperthermia and/or those with phenotypes similar to those of patients with *RYR1* or *DHPR* mutations.

Figure 2.1

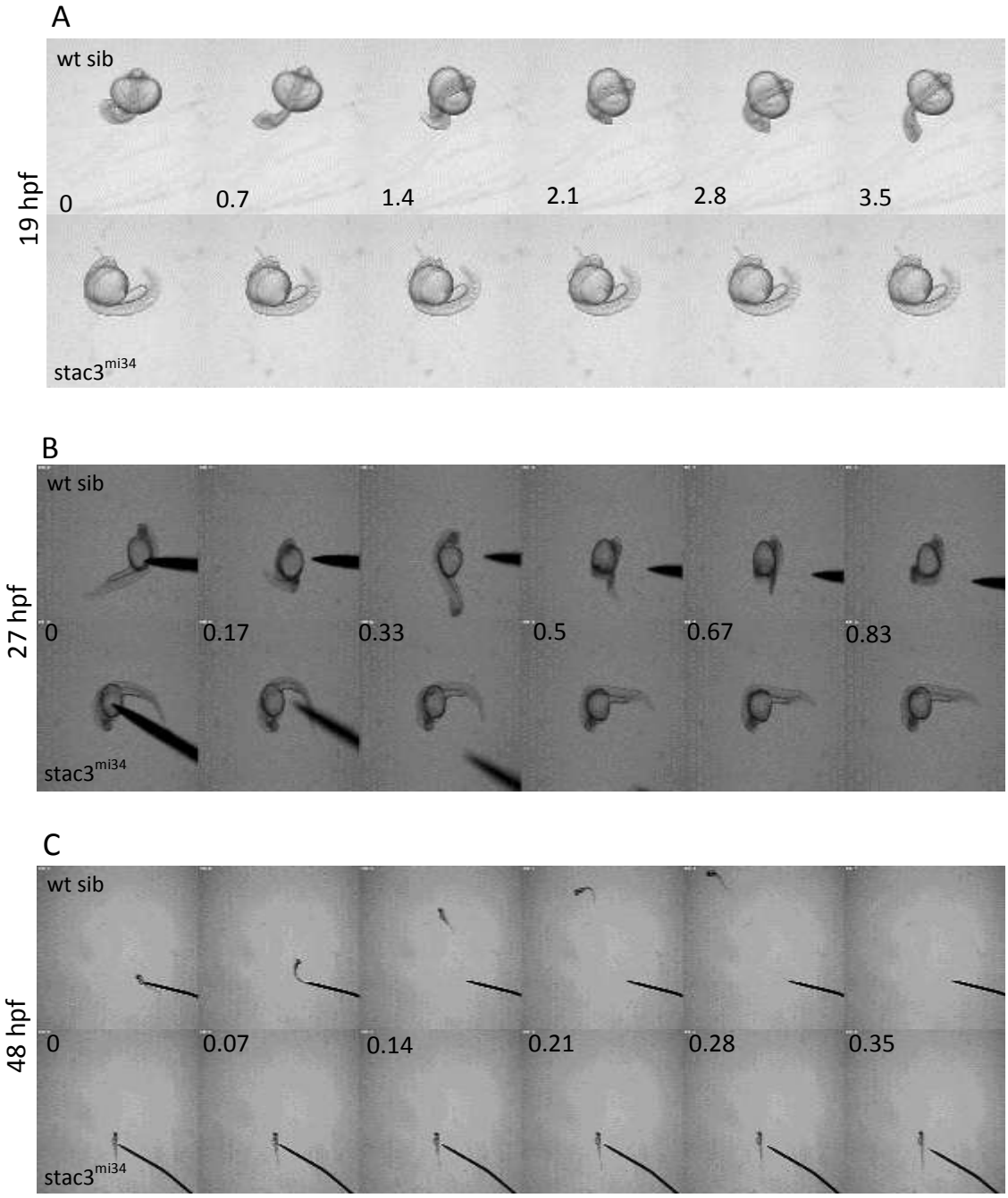
A
wt sib
19 hpf
0
0.7
1.4
2.1
2.8
3.5
stac3mi34
B
wt sib
27 hpf
0
0.17
0.33
0.5
0.67
0.83
stac3mi34
C
wt sib
48 hpf
0
0.07
0.14
0.21
0.28
0.35
stac3mi34

Figure 2.1: Spontaneous and touch induced responses from *stac3*^{mi34} mutants compared to siblings. (A) Spontaneous coiling recorded at 19 hpf wt siblings (top) and *stac3*^{mi34} (bottom). Montage shows behavior sampled every 0.7 seconds. (B) Touch induced tail flips recorded at 27 hpf wt siblings (top) and *stac3*^{mi34} (bottom). Montage shows behavior sampled every 0.17 seconds. (C) Touch induced swimming recorded at 48 hpf wt siblings (top) and *stac3*^{mi34} (bottom). Montage shows behavior sampled every 0.07 seconds. Partially contributed by Dr. Hiromi Hirata.

Figure 2.2

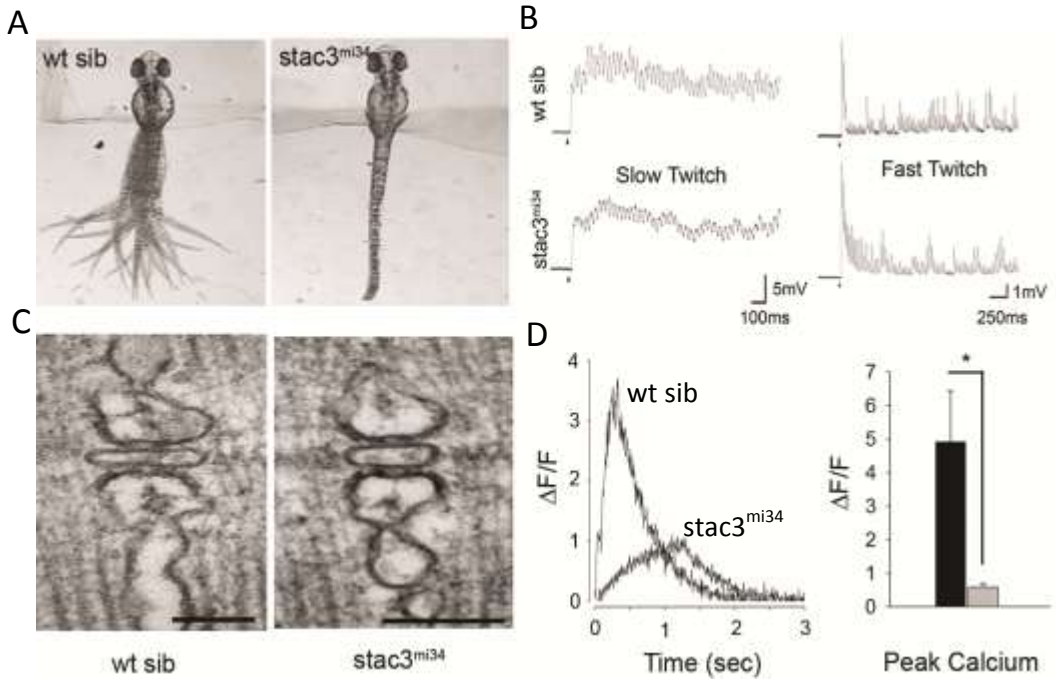

Figure 2.2: EC coupling is defective in *stac3*^{mi34} mutant embryos. All panels show data from 48 hpf embryos. (A) Response to tactile stimulation in wt and *stac3*^{mi34} embryos. Panels show superimposed frames (30 Hz) of swimming motion from wt sibling but not *stac3*^{mi34} embryos with heads embedded in agar. (B) Voltage recordings showing touch evoked synaptic responses of slow twitch and fast twitch muscles of wt sibling and *stac3*^{mi34} mutants. Arrowhead denotes moment of applied tactile stimulation. (C) TEM of wildtype (left) and *stac3*^{mi34} (right) showing t-tubule structure. Scale bar 100nM. (D) Activity induced calcium release in fast twitch muscle. Left shows representative Ca^{2+} transient traces from fast twitch fibers. Right is quantification of peak Ca^{2+} transients recorded from GCaMP3 expressing fast twitch fibers. Peak response is significantly decreased in *stac3*^{mi34} mutants with black and gray bars representing wt sib (fast, n=5) and *stac3*^{mi34} (fast, n=9) fibers, respectively. Asterisk signifies $p<0.01$. Fictive swimming (B) courtesy of Dr. Louis Saint-Amant. TEM (C) courtesy of Dr. Clara Franzini-Armstrong.

Figure 2.3

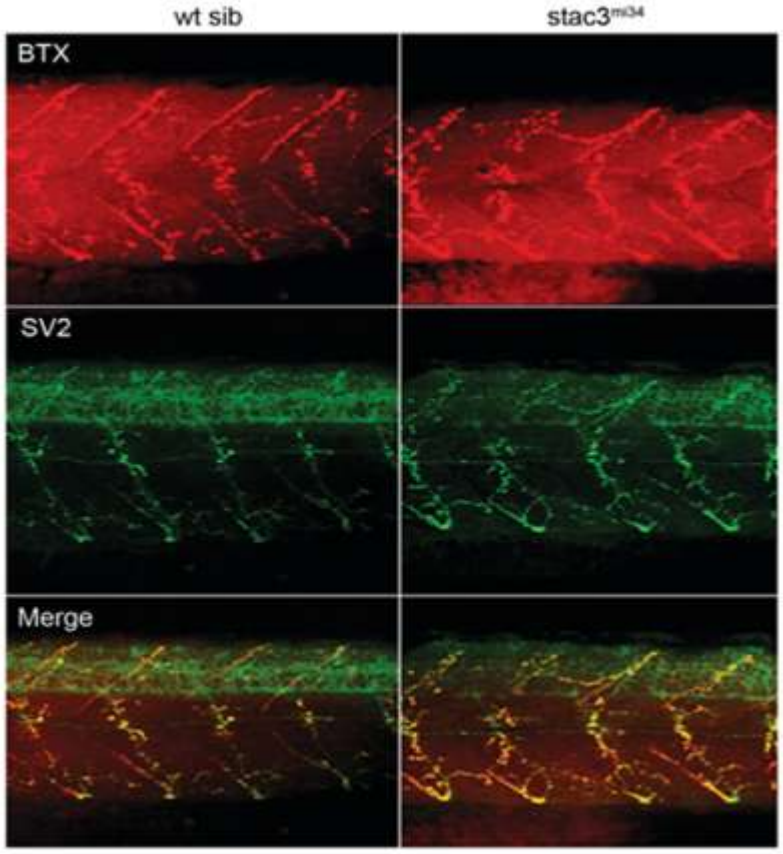

Figure 2.3: Distribution of the neuromuscular junction (NMJ) is unperturbed in *stac3*^{mi34} embryos. Sideview of the trunk of a 48 hpf wt sib and *stac3*^{mi34} embryo showing bungarotoxin-Alexa594 (BTX) labeled distribution of AChRs (red) is normal (top) as is the anti-SV2 (green) labeled presynaptic terminals (middle). The BTX and anti-SV2 labeled panels are merged to show co-localization (bottom).

Figure 2.4

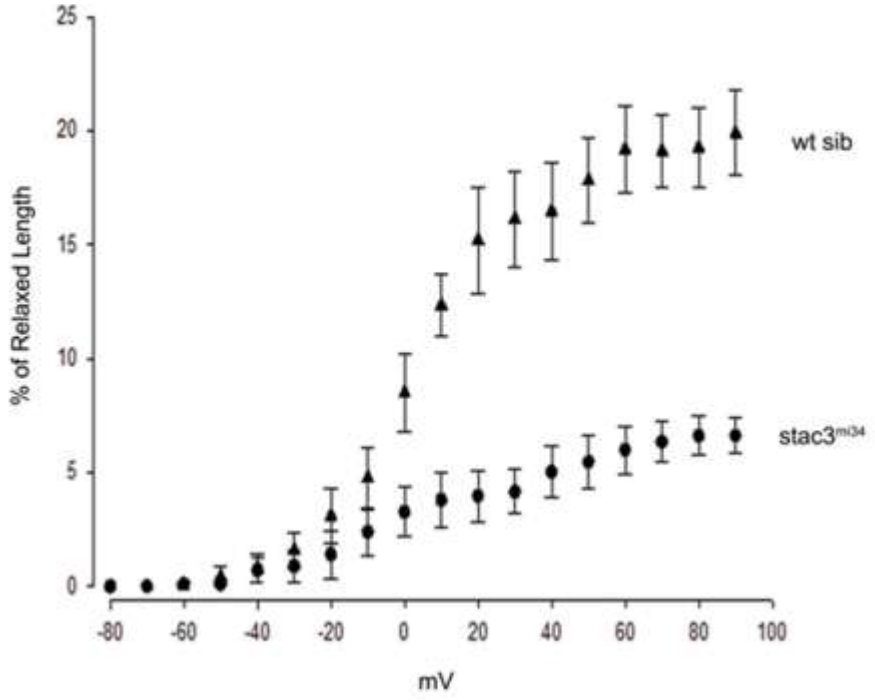

Figure 2.4: Depolarization initiated muscle contraction is decreased in *stac3*^{mi34} embryos at 48 hpf. Muscle fibers were voltage clamped *in vivo* to different membrane potentials for 200 ms and imaged at 60 Hz to measure the amount of contraction as a % of the relaxed fiber length was measured. Wt sib fibers (n=5) and *stac3*^{mi34} fibers (n=4) are denoted by triangles and circles, respectively. The difference in contraction was first significant ($p<0.01$) starting at 10 mV through to 90 mV.

Figure 2.5

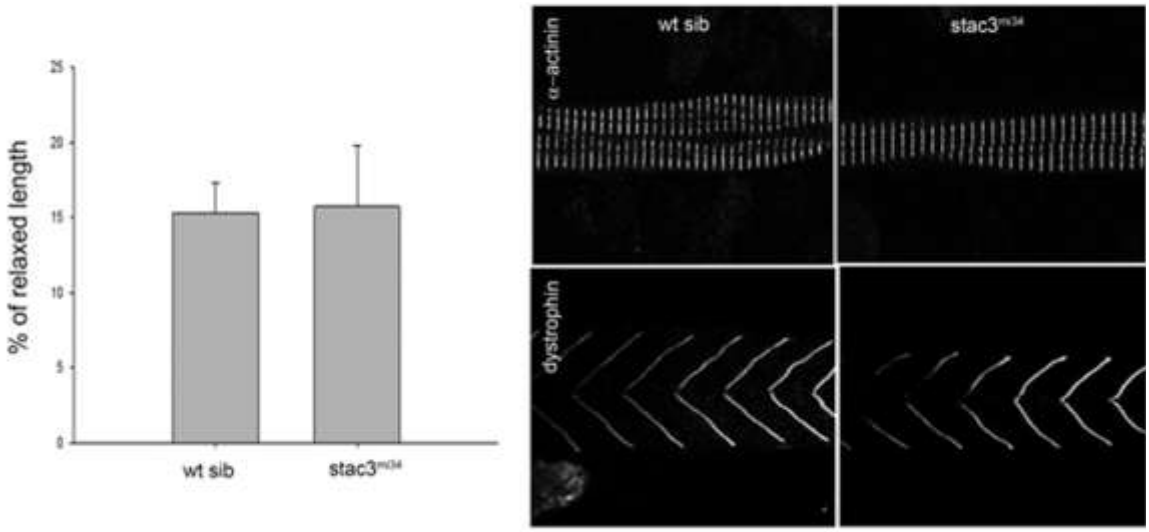

Figure 2.5: Caffeine induces skeletal muscle contractions that were similar between wt sib and *stac3*^{mi34} embryos at 48 hpf. Left, histogram of contraction induced by 5 mM caffeine in the presence of 50 mM curare. Right, the distribution of α-actinin and dystrophin are normal in *stac3*^{mi34} embryos. α-actinin labeling is shown on dissociated muscle fibers while dystrophin is on whole-mounted embryos.

Figure 2.6

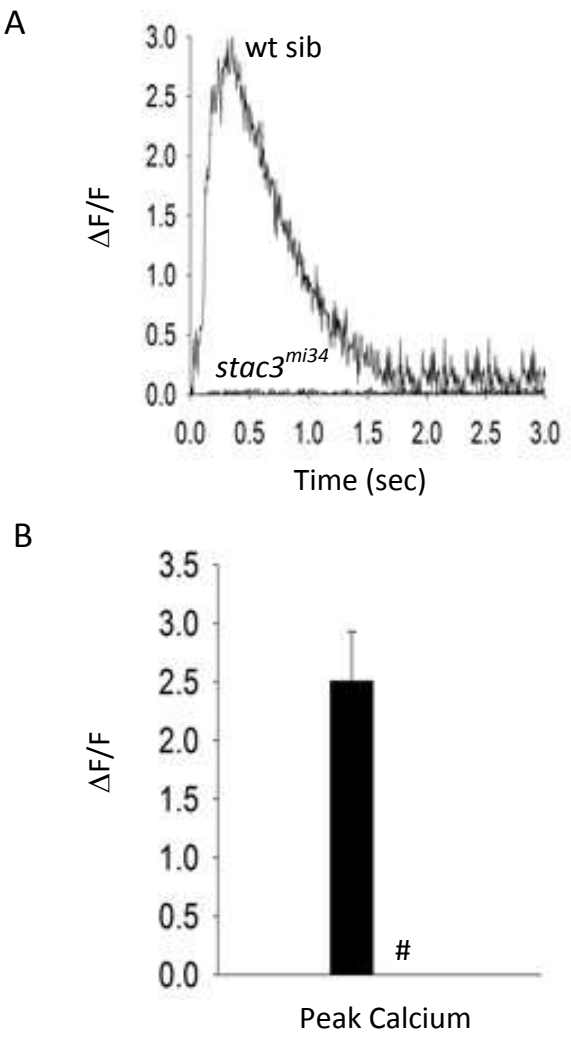

Figure 2.6: Calcium release is decreased in *stac3*^{mi34} zebrafish slow twitch muscle fibers. Ca^{2+} transients recorded from GCaMP3 expressing slow twitch fibers are significantly decreased in *stac3*^{mi34} mutants. (A) Shows quantification of peak Ca^{2+} release with the black bar representing wt sib (slow, n=5) and *stac3*^{mi34} (slow, n=7) fibers. # denotes that peak Ca^{2+} was 0. Recordings performed with 48 hpf embryos.

Figure 2.7

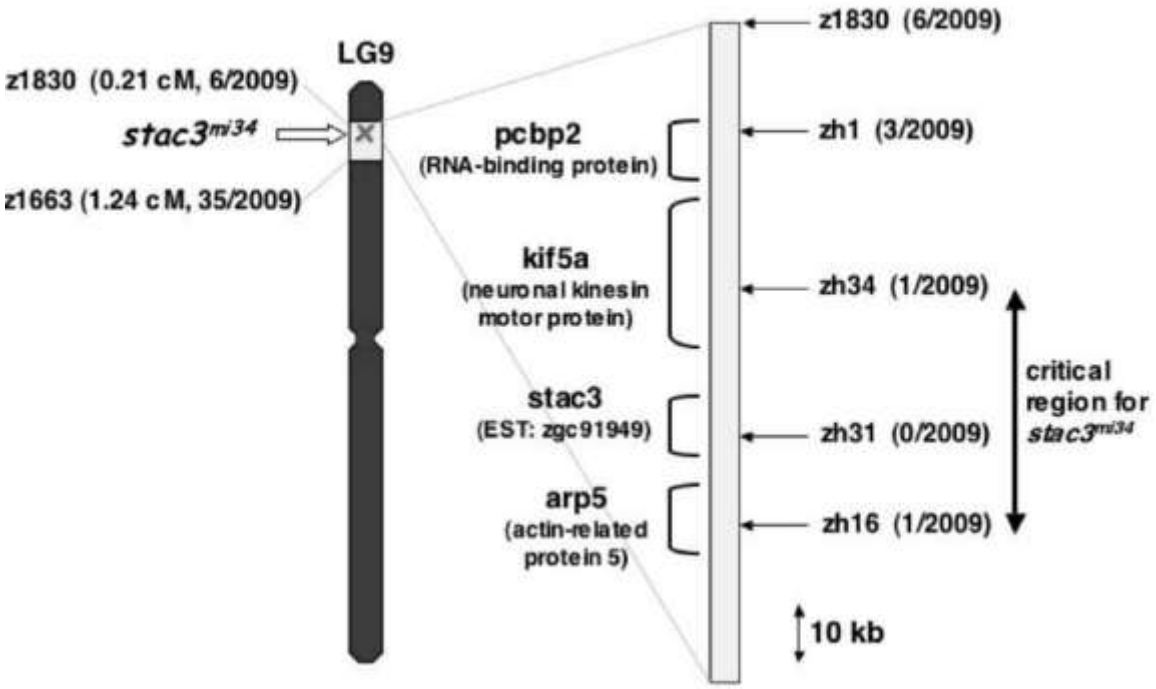

Figure 2.7: Meiotic mapping of the *stac3*^{mi34} locus to the *stac3* gene. Initial meiotic mapping of *stac3*^{mi34} located it to chromsome 9 between markers z1830 and z1663. Numbers in parentheses denote x recombinants in y mutants. A sequenced 156 kb BAC (CR848672) was identified that contained z1830 and high resolution mapping identified new markers (zh1, zh34 and zh16) that flanked the mutation within the BAC. A 4th marker, zh31, located in the *stac3* gene showed no recombination with the mutation out of 2009 mutant embryos suggesting that the mutant locus was *stac3*. Mapping and cloning of zebrafish stac3 courtesy of Dr. Hiromi Hirata.

Figure 2.8

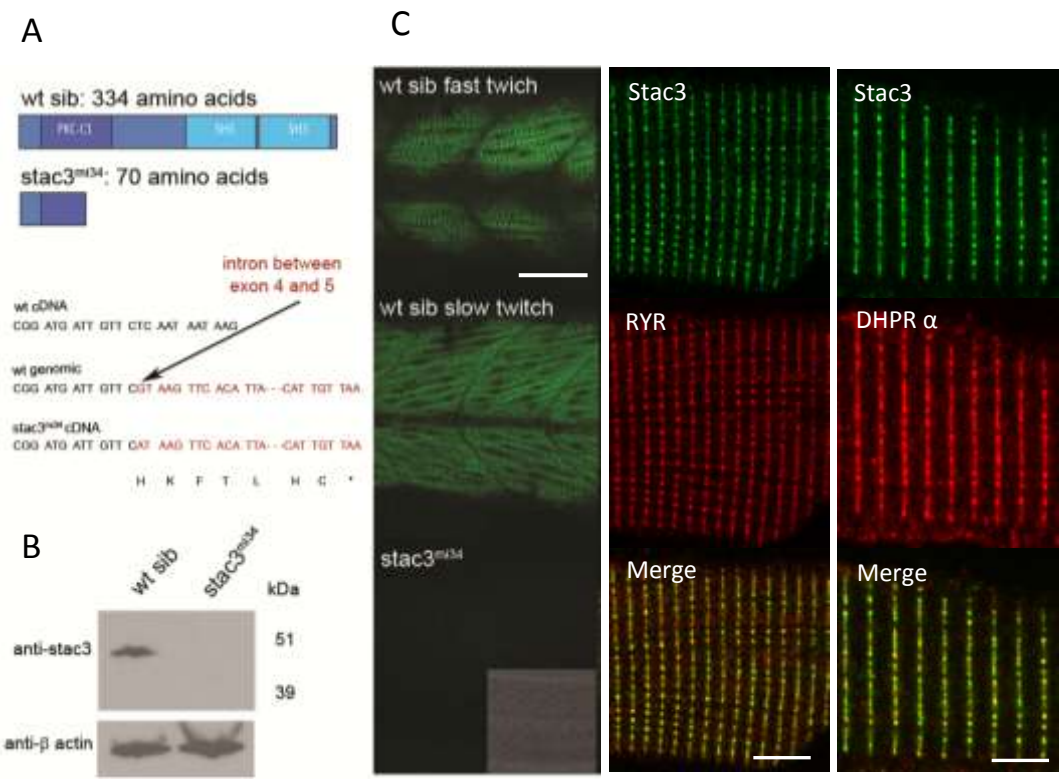

Figure 2.8: *stac3* a muscle specific gene is the basis for the *stac3*^{mi34} phenotype. (A) Diagram of the predicted wt and mutant Stac3 protein (top). DNA sequence of corresponding regions of wt cDNA, wt genomic DNA, and *stac3*^{mi34} cDNA showing that a missense mutation in a splice donor site lead to the inclusion of the intron (red lettering) and stop codon (asterisk) in the mutant cDNA. (B) Western blot of pooled sib and mi34 mutant embryos protein probed with anti-zebrafish Stac3 antibody. β-actin was the loading control. (C) Stac3 co-localizes with RyR and DHPRα1 in skeletal muscles. Left, side view of the trunk of 48 hpf embryos labeled with anti-Stac3 showing that both fast twitch and slow twitch express Stac3 in wt but not mutant embryos. Scale: 60 um. Inset shows the brightfield image of the trunk of the mutant. Right, dissociated 48 hpf wildtype muscle fibers labeled with anti-Stac3 and anti-RyR or anti-DHPRα1 showing that Stac3 co-localizes with RyR and DHPRα1. Scale: 5 um. Western blot (B) courtesy of Jeremy Linsley.

Figure 2.9

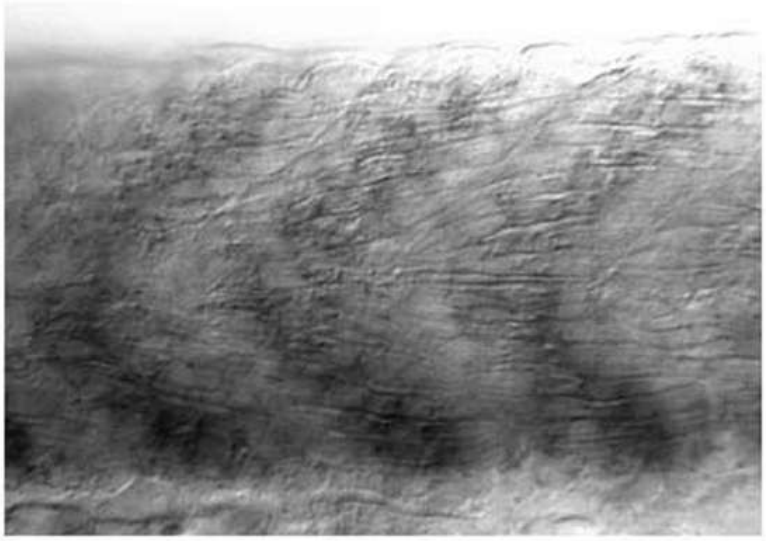

Figure 2.9: *stac3* is expressed specifically by skeletal muscles in zebrafish embryos. Sideview of the trunk of a wildtype embryo (27 hpf) labeled with an antisense riboprobe against *stac3* mRNA showing several segments of *stac3* positive skeletal muscles. *stac3* was not expressed in any other cells at this stage. The sense riboprobe did not label any cells (not shown).

Figure 2.10

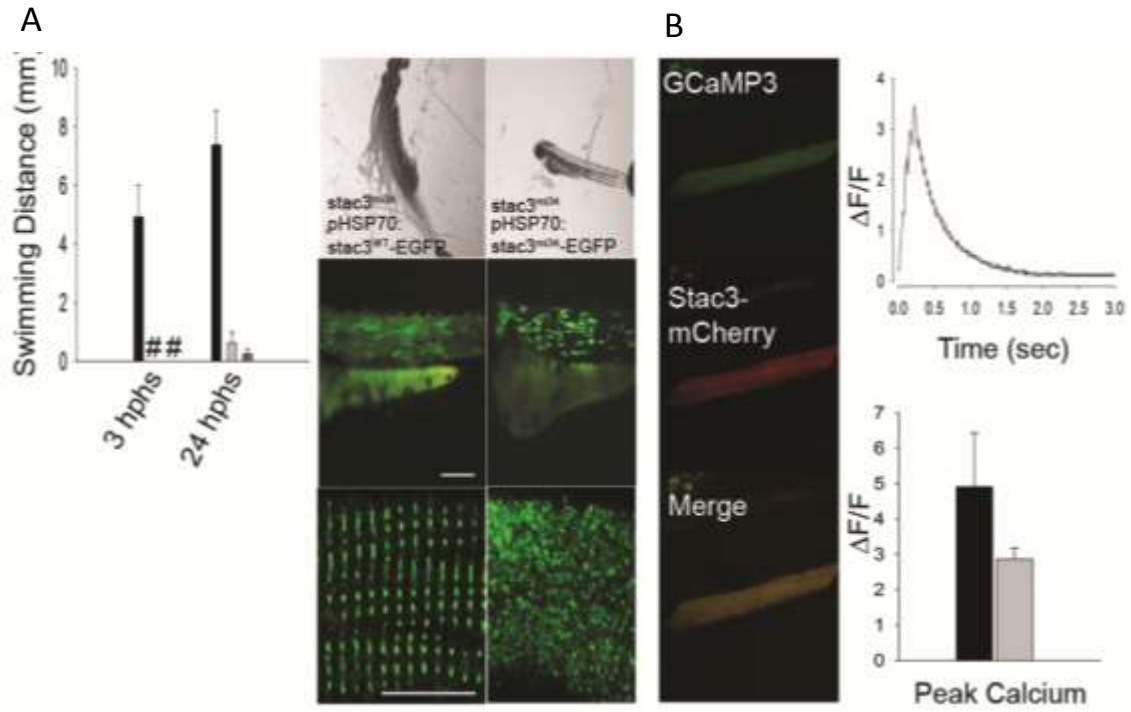

Figure 2.10: Expression of wt Stac3 in muscles rescues the *stac3*^{mi34} phenotype. (A) Left, bar graph showing that mutant embryos expressing heat inducible *stac3*^{wt}*-egfp* (black, n=32) but not *stac3*^{mi34}*-egfp* (light gray, n=4) nor uninjected mutant embryos (dark gray, n=10) exhibited touch evoked swimming at both 3 h post heat shock (hphs) and 24 hphs. # denotes a value of 0. Right panels. Superimposed frames (30 Hz, 1 sec) (top) show that mutant embryos expressing *stac3*^{wt} but not *stac3*^{mi34} swim in response to touch although both are similarly expressed by muscles (middle, scale: 60 um). In dissociated mutant muscles Stac3^{wt}-EGFP localizes to striated bands but Stac3^{mi34}-EGFP does not show a distinct pattern (bottom, scale: 10 um). (B) *In vivo* expression of Stac3^{wt}-mCherry by mutant muscle fibers rescues Ca^{2+} transients. Left panels, examples of *stac3*^{mi34} mutant fast twitch fibers co-expressing *α-actin* driven GCaMP3 and heat induced Stac3^{wt}-mCherry. The triadic localization of Stac3^{wt}-mCherry cannot be seen due to the low resolution of the resonance scans used to detect the fluorescent proteins. Right top, Ca^{2+} transients from mutant fast fibers co-expressing Stac3^{wt}-mCherry and GCaMP3. Bottom, bar graph showing that peak Ca^{2+} release is comparable between wt (black) fast (n=5) and rescued mutant (gray) fast (n=6) fibers.

Figure 2.11

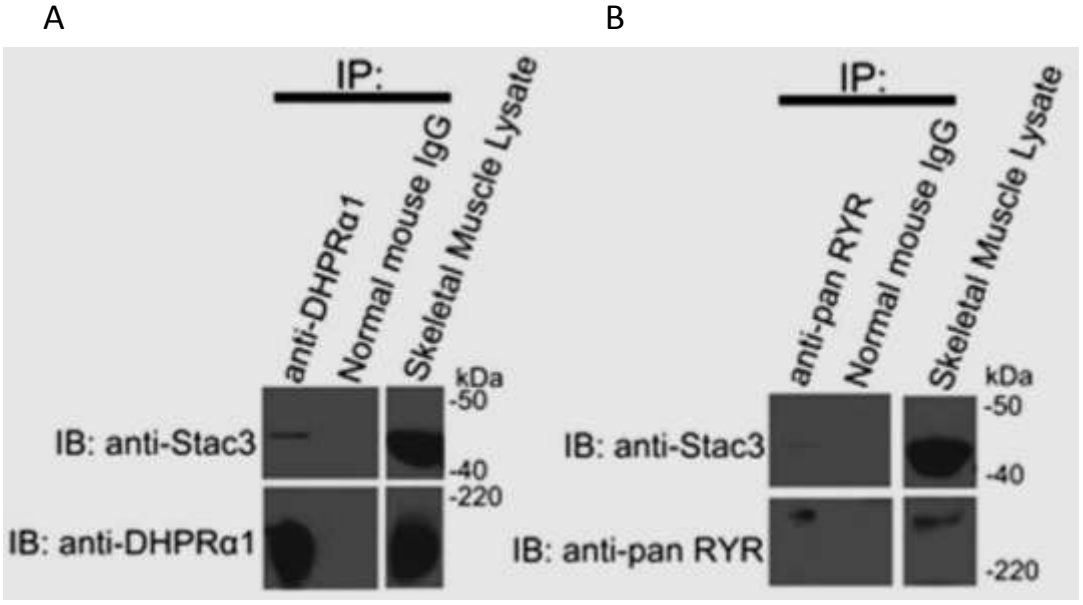

Figure 2.11: Stac3 is in a molecular complex with and DHPR and RyR. (A) Immunoblots showing that immunoprecipitation with anti-DHPRa1 pulls down Stac3 from adult skeletal muscle lysate. (B) Immunoblots showing that immunoprecipitation with anti-pan RyR pulls down Stac3 from adult skeletal muscle lysate. Courtesy of Jeremy Linsley.

Figure 2.12

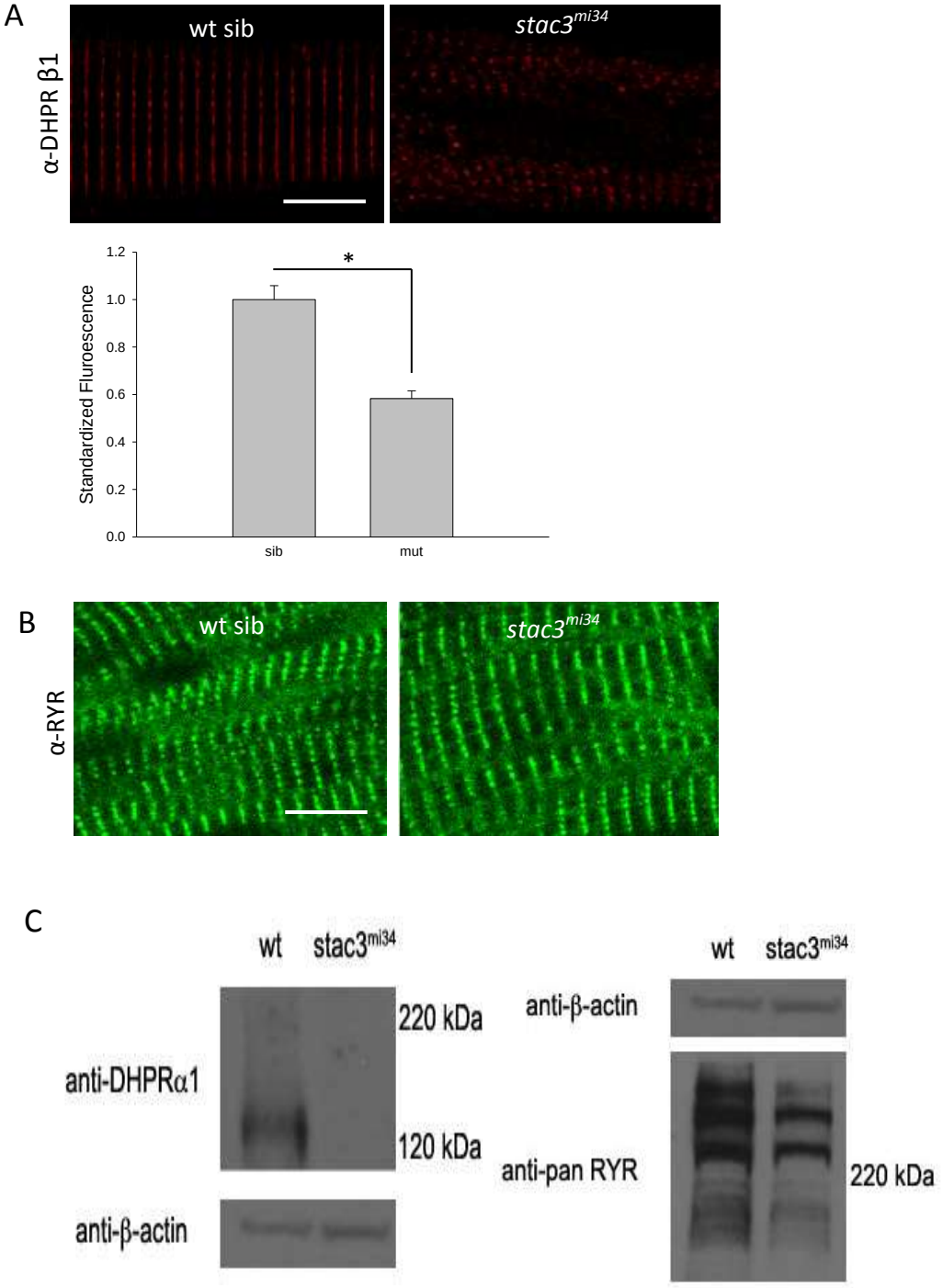
A
wt sib
stac3mi34
α-DHPR β1
Standardized Fluroescence
1.2
1.0
0.8
0.6
0.4
0.2
0.0
*
sib
mut
B
wt sib
stac3mi34
α-RYR
C
wt
stac3mi34
220 kDa
anti-DHPRα1
120 kDa
anti-β-actin
wt
stac3mi34
anti-β-actin
anti-pan RYR
220 kDa

Figure 2.12: DHPR complex protein levels are reduced in *stac3*^{mi34}. (A) Immunolabeling of the DHPR β1 subunit (top) in dissociated wt sibling (left) and *stac3*^{mi34} (right) mutant myofibers. Wildtype siblings show striated bands of labeling. In *stac3*^{mi34} faint bands can still be observed. Scale bar 15 um. Below shows quantification of fluorescence intensity along striated bands of labeling between sibs (n=3) and *mi34* mutants (n=4). * denotes $p<0.01$. (B) Show whole-mounted embryo labeling of ryanodine receptor between sibs (left) and *stac3*^{mi34} (right) both showing banded labeling along muscle fibers. Scale bar 12 um. (C) Western blot for DHPRα (left) and RYR (right) protein from pooled whole embryo protein (~100). Western blots loading control is β-actin. All experiments performed using 48 hpf embryos. Western blots (C) courtesy of Jeremy Linsley.

Figure 2.13

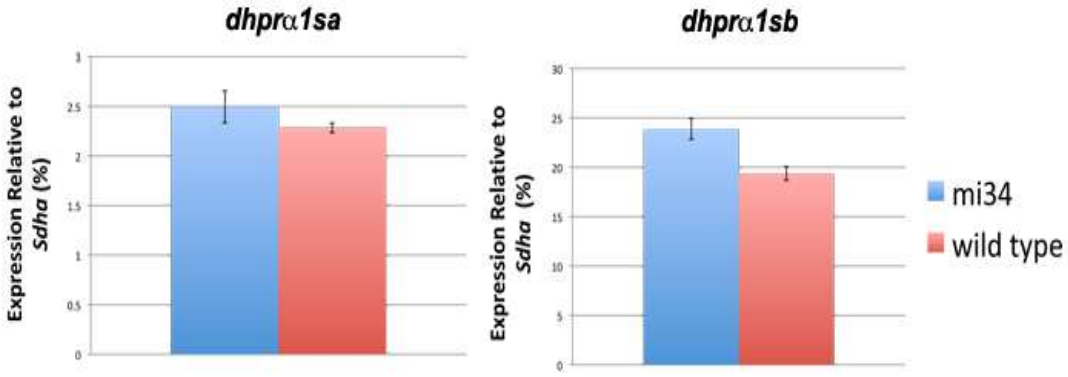

Figure 2.13: Levels of DHPR α transcript normal in *mi34* mutants. qPCR showing transcript levels of slow (dhprα1sa) and fast twitch (dhprα1sb) muscle isoforms of DHPRα are unperturbed in *stac3*^{mi34} compared to wildtype siblings. Standardization to succinate dehydrogenase complex, subunit A. All experiments performed using 48 hpf embryos. Courtesy of Jeremy Linsley.

Figure 2.14

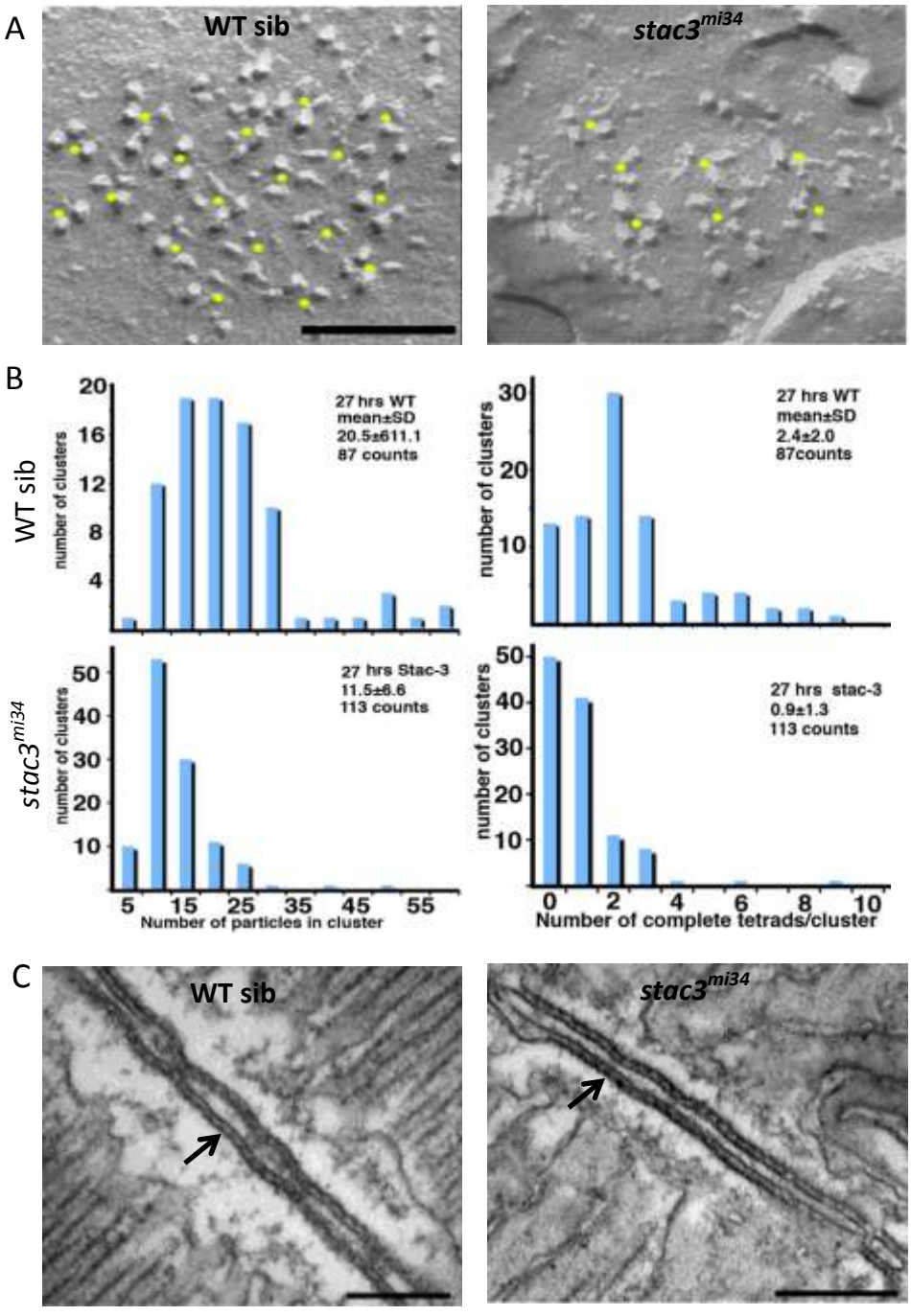
A
WT sib
stac3mi34
B
WT sib
stac3mi34
number of clusters
27 hrs WT
mean±SD
20.5±611.1
87 counts
27 hrs WT
mean±SD
2.4±2.0
87counts
27 hrs Stac-3
11.5±6.6
113 counts
27 hrs stac-3
0.9±1.3
113 counts
Number of particles in cluster
Number of complete tetrads/cluster
C
WT sib
stac3mi34

Figure 2.14: DHPR particles are less frequent in tetrad clusters. (A) Representative freeze fracture images showing tetrad clusters (center of tetrad yellow dot) between wt and *stac3*^{mi34}. Scale bar 100 nm. (B) Histograms showing distribution of DHPR particles within tetrad clusters (left) or particles within complete tetrads (right). A complete tetrad is considered a tetrad with a minimum of 3 DHPR particles. Both (A) and (B) collected at 27 hpf embryos. (C) Thin section EM from 4 dpf embryos showing triadic feet representing RYR. Both wt siblings and *stac3*^{mi34} show long rows of electron dense spots (arrow). Scale 250 nm. Courtesy of Dr. Clara Franzini-Armstrong.

Figure 2.15

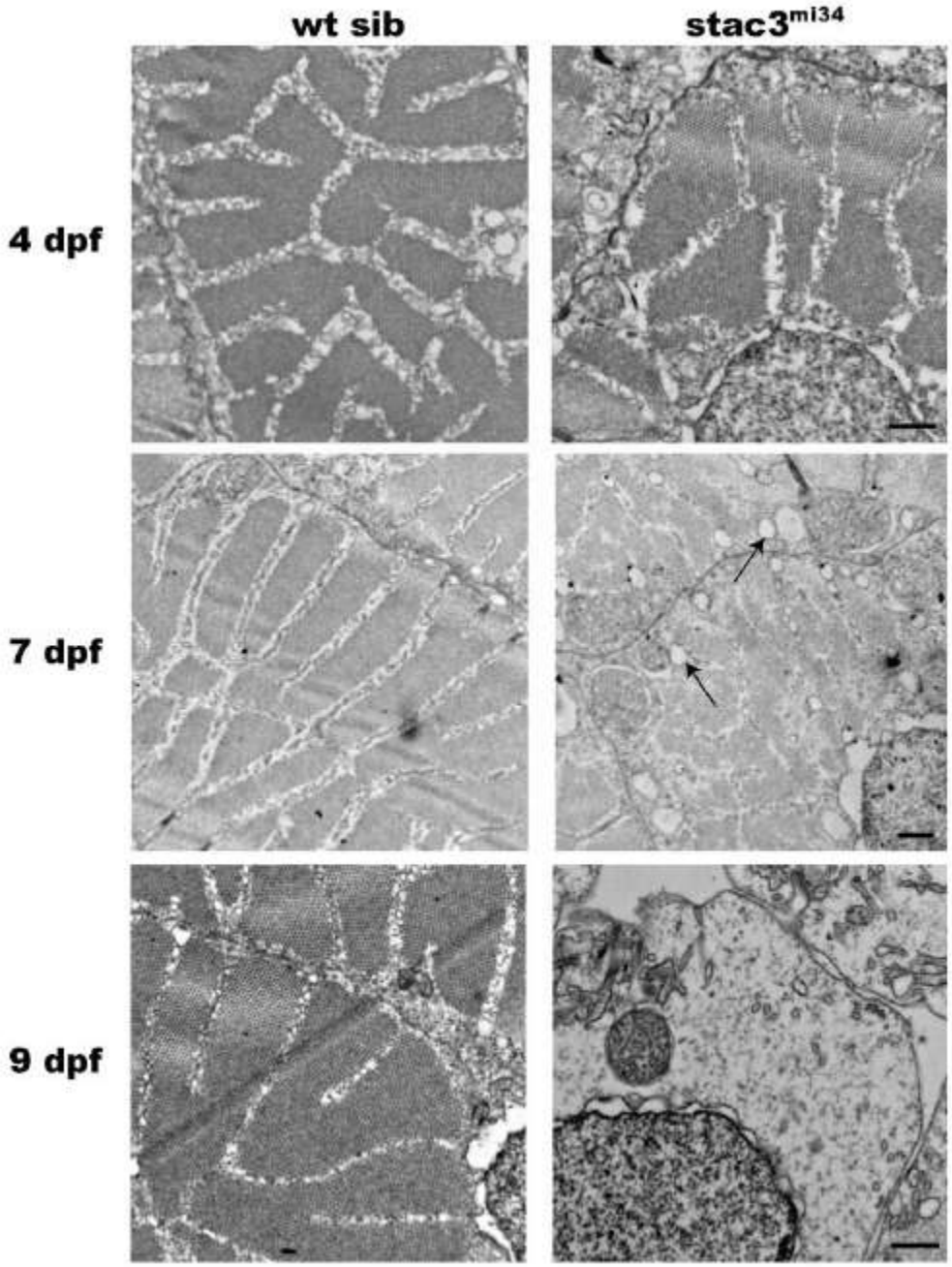

Figure 2.15: Skeletal axial muscles from *stac3*^{mi34} mutants exhibit progressively defective SR. Electron micrographs of SR (arrayed circular profiles) from wtsib and mutant skeletal muscles showing that mutant muscles have relatively normal SR at 4 dpf and swollen ones (arrows) by 7 dpf. Mutant myofibers are breaking down at 9 dpf. Scale: 500 nm. Courtesy of Dr. Jim Dowling.

Figure 2.16

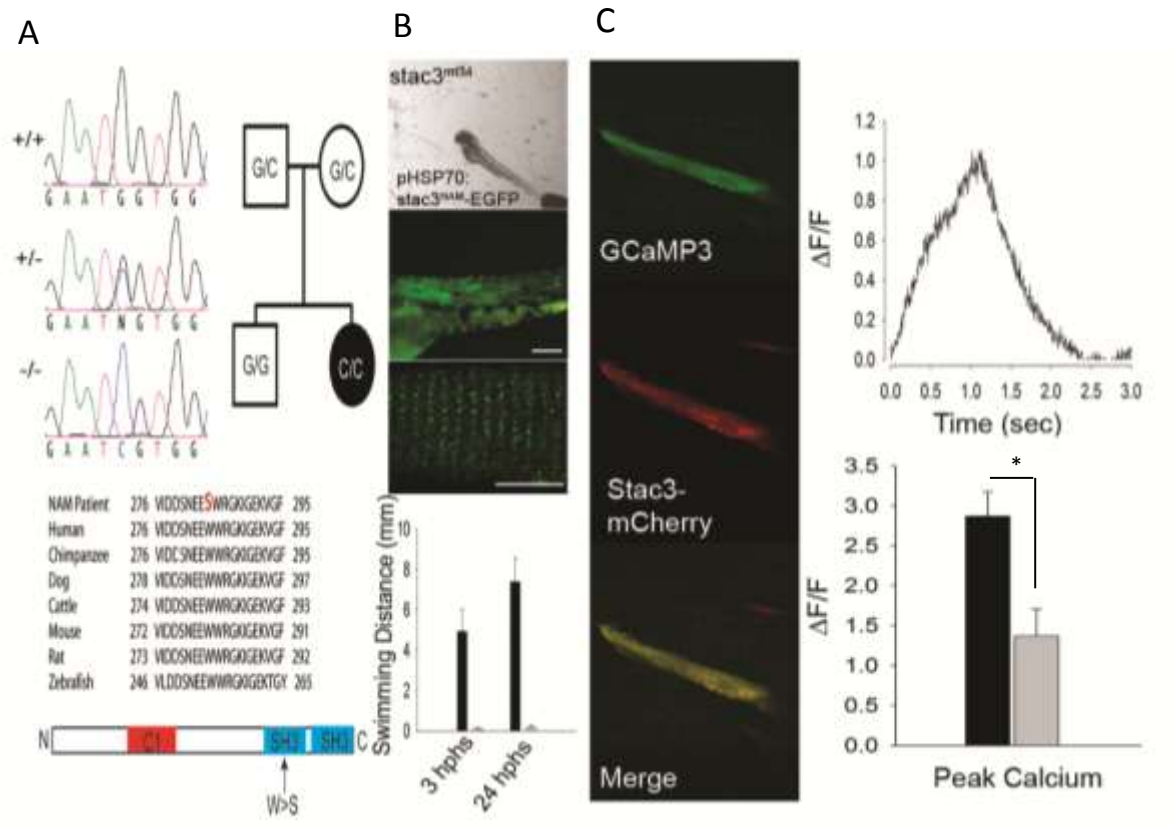
A
B
C
+/+
+/-
-/-
G/C
G/C
G/G
C/C
NAM Patient 276 VIDDSNEESWRGKKGEKVGF 295
Human 276 VIDDSNEEWWRGKKGEKVGF 295
Chimpanzee 276 VIDDSNEEWWRGKKGEKVGF 295
Dog 278 VIDDSNEEWWRGKKGEKVGF 297
Cattle 274 VIDDSNEEWWRGKKGEKVGF 293
Mouse 272 VIDDSNEEWWRGKKGEKVGF 291
Rat 273 VIDDSNEEWWRGKKGEKVGF 292
Zebrafish 246 VLDDSNEEWWRGKKGEKTGY 265
N
C1
SH3
SH3
C
W>S
stac3
pHSP70:
stac3NAM-EGFP
Swimming Distance (mm)
3 hphs
24 hphs
GCaMP3
Stac3-
mCherry
Merge
ΔF/F
Time (sec)
ΔF/F
*
Peak Calcium

Figure 2.16: Missense mutation in human STAC3 causes Native American Myopathy (NAM). (A) Left top, sequence chromatographs of corresponding exonic region of the stac3 gene of individuals +/+, +/- and -/- for the NAM locus showing the G>C missense mutation in the stac3 gene. Right top, pedigree of an individual exhibiting NAM (black) and conserved missense mutation (C/C). Middle, alignment of the corresponding region of Stac3 containing NAM mutation showing that the missense mutation results in a W>S substitution in NAM individuals and that this W is completely conserved between various mammals and zebrafish. Bottom, diagram showing that the missense mutation in $Stac3^{NAM}$ is located in a SH3 domain. (B) Expression of $Stac3^{NAM}$ by muscle fibers in $stac3^{mi34}$ embryos does not rescue touch evoked swimming. Superimposed frames (30 Hz) showing that a heat induced mutant embryo previously injected with pHSP70:$zstac^{NAM}$-egfp does not swim following tactile stimulation (top) despite expression of $zStac3^{NAM}$-EGFP in myotomes and triadic localization of $zStac3^{NAM}$-EGFP (middle, scale bars: 80 um and 10 um). Bar graph (bottom) quantify the comparable lack of touch evoked swimming of $stac3^{mi34}$ mutants expressing the NAM allele (black) and wt Stac3 rescued mutants (gray) both 3 and 24 hphs. (C) Expression of $Stac3^{NAM}$ by muscle fibers in $stac3^{mi34}$ embryos partially rescues Ca^{2+} transients in vivo. Left panels, examples of $stac3^{mi34}$ mutant slow and fast twitch fibers co-expressing α-actin driven GCaMP3 and heat induced $zStac3^{NAM}$-mCherry. The triadic localization of $Stac3^{wt}$-mCherry cannot be seen due to the low resolution of the resonance scans used to detect the fluorescent proteins. Right top, representative Ca^{2+} transients from mutant fast fibers co-expressing $Stac3^{NAM}$-mCherry and GCaMP3. Right bottom, bar graph showing that peak Ca^{2+} release is decreased between fast fibers from NAM allele expressing (gray, n=6) and wt Stac3 expressing mutant fibers (black, n=6) embryos. Asterisk signifies $p<0.01$. NAM mapping and human mutation characterization (A) courtesy of Dr. Jim Dowling.

Figure 2.17

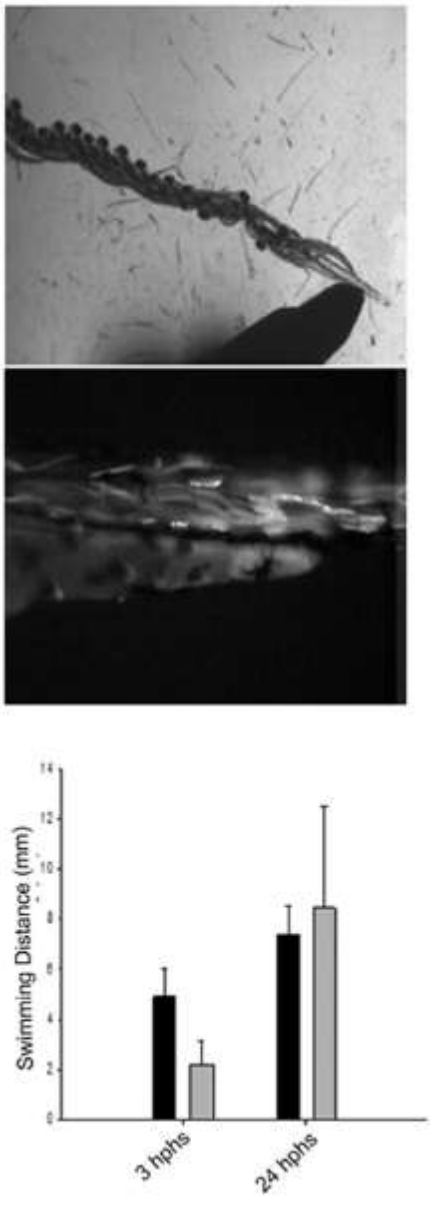

Figure 2.17: Expression of human *STAC3* by skeletal muscles in *stac3*^{mi34} embryos rescues the mutant behavior. Top, superimposed frames (30 Hz) showing swimming by a *stac3*^{mi34} mutant embryos injected with heat inducible constructs for human stac3 fused to EGFP following heat induction. Middle, sideview of the trunk of a *pHSP70:hstac3wtegfp* injected *stac3*^{mi34} embryo showing expression of human Stac3-EGFP in myotomes in the embryo shown above. Bottom, histogram showing that mutant embryos expressing human Stac3-EGFP (gray, n=4) swim as effectively as mutant embryos expressing zebrafish Stac3-EGFP (black,n=32). Human *STAC3* cloned courtesy of Jeremy Linsley and Akhila Satish.

CHAPTER 3

ZEBRAFISH STAC3 MEDIATES THE TRAFFICKING OR STABILITY OF THE SKELETAL MUSCLE DIHYDROPYRIDINE RECEPTOR

Abstract

Excitation-contraction (EC) coupling is the process of converting electrical input to a chemical output in skeletal muscle necessary for contraction and movement. In skeletal muscle, the primary complexes involved in EC coupling are well known, but the mechanisms and proteins that regulate EC coupling are poorly understood. The novel adapter protein Stac3, associates with the triadic complex, and is critical for normal excitation induced calcium release (Chapter 2). However, the EC coupling proteins necessary for Stac3 localization are unknown. A second issue raised by the identification of stac3 is the mechanism by which the loss of Stac3 impairs calcium release. Here we show by using previously known zebrafish EC coupling mutants that the dihydropyridine receptor (DHPR) complex is required for normal localization of Stac3. In addition, the proper spatial interactions of DHPR and RYR do not appear necessary for Stac3 targeting. Furthermore, the previously identified congenital myopathy, Native American Myopathy (NAM), caused by a partial loss of function allele in Stac3 was employed to understand the mechanism of Stac3 function. We found that the homologous zebrafish NAM mutation expressed in Stac3 null zebrafish can rescue swimming behavior in a temperature sensitive fashion. Permissive temperatures allow $Stac3^{NAM}$ to localize in a pattern similar to the triadic localization in $stac3^{wt}$, while non-permissive temperatures result in predominately peri-nuclear localization. These

findings are consistent with the possibility that Stac3 mediates the trafficking or stability of the DHPR complex.

Introduction

Skeletal muscle is a specialized tissue for the generation of force responsible for movement. Electrical input into the muscle from the nervous system is converted into chemical signals, which initiate contraction in skeletal muscle by a process known as excitation-contraction (EC) coupling. The primary components of EC coupling are the dihydropyridine receptor (DHPR) and the ryanodine receptor (RYR). The DHPR is an L-type calcium channel, which serves as a voltage sensor that in turn directly activates the RYR. The RYR is the primary calcium release channel found in the membrane of the sarcoplasmic reticulum (SR), the calcium storage organelle of muscle (Bannister, 2007; Paolini et al., 2004b; Protasi et al., 2002; Tanabe et al., 1990; Tanabe et al., 1988). The entire set of components for EC coupling are localized in triads, specialized junctions between the transverse tubules (t-tubules, invaginations of the sarcolemma), with the SR membrane (Flucher et al., 1993b). Furthermore, specialized spatial formations of four DHPRs positioned over a single RYR, referred to as a tetrad, aggregate in organized arrays necessary for calcium release (Block et al., 1988; Protasi et al., 1998). Despite considerable understanding of the physiology and molecular anatomy of EC coupling, how the specialized structures form and how the molecular EC coupling complex is targeted is poorly understood.

One component known to be important for triadic localization of the DHPR complex is the β subunit of DHPRα. DHPR is comprised of a pore forming α1 subunit and β, α2δ1, and γ subunits (Catterall et al., 2005). Knockouts of the β subunit in both mice (Gregg et al., 1996) and zebrafish (Schredelseker et al., 2005; Zhou et al., 2008) demonstrate that this subunit is essential for functional DHPRs to be localized to triads. In addition, the β subunit is necessary to support the interactions between the DHPR and RYR required for tetrad formation (Schredelseker et al., 2005). The β subunit can regulate the DHPR complex by binding small G-proteins of the RGK family such as Rem and Rad (Finlin et al., 2003). Studies from heterologous systems illustrate that a RGK/β interaction can suppress L-type calcium channels by either immobilizing the voltage sensor or reducing the number of functional channels in the membrane (Bannister et al., 2008a; Yang et al., 2010), through dynamin mediated endocytosis (Yang et al., 2010). Interestingly, dimerization of the SH3 domain of the calcium channel β subunit can recruit dynamin (Miranda-Laferte et al., 2011).

Other trafficking mechanisms have been demonstrated using the cardiac DHPR β subunit. These studies show that β protects the channel pore subunit from the endoplasmic reticulum-associated protein degradation (ERAD) quality control system. DHPR β blocks a specific ubiquitination sequence within the DHPR and allows proper ER export and subsequent targeting (Altier et al., 2011). These studies collectively demonstrate a diverse range of modulatory pathways in which the DHPR can be trafficked and regulated. Further work elucidating novel pathways of regulation will

significantly assist in understanding an essential and complex process critical to muscle biology.

A null mutant of the adapter-like protein Stac3 was identified in zebrafish and referred to as *stac3*^{mi34} (Chapter 2) . Stac3 is unique to skeletal muscle, associates with the EC complex, and appears to predominately affect triadic localization of the DHPR complex (Chapter 2). Indeed, EC coupling is significantly impaired by the absence of Stac3 in muscle. In addition, a missense mutation of STAC3 in humans is the basis of a congenital disease known as Native American Myopathy (NAM) (Chapter 2). NAM results in muscle weakness, cleft palate, ptosis, and susceptibility to malignant hyperthermia (MH) (Stamm et al., 2008a).

Despite the identification of Stac3 as a key component of the EC complex, numerous questions remain about its function and the mechanisms by which it influences EC coupling. Here we use the *stac3*^{mi34} line, along with other EC coupling protein mutants to investigate which complexes or interactions are critical for the normal localization of Stac3. In addition, we demonstrate that zebrafish Stac3^{NAM}, the homologous mutation to NAM, rescues behavior and Stac3 localization in a temperature sensitive manner. Considering previously published reports of temperature sensitive rescue of ion channel function being related to protein trafficking or protein stability (Maljevic et al., 2011; Rusconi et al., 2007; Sharkey et al., 2009), we have begun exploring whether the mechanism of Stac3 is to regulate trafficking of DHPR.

Materials and Methods

Animals, Behavioral Analysis and Statistical Analysis

Zebrafish were bred and maintained according to approved guidelines of the University Committee on Use and Care of Animals at the University of Michigan. The *stac3*^{mi34} mutation was isolated from a mutagenesis screen using procedures previously reported (Driever et al., 1996; Haffter et al., 1996). Embryonic behaviors were video-recorded using a Point Grey Firefly MV USB camera mounted on a stereomicroscope and analyzed with ImageJ.

Immunolabeling

Wholemounted embryos were immunolabeled as described previously (Hirata et al., 2005). For labeling dissociated skeletal muscle fibers, 48 hpf embryos were incubated in collagenase type II (3.125 mg/ml in CO_2-independent medium (Gibco)) at 20°C for 1.5 h with the muscle fibers triturated every 30 min. Fibers were spun at 380*g* in a benchtop centrifuge for 5 min, supernatant removed and fibers resuspended in CO_2-independent medium and allowed to settle on polyornithine coated coverslips. Fibers were washed in CO_2-independent medium then fixed. Dissociated muscles were labeled using 0.25% Triton X100 detergent in the incubation solutions containing the following primary antibodies/toxin: 1/200 dilution of anti-RyR (34C IgG1, Sigma); 1/200 anti-DHPRα1 (1A IgG1, Affinity BioReagents); 1/1000 anti-mCherry (IgG1, Clontech); 1/500 anti-calnexin (IgG1, Sigma). Secondary antibodies were anti-mouse Alexa 488/568 and anti-rabbit Alexa 488/568 (Invitrogen). All immunolabeled embryos or fibers were imaged by confocal microscopy.

Quantification of Fluorescence

For all immuno-fluorescence quantification of Stac3, labeling between sibs and mutants was performed side by side to maintain conditions per experiment. All confocal setting were identical between sibs and mutants during imaging per experiment. To obtain a fluorescent measure a rectangular region of interest encompassing part of a band of labeling (band consistent with triadic localization) of muscle labeling was selected, roughly 3-4 micron square. In a single muscle fiber, 5 different fluorescent measures were taken at evenly spaced distances along a single fiber. All 5 measures were averaged to represent a single fiber fluorescent signal. Similar measures were taken over several embryos between sibs and mutants. Since bands could not be observed in ryr mutants, measurements were taken as closely to the location of a putative band location as possible. Fluorescence was standardized to sibs for comparison with mutants.

Fluorescence Banding Pattern Index

A three part qualitative banding index was applied to the whole mount labeling of zStac3 from *red* and *ryr* mutants. First, images were converted to black and white using ImageJ under consistent thresholds for either experimental group. This established consistent images for comparison with the elimination of background. Next, one somite within a whole embryo was divided into quarters to further sample variability in banding over a single embryo. From each quarter somite a value was given based on strength of the banding pattern (1-3) indicating: 1) No apparent organized banding, all signal random, 2) Some indication of banding on fibers. Banding not always continuous across

fibers, 3) Strong banding observed with clear areas of signal and no signal obvious across the entire length of fibers.

Expression of β2a

Rat CACNB2a was a kind gift from the Grabner lab. For expression in *mi90 red* embryos the CACNB2a was subcloned in *pHSP70:mCherry* in frame with the mCherry. Induction of expression was performed as previously described (Chapter 2). In brief, injected embryos were raised to 48 hpf, when phenotypic *mi90* mutants were separated and heat shocked for 1 hour at 37^0C. Embryos were given 24 hours to allow protein production before being fixed for labeling. Labeling was performed for anti-mCherry and anti-zStac3 as described in immunolabeling methods. Whole embryos were imaged and muscle fibers showing mCherry signal were selected.

Generation and Expression of Stac3^{NAM}

Expression of *stac3^{NAM}* was performed by subcloning zebrafish *stac3* into *pSKM-EGFP*. Zebrafish *stac3^{NAM}* was generated by site-directed mutagenesis (SDM) converting W254 into S. Forward mutagenic primer 5` CTAATGAGGAGTCCTGGAGGGGCAAGATTG 3` and reverse mutagenic primer 5` CAATCTTGCCCCTCCAGGACTCCTCATTAG 3` . A standard Stratagene Quick-change PCR SDM protocol was used to introduce the missense mutation. Successful SDM reactions were confirmed by DNA sequencing. Constructs (10 ng/µl) were injected into one cell stage embryos of a cross between *stac3^{mi34}* heterologous carriers with a Nanoject II (Drummond Scientific Company). Embryos were raised at 28.5^0C. At 48 hpf *stac3^{mi34}* mutant embryos were behaviorally identified by

absence of swimming behavior. Embryos with approximately 10% or more skeletal muscle fibers expressing EGFP were used for behavioral assays.

Temperature Assay of Stac3^{NAM} expressing embryos

Heterozygous in-crosses of *mi34* carriers were injected with *pHSP70:zstac3^{NAM}-EGFP*. Induction of construct expression was carried out as previously described. In brief, injected embryos were raised at 28.5^{0}C till 48 hpf and mutants were separated based on lack of swimming. Mutants were induced for 1 hour at 37^{0}C and then returned to 28.5^{0}C for 3 hours. After 3 hours at 28.5^{0}C embryos with 10% or more mosaic EGFP in muscle were assayed for touch response. Construct expressing mutants were then placed at 20^{0}C overnight for approximately 18 hours and touch response was assayed again. In addition, the construct *pSKM: zstac3^{NAM}-EGFP* was generated. Carrier in-crosses were injected as previously described and raised to 48hpf at 28.5^{0}C. At this time point wildtype siblings and *mi34* mutants were separated based on the presence or absence of a swimming response, respectively. Each set of embryos was then subjected to various temperatures. At 48 hpf (time point t0), embryos expressing Stac3^{NAM}-EGFP were assayed after being raised at 28.5^{0}C. All numbers collected are from embryos that were exposed to each temperature time point in succession. Swimming distance was recorded in response to a tactile stimulation provided by forceps. Expressing embryos were then placed at 20^{0}C for 18 hours (time point t18) and swimming distance assayed as before. All embryos were then returned to 28.5^{0}C for 2 hours (time point t20) before again recording swimming distance. During recording of swimming behavior, any given embryo was not outside of stated target temperature for more then 6 minutes.

Temperature Dependent Localization of Stac3^{NAM}

In-crosses of *mi34* carriers were performed and embryos were injected with the construct *pHSP70:stac3^{NAM}-mCherry* as previously described (Chapter 2). Embryos were raised at 28.5^{0}C till 48hpf and phenotypic *mi34* mutants separated. Expression of the constructed was induced with a 1 hour heat shock at 37^{0}C. After heat shock embryos were separated into two populations. One group was raised at 28.5^{0}C and the other at 20^{0}C. At approximately 24 hour post heat shock (embryos approximately 66-72 hpf) whole embryos were immunolabeled with anti-mCherry as previously described. For calnexin labeling, used as comparative marker for Stac3^{NAM}, dissociated myofibers were used.

Results

Stac3 requires the EC complex for normal localization

The proteins required to localize Stac3 are unknown. To explore this question we used the *relatively relaxed (ryr)* zebrafish mutant, which lacks RYR1b, the isoform found specifically in fast twitch fibers (Hirata et al., 2007). The work of Hirata et al demonstrated that in fast twitch fibers the lack of RYR1b resulted in a loss of many other components of the EC coupling complex including DHPR and all associated subunits, yet without disrupting the formation of the triad. Representative images of zStac3 labeling showed a banded pattern in a sibling and a random punctate pattern in mutants (Figure 3.1A). A similar observation is seen when the same representative images are converted to black and white and background reduced (Figure 3.1B).

Quantification of the fluorescent signal in sibs and *ryr* shows a significant decrease of the signal intensity in *ryr* (Figure 3.1C). Furthermore, the banded pattern observed in siblings is reduced to a random punctate pattern in mutants (Figure 3.1D).

RYR is not sufficient for Normal localization of Stac3

To determine the critical proteins necessary for Stac3 association and targeting, we employed another previously described EC coupling zebrafish mutant. The *mi90* allele of the *relaxed (red)* zebrafish mutant is a null of the L-type calcium channel subunit β1a, and results in a total loss of the DHPR α1S from skeletal muscle in both fast and slow twitch fibers (Zhou et al., 2006). Despite the absence of the DHPR complex in *red* mutants, immunolabeling shows banded RYR labeling similar to wildtypes (Figure 3.2A). In addition, inducing calcium release with the RYR agonist caffeine, results in levels of contraction similar to wildtype siblings (Figure 3.2B). These results suggest that in *red* muscles there are grossly normal levels of functional RYR localized in the SR membrane.

Representative images showing zStac3 labeling in a banded pattern in siblings embryos while weaker and more disorganized labeling is observed in *red* mutants (Figure 3.3A). Similar patterns are observed when the same images are converted to black and white with a background reduction (Figure 3.3B). Quantification of the fluorescent signal shows that overall fluorescence intensity is significantly reduced in *red* mutants (Figure 3.3C). Analysis of the degree of patterning in *red* mutants shows a significant reduction from siblings (Figure 3.3D). However, a banding index value approaching two shows a degree of discernible pattern within some somatic sections.

The DHPR complex is capable of localizing Stac3

Previous work from the Grabner lab has shown that targeting the DHPRα to the triad is an intrinsic property of all L-type calcium channel β subunits, including the cardiac and neurally expressed β2a subunit. This study also demonstrated that only the skeletal muscle specific β1a was capable of supporting the necessary interactions between the DHPR and RYR to allow physical coupling, as observed by the presence of tetrads (Schredelseker et al., 2009). Therefore, we induced expression of β2a fused to mCherry in *red* embryos and assayed for localization of Stac3. With expression of β2a it is expected that the DHPR and RYR would be localized to triads yet without being coupled. Membrane and striated banded β2a-mCherry labeling was observed in *red* mutant muscle (Figure 3.4 top panel). In these muscle fibers banded labeling of endogenous Stac3 was observed (Figure 3.4, middle panel) co-localizing with the banded β2a-mCherry fluorescence (Figure 3.4, bottom panel).

Stac3^{NAM} Rescues Swimming and Localization in a Temperature Sensitive Manner

Studies show that some loss of function mutations in ion channels could be rescued in a temperature sensitive manner (Maljevic et al., 2011; Rusconi et al., 2007; Sharkey et al., 2009). Stac3^{NAM} differs from wildtype by only a single amino acid, and so might be temperature sensitive. In contrast, the *stac3^{mi34}* mutant is a null, lacking most of the protein, so its function was not expected to be temperature sensitive. Induced expression of zebrafish Stac3^{NAM} , using the *pHSP70:zstac3^{NAM}-EGFP* construct, in the skeletal muscle of *stac3^{mi34}* does not result in a swimming rescue compared to un-injected mutants at physiological temperature (28.5^{0}C) at observed time points up to 72

hpf, or 24 hours post heat shock (hphs) (Chapter 2). We therefore decided to test the effect of a lower temperature. As previously described (Chapter 2), *mi34* mutants raised at 28.5^{0}C were induced to express Stac3^{NAM} at 48 hpf (time point T0), and showed minimal touch response. After assaying behavior, embryos were placed at 20^{0}C overnight (time point T2) before assaying touch response again. Stac3^{NAM} expressing mutants raised overnight at 20^{0}C showed a significant increase of touch response. Finally, embryos were returned to 28.5^{0}C for 2 hours (time point T3) and minimal touch response was recorded (Figure 3.5).

Since temperature influenced the behavior of Stac3^{NAM} expressing *mi34* mutants, we wanted to negate the potential influence of a temperature sensitive promoter. Therefore, we used the α-actin promoter to generate the construct *pSKM:zstac3^{NAM}-EGFP* to drive expression specifically in skeletal muscle. The *pSKM:zstac3^{NAM}-EGFP* construct was injected into *mi34* carrier in-crosses and the embryos were raised to 48 hpf at physiological temperatures (28.5^{0}C). Phenotypic *mi34* mutants were identified and screened for EGFP fluorescence in skeletal muscle to indicate mosaic expression of Stac3^{NAM} (Figure 3.6A). The swimming response to tactile stimulation of Stac3^{NAM} expressing embryos was then observed at 48 hpf (referred to as time point zero (t0)) (Figure 3.6B, left panel). Stac3^{NAM} expressing embryos were then placed at 20^{0}C for 18 hours (approximately 66 hpf (time point t18)), and the tactile response was again examined (Figure 3.6B, middle panel). Finally, embryos were returned to 28.5^{0}C for 2 hours (time point t20 or approximately 68 hpf) and response to tactile stimulation assayed (Figure 3.6B, right panel). Quantification of 23 *mi34* mutant embryos

expressing Stac3^{NAM} shows significant restoration of swimming in response to touch at the tested permissive temperature (20^{0}C), which was reversed with non-permissive temperatures (Figure 3.6C). Likewise, the influence of temperature was observed in wildtype sibling embryos injected with *pSKM:zstac3^{NAM}-EGFP* to rule out a potential dominant-negative influence. At 48 hpf wildtype siblings were identified with mosaic expression of Stac3^{NAM}-EGFP in skeletal muscle (Figure 3.7A). Embryos were exposed to the same temperature paradigm as the previously described *mi34* mutants (above). At each time point the swimming behavior was observed in response to touch (Figure 3.7B). Quantification of the touch response of wildtype siblings expressing Stac3^{NAM} showed no significant changes based on varying temperature (Figure 3.7C).

To further identify the impact of temperature on Stac3^{NAM}, we looked at the localization of induced Stac3^{NAM} in the *mi34* background at permissive or non-permissive temperatures. Physiological temperatures (28.5^{0}C), yielded little to no banded localization of Stac3^{NAM} in muscle; however, the signal for Stac3^{NAM} appeared centrally in muscle fibers around the area surrounding the nuclei (Figure 3.8A). Conversely, Stac3^{NAM} expressing mutant embryos raised at the permissive temperature (20^{0}C) pre-dominantly showed Stac3^{NAM} localization in banded patterns (Figure 3.8B). To understand the subcellular localization of Stac3^{NAM} at physiological (non-permissive) temperatures we compared labeling with a known ER marker, calnexin. This specific marker was selected due to the peri-nuclear localization of Stac3^{NAM} at non-permissive temperatures. Labeling of zebrafish skeletal muscle with calnexin shows signal centrally located in a muscle fiber around the nuclei (Figure 3.8C).

Discussion

The EC complex includes the DHPR and RYR localized to triads and are visible as a banded pattern in muscle fibers. Previously, we demonstrated Stac3 co-localizes with DHPR and RYR as well as binds to the DHPR/RYR molecular complex. These data show that Stac3 is part of the EC coupling molecular complex localized to triads.

From this current study, we found that removal of the DHPR complex, in *red* mutants, significantly reduced the normal banded localization of Stac3 despite normal triadic RYR. Furthermore, our evidence suggests that triadic DHPR uncoupled from triadic RYR is capable of localizing Stac3 in a pattern consistent with wildtype skeletal muscle. Together these experiments imply that the DHPR complex or an associated protein(s) have a significant impact on the localization of Stac3, whereas, RYR appears to have a minimal influence on the localization of Stac3. However, the complex interaction of DHPR and RYR could have unforeseen consequences in the localization or function of Stac3. In addition, our current results do not directly demonstrate Stac3 interacts with a protein within the DHPR complex.

Here we have made the novel discovery that zebrafish Stac3^{NAM} can rescue the touch induced swimming behavior of *mi34* in a temperature sensitive manner. In order to show that Stac^{NAM} was not acting as a dominant negative at any of the tested temperatures, we investigated the impact of Stac3^{NAM} on wildtype siblings. At no point did expression of Stac3^{NAM} in wildtype siblings impair touch induced swimming. This suggests that permissive temperatures were permitting Stac3^{NAM} to rescue *mi34* mutant behavior. Furthermore, the localization of the Stac3^{NAM} protein is influenced by

temperature. Comparison of calnexin labeling and Stac3^{NAM} at non-permissive temperatures suggests localization consistent with the ER. If Stac3^{NAM} is localizing with the ER, the lack of any known ER retention signals within the Stac3 sequence would suggest localization to the cytoplasmic side of the ER membrane. However, further experiments are required to confirm this hypothesis. Interestingly, Stac3^{NAM} expressing muscle fibers from embryos raised at permissive temperatures show localization consistent with wildtype Stac3. These results would suggest that permissive temperatures allow Stac3^{NAM} to achieve the conformation or functional interaction necessary to target to its normal endogenous location. It will be interesting to determine if normal levels of triadic DHPR are also rescued at permissive temperatures. Considering that we achieve a behavioral rescue, and that Stac3 requires the DHPR complex for targeting, we would expect a DHPR complex rescue.

The fact that temperature rescues behavior and Stac3^{NAM} localization suggests several possible mechanisms of regulating EC coupling. One model is that Stac3 is necessary for DHPR trafficking from the ER to the area of the triad. Similar mechanisms are known from other studies showing that the DHPR β subunit in cardiac tissue protects the DHPR from the ERAD system and thus allow normal channel targeting (Altier et al., 2011). Whether the β1a serves this role in skeletal muscle is not known, or if Stac3 could be a co-regulator of this mechanism. A second model is that once Stac3 is at the vicinity of the triad it increases the stability of the DHPR and reduces endocytotic removal. Known mechanisms exist involving dynamin mediated endocytosis of L-type calcium channels directed by interactions of the β subunit with small G-proteins of the

RGK family (Yang et al., 2010). Stac3 could potentially be involved with a β/RGK mechanism or a separate mechanism independently regulating turnover. Future experiments using live time-lapse imaging of the DHPR in Stac3^{NAM} expressing skeletal muscle may elucidate details of the Stac3 mechanism. The change in DHPR localization or intensity at triads at permissive or non-permissive temperatures could demonstrate how the activity of Stac3 affects the DHPR. Similar experiments with RYR1 would determine if Stac3 influences RYR by any similar mechanisms. However, future studies will also need to include a more detailed timeline of temperature dependent rescue in order to fully explore the impact of temperature on Stac3^{NAM} activity. Continuing work exploring the precise mechanism for the action of Stac3 in skeletal muscle may reveal a novel interaction regulating EC coupling or calcium channels.

Figure 3.1

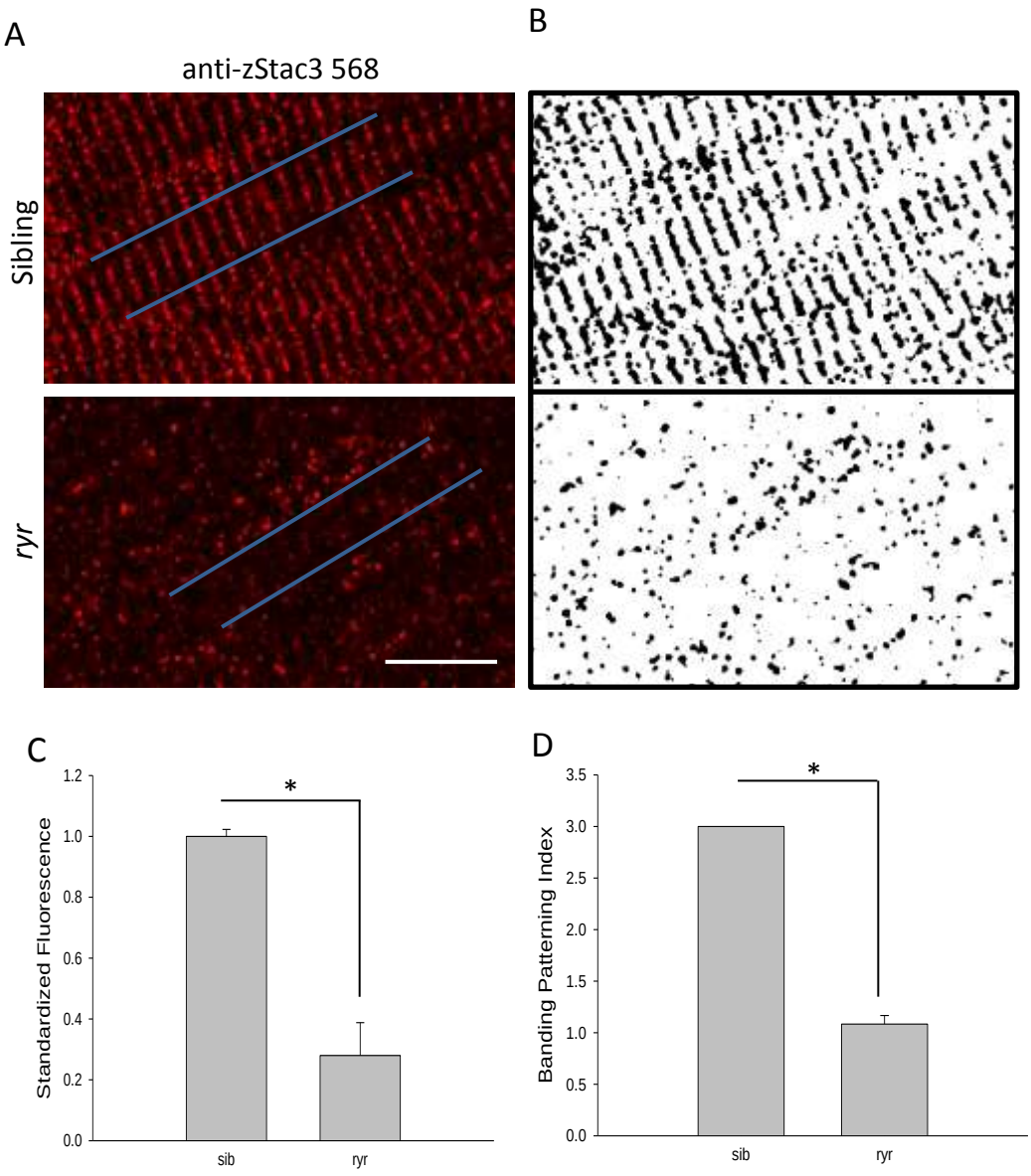
A
B
anti-zStac3 568
Sibling
ryr
C
D
Standardized Fluorescence
1.2
1.0
0.8
0.6
0.4
0.2
0.0
*
sib
ryr
Banding Patterning Index
3.5
3.0
2.5
2.0
1.5
1.0
0.5
0.0
*
sib
ryr

Figure 3.1: Stac3 requires the EC complex to localize in skeletal muscle. A) Representative images of whole mount zStac3 labeling in sib (top) or *ryr* (bottom) fast twitch skeletal muscle. Blue bars partially delineate a single muscle fiber. B) Black and white converted images of (A) to standardize and reduce background. C) Quantification of fluorescence intensity along bands of signal in either sibs (n=2) or *ryr* (n=3). In *ryr* closest approximation to where band should be present was used. D) Banding pattern index as sampled from black and white images. The same group of labeled embryos quantified in (C) was used for patterning measure. In *ryr* index is approximately one showing no discernible pattern of zStac3. * denotes $p<0.01$. Labeling performed on whole mounted embryos at 48 hpf. Scale bar 10um.

Figure 3.2

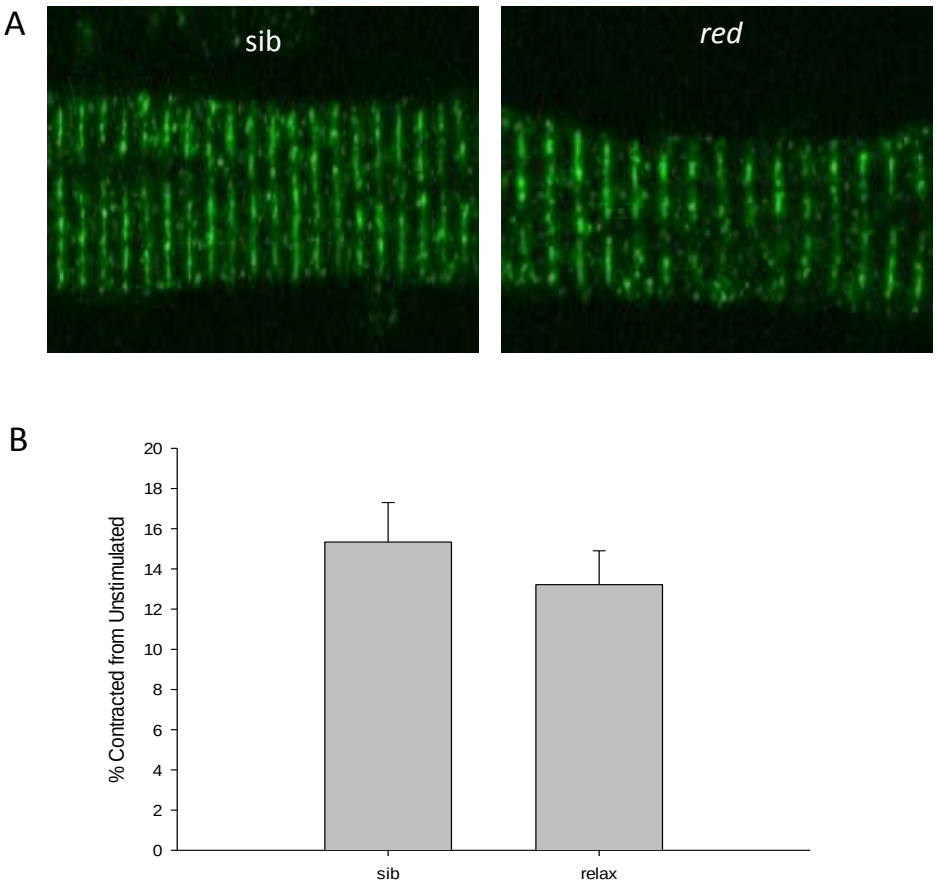

Figure 3.2: RYR is localized and caffeine responsive in *red* mutants. A) Dissociated myofiber labeling with anti-RYR antibody and secondary antibody Alexa-488. In both sib (left panel) and *red* mutants (right panel) banded labeling is observed. B) Quantification of the percent somite displacement from rest (unstimulated) after exposure to 5mM caffeine. Percent contraction from unstimulated is not significantly different between sibs and *red* mutants.

Figure 3.3

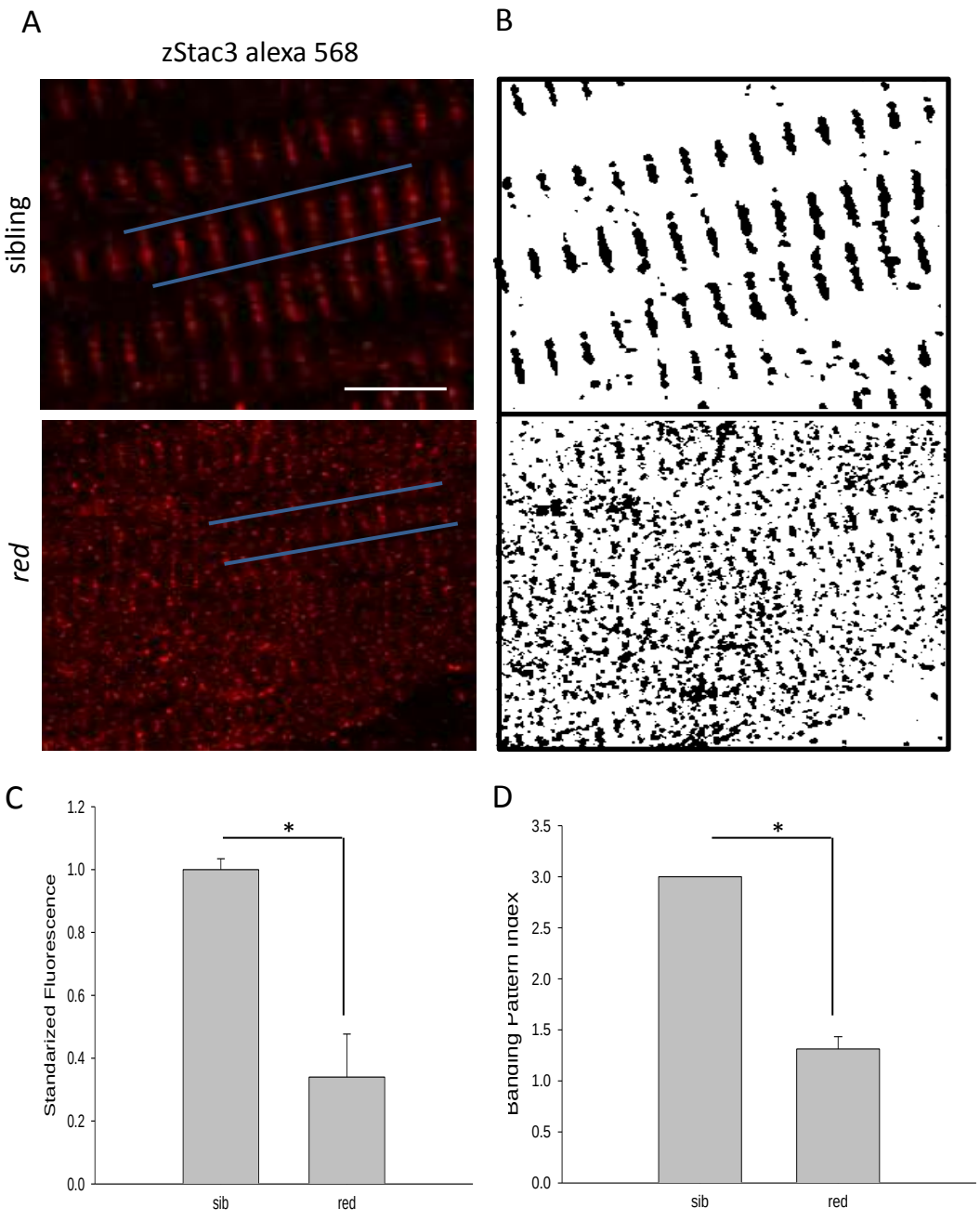
A
zStac3 alexa 568
sibling
red
B
C
Standarized Fluorescence
1.2
1.0
0.8
0.6
0.4
0.2
0.0
*
sib
red
D
Banding Pattern Index
3.5
3.0
2.5
2.0
1.5
1.0
0.5
0.0
*
sib
red

Figure 3.3: RYR is not sufficient for normal Stac3 localization. A) Representative images of whole mount zStac3 labeling in sib (top) or *red* (bottom) fast twitch skeletal muscle. Blue bars partially delineate a single muscle fiber. B) Black and white converted images of (A) to standardize and reduce background. C) Quantification of fluorescence intensity along bands of signal in either sibs (n=3) or *red* (n=4). D) Banding pattern index as sampled from black and white images. The same group of labeled embryos quantified in (C) was used for patterning measure. In *red* index is approximately 1.5 showing some discernible pattern of zStac3. * denotes $p<0.01$. Labeling performed on whole mounted embryos at 48 hpf. Scale bar 10um

Figure 3.4

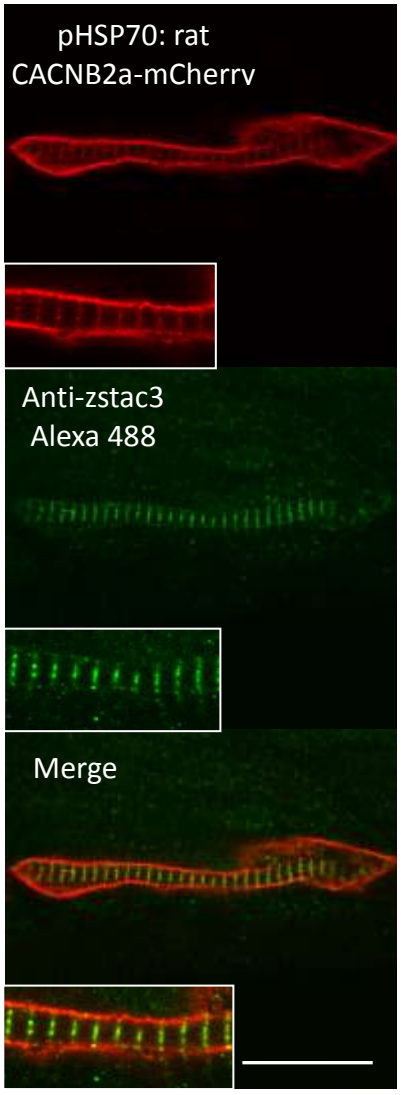

Figure 3.4: Non-endogenous calcium channel β subunits can restore Stac3 localization in *red* mutants. Top panel is a *red* muscle cell expressing rat CACNB2a-mCherry labeled with anti-mCherry with Alexa 568 secondary antibody in a banded pattern along a single muscle fiber. Middle panel shows the same fiber labeled with the anti-Stac3 antibody and secondary Alexa 488. The bottom panel is the merged image showing the banded pattern in the top and middle panel co-localize. Notice the surrounding muscle tissue shows no CACNB2a or Stac3 positive signal. Insets in all panels show higher magnification image. All labeling is a whole mount embryo at 48 hpf. Scale bar 30 um. The rat *CACNB2a* construct was a kind gift from the Grabner lab.

Figure 3.5

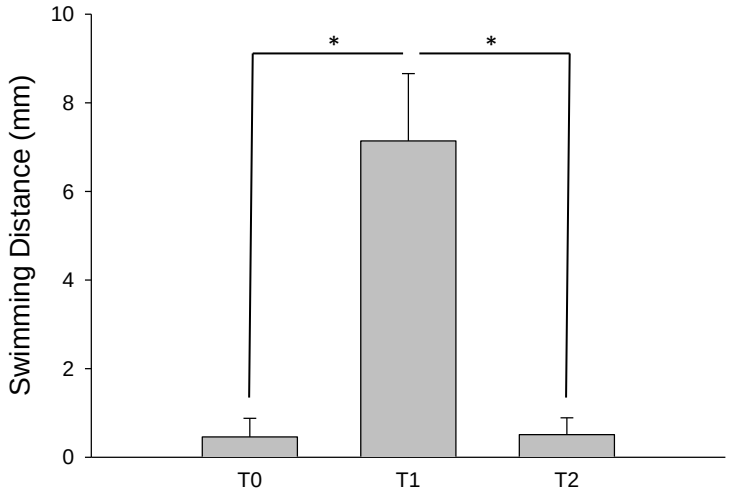

Figure 3.5: Quantification of the touch response of *mi34* mutants with induced expression of Stac3^{NAM} at varying temperatures. T0 represents the time point at 48 hpf with embryos raised at 28.5^{0}C. T1 is the time point when embryos were moved to 20^{0}C overnight. T2 is the time point after embryos were returned to 28.5^{0}C for 2 hours. n=8. * denotes $p<0.01$.

Figure 3.6

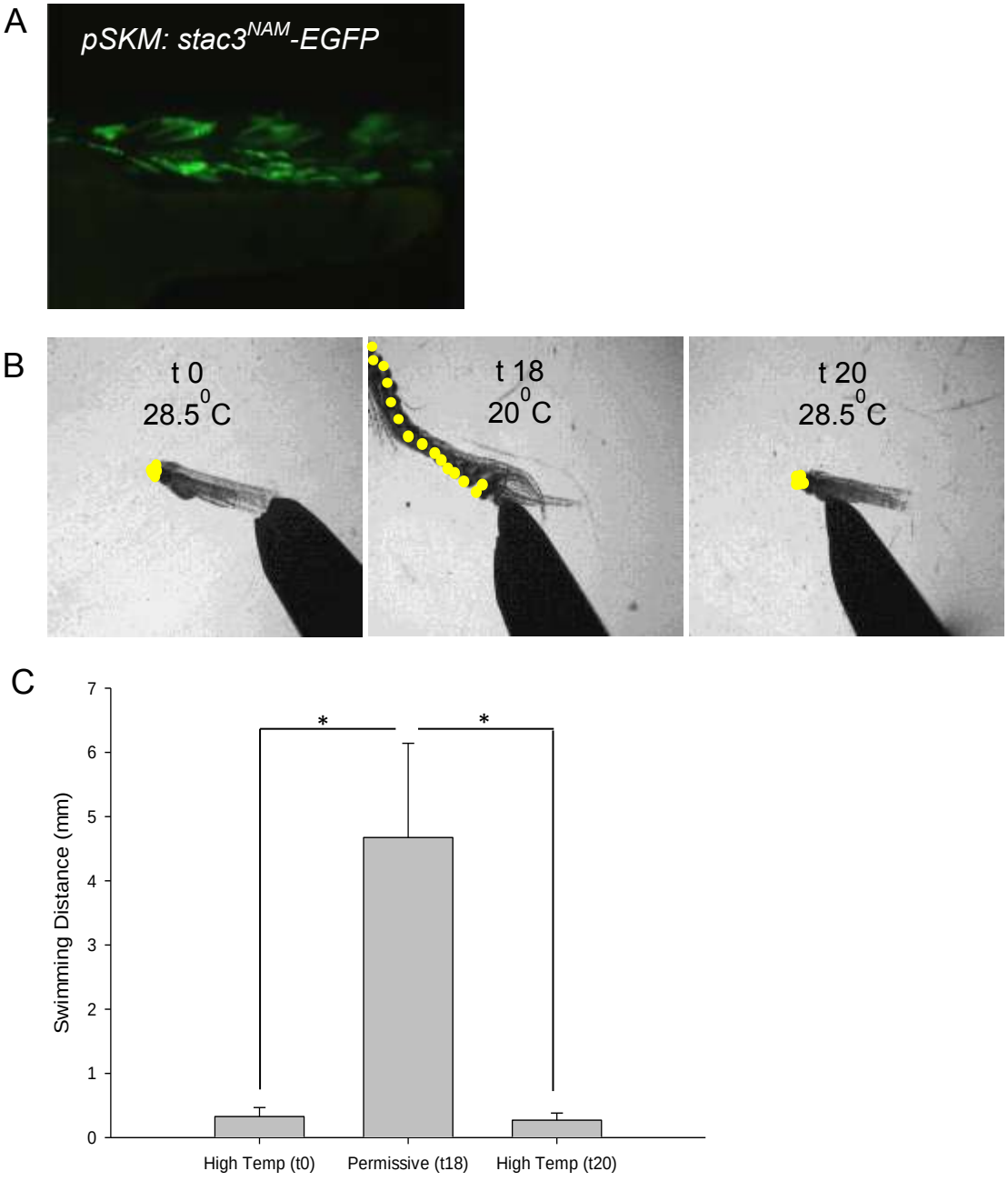
A
pSKM: stac3NAM-EGFP
B
t 0
28.5 0C
t 18
20 0C
t 20
28.5 0C
C
Swimming Distance (mm)
0
1
2
3
4
5
6
7
*
*
High Temp (t0)
Permissive (t18)
High Temp (t20)

Figure 3.6: Response of *mi34* mutants expressing Stac3^{NAM} in response to tactile stimulation after exposure to different temperatures. A) Representative live fluorescent image of *mi34* mutant embryo expressing Stac3^{NAM}-EGFP at 48 hpf. B) Representative of tactile responses. Each panel shows 30 stacked frames sampled at 30 Hz beginning at the moment of tactile stimulation applied by forceps (black wedge). Each panel shows the same embryo at different time points. Embryo displayed in A) is same embryo shown in (B). The presence or absence of swimming is indicated by the displacement of the embryo marked by yellow dots placed at the head of the embryo in each frame. Left panel shows Stac3^{NAM} expressing *mi34* mutant at 48 hpf (time point t0) raised at 28.5^{0}C when tactile responses were first recorded. Immediately after tactile assay the embryos was placed at 20^{0}C for 18 hours (time point t18, ~66 hpf) and tactile response was recorded again. Immediately after the second assay the embryos were transferred back to 28.5^{0}C for 2 hours (time point t20, embryos ~68 hpf) before touch response was retested. C) Quantification of tactile response at all 3 time points with a n=23 for Stac3^{NAM} expressing *mi34* mutants. * denotes $p<0.01$.

Figure 3.7

A

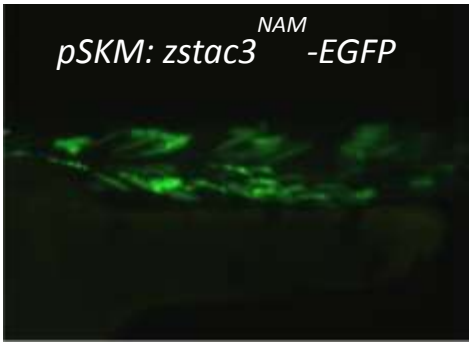

B

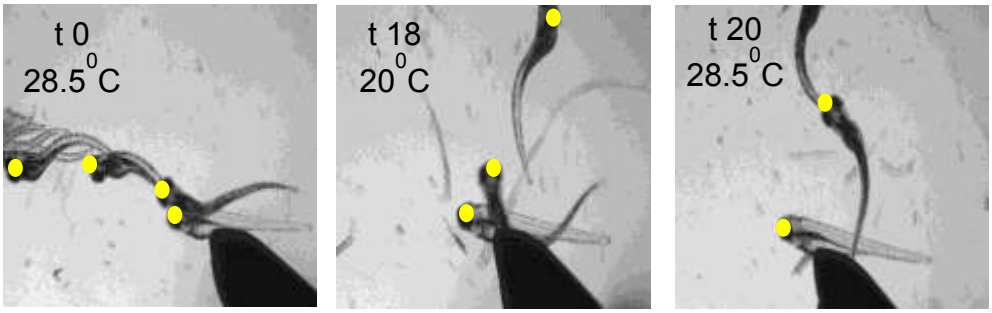

C

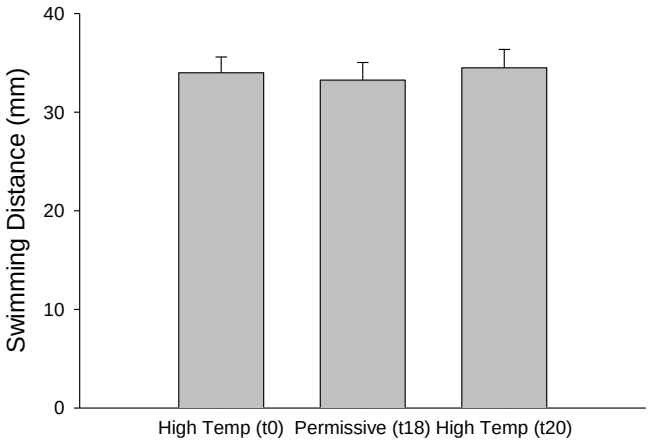

Figure 3.7: Response of wildtype siblings expressing Stac3^{NAM} in response to tactile stimulation after exposure to different temperatures. A) Representative live fluorescent image of wildtype embryos expressing Stac3^{NAM}-EGFP at 48 hpf. B) Representative of tactile responses. Each panel shows 30 stacked frames sampled at 30 Hz beginning at the moment of tactile stimulation applied by forceps (black wedge). Each panel shows the same embryo at different time points. Embryo displayed in A) is same embryo shown in (B). The presence of swimming is indicated by the displacement of the embryo marked by yellow dots placed at the head of the embryo in each frame. Left panel shows Stac3^{NAM} expressing wildtype sibling at 48 hpf (time point t0) raised at 28.5^{0}C when tactile responses were first recorded. Immediately after tactile assay the embryos was placed at 20^{0}C for 18 hours (time point t18, ~66 hpf) and tactile response was recorded again. Immediately after the second assay the embryos were transferred back to 28.5^{0}C for 2 hours (time point t20, embryos ~68 hpf) before touch response was retested. C) Quantification of tactile response at all 3 time points with a n=10 for Stac3^{NAM} expressing wildtype siblings.

Figure 3.8

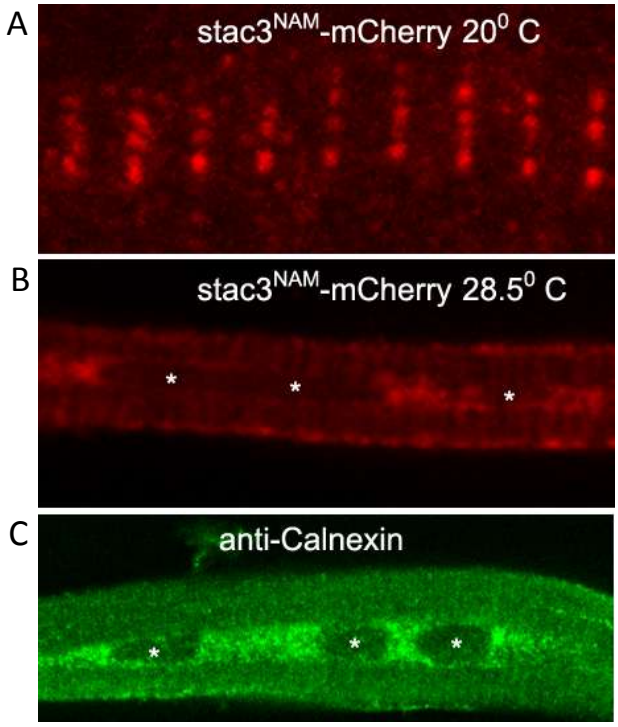

Figure 3.8: Permissive temperatures allow Stac3^{NAM} to localize in a pattern consistent with wildtype Stac3. Expression of Stac3^{NAM} was induced at 48hpf in injected *mi34* mutants identified by phenotype. After induction, injected *mi34* embryos were divided into two groups raised at either 20^{0}C or 28.5^{0}C. Induced embryos were labeled at 72 hpf (24 hours post heat shock). A) Whole mount labeling of Stac3^{NAM}-mCherry from injected mutants raised at 20^{0}C. Labeling shows a banded pattern. B) Localization of Stac3^{NAM} from an embryo raised at 28.5^{0}C. No banded labeling observed. At 28.5^{0}C labeling of Stac3^{NAM} is located centrally in the muscle fiber proximal to the nuclei labeled with asterisks. Fish shown from (A) and (B) are all from the same clutch and injection. In C), labeling is from a different clutch of embryos than in (A) and (B), and shows anti-Calnexin, an ER marker showing centrally located labeling around the nuclei. Asterisks denote muscle nuclei.

CHAPTER 4

ZEBRAFISH STAC1 IS EMBRYONICALLY EXPRESSED IN A VENTRAL SET OF SPINAL CORD NEURONS

Abstract

The STAC protein family is comprised of three genes in mammals. Each STAC protein is an adapter-like protein containing a cysteine rich C1 domain and two SH3 domains. In zebrafish, the Stac3 protein is specific to skeletal muscle and critical for normal function and behavior. In mammals, the STAC1 ortholog of STAC3 shows neural expression, yet no functional data are available. Here we identify and clone the zebrafish *stac1* gene. In addition, we demonstrate that *stac1* is expressed in a small set of ventrally located neurons in the embryonic zebrafish spinal cord. This information will assist in developing functional studies exploring this novel member of the STAC family.

Introduction

The identification and characterization of novel genes is an important and ongoing part of piecing together biologic mechanisms. The STAC family of proteins is poorly understood with minimal functional analysis. Recent investigation has shown that Stac3 is a key regulator of excitation-contraction coupling in skeletal muscle, and the underlying genetic cause of a congenital human myopathy. Unlike *STAC3*, the *STAC1* gene is expressed in neural tissue (Suzuki et al., 1996). In the dorsal root ganglion (DRG), *STAC1* and *STAC2* are expressed in distinct subsets of neurons (Legha et al.,

2010). However, the function of the neuronally expressed STACs is unknown. We cloned and analyzed *stac1* in zebrafish to gain functional understanding of STAC1. Zebrafish provide a good model as they are clear and easily to manipulate (Detrich et al., 1999), and the developing nervous system of zebrafish is well characterized (Bernhardt et al., 1990; Bernhardt et al., 1992; Kuwada et al., 1990).

Material and Methods

Animals

Zebrafish were bred and maintained according to approved guidelines of the University Committee on Use and Care of Animals at the University of Michigan.

Molecular Biology

cDNA was synthesized from TRIzol (Invitrogen) extracted RNA from adult zebrafish brains. PCR amplification was performed using Vent Polymerase and gene specific primers: forward 5' ATGATTCCGCCAGCAAACATGATTCA 3' and reverse 5' TCATATATTCTCCAGGACGTCACAGGGCACATA 3'. Primers were designed to the immediate 5` and 3` regions of the predicted zebrafish stac1 cDNA (XM_001344434). PCR produced a single band which was A-tailed using Taq Polymerase and subcloned into pGEM-T Easy vector (both Promega). Multiple clones were isolated and sequenced.

In-situ

In-situ procedure was performed as previously described (Li et al., 2004). In brief, embryos at 24 hpf were fixed and washed in 1X PBS containing 0.1% Tween20 (Sigma). Anti-sense digoxigenin (DIG) riboprobes were synthesized from linear plasmid DNA of

the entire stac1 cDNA. Probe integrity was assayed by gel electrophoresis prior to use. Full length anti-sense riboprobe was used. Detection of probe was performed using anti-DIG antibody conjugated to alkaline phosphatase. Chromagenic detection used NBT/BCIP solutions. Color reactions were ran till clear signal was detected before stopping the reaction. All probe synthesis and detection reagents from Roche.

Results

Identification and Cloning of Zebrafish *stac1* from Adult Brain

In order to identify the zebrafish ortholog of mammalian *STAC1* we prepared cDNA from adult zebrafish brains. Adult brains were selected since the Allen Brain Atlas (http://mouse.brain-map.org/) and initial publications of *STAC1* showed expression in adult mammalian brain tissue (Suzuki et al., 1996). Cloning and sequencing of the zebrafish stac1 was necessary in order to confirm the predicted cDNA (XM_001344434) and ensure no dramatic sequence differences prior to further study. PCR of adult zebrafish brain cDNA produced a single band of the correct predicted size of 1.1kb. The band was subcloned and sequenced. The isolated clone showed high sequence homology to known mammalian Stac1 sequences. In addition, the sequence confirmed the presence of a C1 domain and two SH3 domains (Figure 4.1) consistent with other STAC proteins, including the previously cloned and described Stac3 in zebrafish (Chapter 2 and 3).

stac1 is expressed in a Set of Ventral Neurons in the Spinal Cord of Embryonic Zebrafish

Anti-sense riboprobes were used to determine the location of *stac1* expression in whole mounted, 24 hpf zebrafish embryos. *stac1* RNA was detected in a small set of neurons located in the ventral spinal cord in close proximity to the floor plate (Figure 4.2). Approximately 2-4 neurons per somatic segment possessed signal for *stac1* expression. Visual examination of the brain and skeletal muscle showed no discernible signal to indicate stac1 expression.

Discussion

Here we have demonstrated that zebrafish possess a highly homologous protein to the mammalian STAC1, that is expressed early in zebrafish development. However, regions of no conservation of the zebrafish Stac1 sequence compared to the mammalians sequences are present. Potentially, these regions of no conservation could be retained intronic sequence. Our comparison of the zebrafish stac1 cDNA with exon-intron boundaries of the fish and mammalian sequence though did not support this hypothesis. This suggests the regions of variation between fish and mammalian sequences are real, yet further study is required to understand the importance of these differences. In any case, the numerous advantages of the zebrafish model may be beneficial to exploring the functional role of Stac1.

In-situ analysis showed that a subset of cells express *stac1*. The location within the ventral spinal cord near the floorplate suggests that *stac1* positive cells are either motorneurons (Myers, 1985) or Kolmer-Agduhr (KA) interneurons (Bernhardt et al., 1992). A single time point was selected for preliminary analysis to confirm neuronal expression of zebrafish stac1 as expected from the mammalian homologue.

Due to the sequence similarity, Stac1 may potentially have a similar function as Stac3. Therefore, Stac1 may regulate calcium currents in neurons and thus influence behavior. Once a behavioral defect in zebrafish is identified, techniques are available to dissect the underlying molecular mechanism (Cui et al., 2005; Hirata et al., 2004). Continuing work with zebrafish Stac1 may provide new functional insight into neuronal activity.

Figure 4.1

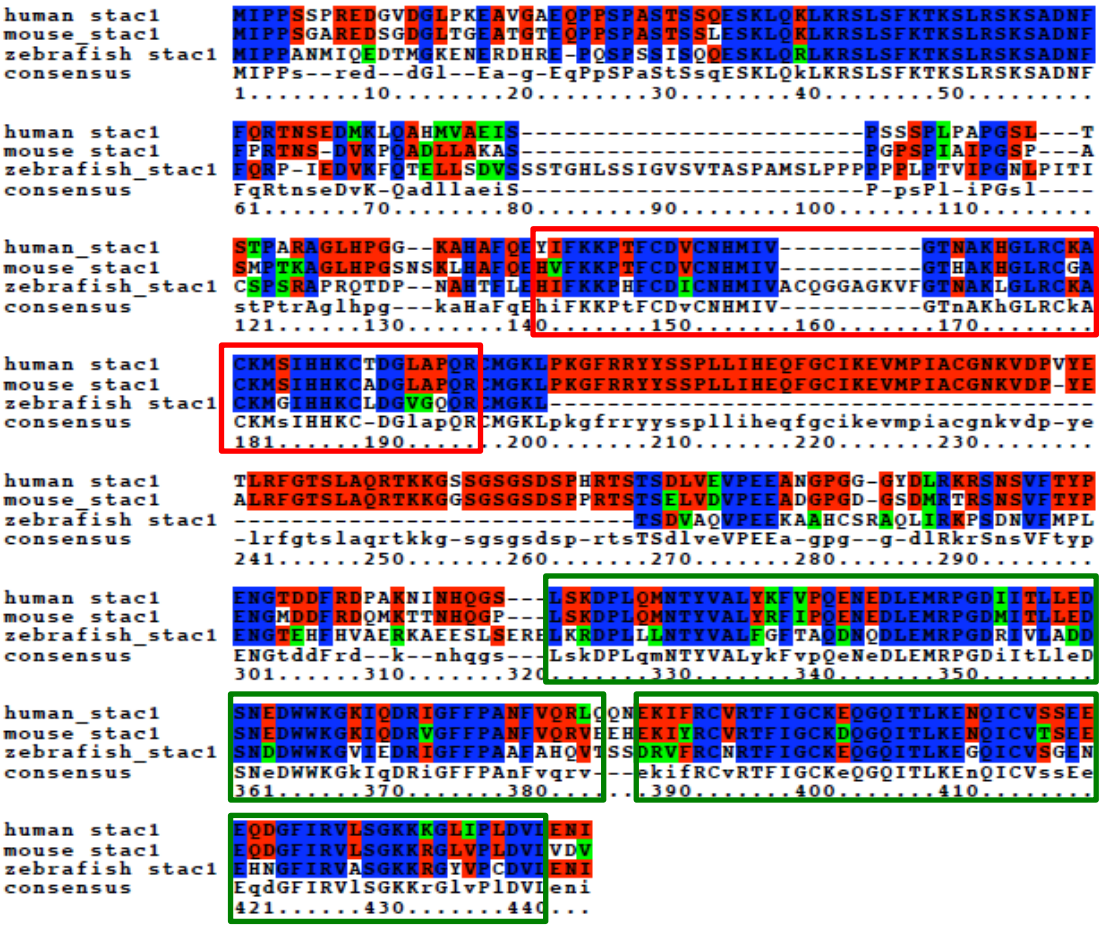

Figure 4.1: Cloned zebrafish Stac1 is similar to known mammalian STAC1 sequences. Blue represents completely conserved residues, red is identical residues, and green is similar residues. The residues within the red box are the C1 domain. The residues within either the blue or the green boxes are the SH3 domains. The alignment was generated using Biology Workbench software.

Figure 4.2

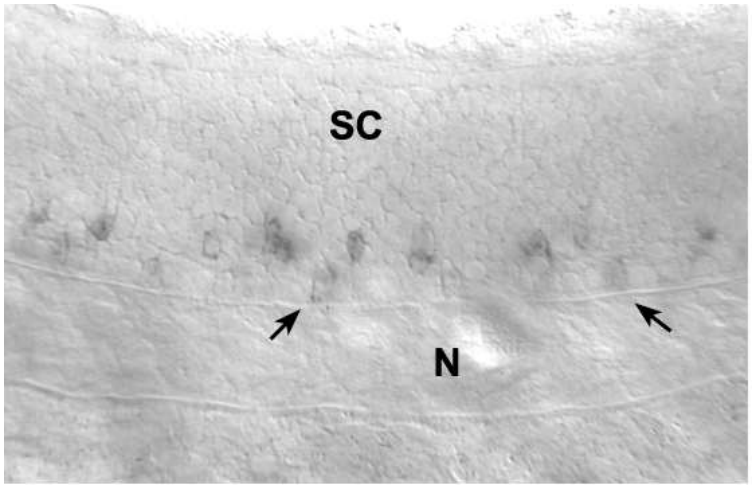

Figure 4.2: Zebrafish *stac1* is expressed in ventral spinal cord neurons. Bright field image of the spinal cord (SC). Arrows indicate the floor plate and the notochord (N) which indicate the labeled neurons are ventrally located. Labeling and imaging performed on 27 hpf embryos.

CHAPTER 5

DISCUSSION AND CONCLUSIONS

Summary

A zebrafish mutagenesis screen was performed to identify mutants with abnormal motor behavior and normal morphology. One mutant named *mi34* had a progressive loss of early motor behaviors. Meiotic mapping of the *mi34* mutant identified the causative gene as *stac3*. Interestingly, stac3 is a novel gene with no known functional role. The *stac3* gene encodes a small adapter-like protein containing a C1 domain and two SH3 domains.

Investigation of the *in vivo* role of Stac3 showed a skeletal muscle-specific defect. We demonstrated that muscle did not contract fully in response to direct depolarization. However, application of the RYR agonist caffeine resulted in normal levels of muscle contraction compared to controls, showing that the contractile machinery is normal. Subsequent calcium imaging showed a significant reduction in peak calcium release during induced activity in $stac3^{mi34}$, supporting a defect in EC coupling. Furthermore, immunolabeling and co-immunopreciptation showed that Stac3 co-localized and associated with the EC coupling complex. Further analysis of the action of Stac3 in EC coupling suggests the primary defect in $stac3^{mi34}$ is a decrease in triadic DHPR possibly due to defective trafficking. However, the mechanism by which Stac3 regulates triadic DHPR is just beginning to be analyzed.

Myopathic features of *stac3*^{mi34} encouraged the analysis of human STAC3 and revealed it as the genetic basis of a human congenital myopathy. Individuals with the congenital disease Native American Myopathy (NAM) possessed a STAC3 missense mutation in a conserved region of the protein. The NAM mutation modeled in zebrafish demonstrated that Stac3^{NAM} could not rescue *stac3*^{mi34} behavior at physiological temperatures. In addition, Stac3^{NAM} could not restore EC coupling in *stac3*^{mi34} mutants. Further analysis showed that expressed Stac3^{NAM} could only poorly localize to triads and predominately remains in an area of the muscle fibers consistent with the ER. Interestingly, we discovered that in zebrafish the Stac3^{NAM} could rescue behavior and protein localization in a temperature sensitive manner.

The discovery of Stac3 prompted the investigation of the other Stac (1 and 2) proteins. We identified zebrafish *stac1* in neurons of the embryonic ventral spinal cord. However, we found no sequence homologous to *stac2* in zebrafish (Horstick et al unpublished).

Here I will discuss the role of Stac3 as a potential regulator of EC coupling proteins and role in human disease. In addition, I will discuss the putative role of Stac1 in the nervous system. I will also briefly discuss the larger biologic question regarding what the presence or absence of Stac proteins in different neurons and/or muscle has on cell function.

The role of Stac3 in Skeletal Muscle Excitation-Contraction coupling Regulation

EC coupling in skeletal muscle is a complex process involving numerous proteins. Indeed, successful EC coupling not only requires the proper set of proteins, but also the proper spatial localization and interactions within specialized muscle domains. The potential roles of Stac3 could include synthesis of the EC coupling proteins, regulating the coupling between DHPR/RYR, or regulation of the trafficking of EC coupling proteins to and from triads. Since Stac3 associates with the EC coupling complex, several of these hypothesizes are possible. However, various experiments assisted in limiting the possible models of Stac3 regulation of EC coupling.

One critical finding is that the DHPR α1S but not RYR1 have reduced protein levels in *stac3*^{mi34}, although transcript levels of DHPR α1S are normal. In addition, freeze fracture EM shows that the DHPRs found at triads are not correctly arranged in tetrads in mutant muscles. This data suggests that Stac3 is required for normal levels of triadic DHPR but not RYR, and for tetradic organization of DHPRs. Furthermore, triadic localization of Stac3 is correlated in all cases with triadic DHPR but not RYR. Stac3 mutants are deficient in triadic DHPR but not RYR and *red* mutants that are null for DHPR β are deficient in triadic Stac3 but not RYR. In addition, expression of non-skeletal muscle forms of the β subunit of DHPR in *red* muscle will restore both triadic DHPRα and Stac3. These findings suggest that Stac3 regulates EC coupling by specifically influencing triadic DHPR protein levels.

A putative model to explain the reduced levels of triadic DHPR is that Stac3 regulates the trafficking of the DHPR. The finding that Stac3^{NAM} rescues in a temperature sensitive manner supports this model. Indeed, observation of temperature

sensitive rescue in other studies is typically connected to restoration of protein folding and subsequent trafficking (Maljevic et al., 2011; Rusconi et al., 2007; Sharkey et al., 2009). In Stac3^{NAM} expressing muscle fibers, permissive temperatures allow putatively ER localized Stac3^{NAM} to successfully target to the triads. This suggests that decreased temperature permits some alteration to Stac3^{NAM} allowing export from the ER. At present, it is unknown if permissive temperatures allow the Stac3^{NAM} rescue to recovers DHPR protein levels and numbers of DHPRs in tetrads. Since the Stac3^{NAM} rescue can restore swimming behavior in *stac3*^{mi34}, the rescue of DHPR protein levels and frequency in tetrads seems likely. However, further experiments are necessary to determine the putative mechanism that Stac3 uses to traffic DHPRs.

Stac3 could modulate DHPR trafficking by several mechanisms. First, Stac3 could support ER export of the DHPR complex to triads. Second, Stac3 could regulate endocytosis of the DHPR complex at the triad. If Stac3 assists DHPR export from the ER, then the DHPR should accumulate in the ER in *stac3*^{mi34}. However, previous experiments did not show ER localized DHPR in *stac3*^{mi34} (Horstick et al, unpublished). The lack of DHPR labeling in mutants might occur because of quality control mechanisms in the ER. Pharmacologic block of the ER quality control systems will be required, using drugs such as kifunensine, for further investigation. In addition, observing fluorescently tagged DHPR in Stac3^{NAM} expressing embryos should show migration of the DHPR from ER to triad in real time dependent on temperature. Interestingly, the calcium channel β subunit in cardiac muscle assists in ER export of the

DHPR. Therefore, Stac3 may support this previously identified mechanism or function as the skeletal muscle specific counterpart.

Alternatively, if Stac3 only mediates endocytosis of the DHPR from triads, we would not expect to see DHPR sequestered in the ER in mutants. However, blocking either proteasome or lysosome degradation may rescue DHPR protein levels in *stac3*^{mi34}. Interactions of the β subunit and small G-protein regulate DHPR endocytosis in a dynamin dependent fashion (Yang et al., 2010). Stac3 may act as a third component of this previously described regulatory pathway or independently modulate DHPR turnover. Consequently, Stac3 trafficking of DHPR does not rule out a regulatory effect on DHPR activity. Stac3 could simultaneously traffic the channel and modulate open probability, voltage sensitivity, etc. In any case, current evidence suggests the mechanism influencing triadic DHPR levels as the primary defect. Regardless continuing effects to identify the exact mechanism of Stac3 are required.

Regardless of the exact mechanism of Stac3 regulation of the DHPR, Stac3 will provide new insight into EC coupling. The identification of a novel protein critical for EC coupling is an exciting addition to biologic knowledge. Indeed, if evidence is found for a direct interaction between the DHPR α1S and Stac3, the Stac3 protein could arguably be considered a novel regulatory subunit of the DHPR complex.

Role of Stac3 in Human Disease

We have shown that a missense mutation in STAC3 is responsible for a congenital human disease NAM. Initial analysis in zebrafish of Stac3^{NAM} has thus far

suggested the NAM mutation results in a partial loss of function. Therefore, a likely hypothesis for the NAM phenotype is a reduction of DHPRs in the triads as in zebrafish stac^{mi34} mutants and predicts decreased EC coupling in NAM patients. Human NAM patients are, however, ambulatory and capable of most motor functions (Stamm et al., 2008a). This suggests that decreased EC coupling in these individuals allows for most motor functions although under more strenuous conditions these individuals may exhibit more severe defects. Thus there might exist differences in the phenotype of the NAM allele in zebrafish and humans. Alternatively, some form of physiological or genetic compensation may occur in NAM individuals that partially diminishes the deleterious effects of the NAM mutation. One would not have expected any compensation in our examination of the Stac3^{NAM} since these experiments were acute and not likely to trigger compensatory mechanisms. More investigation is required to fully understand the impact of temperature on Stac3^{NAM} function. The generation of a transgenic line of zebrafish that express Stac3^{NAM} in skeletal muscles could be useful to examine this possibility as well as to better characterizes the mechanisms that lead to the NAM congenital myopathy.

With a transgenic Stac3^{NAM} zebrafish line, we can also perform drug screens to find potential therapeutic agents for NAM. In addition, NAM exhibits MH susceptibility in humans (Stamm et al., 2008a). MH susceptibility is a relatively prevalent muscle condition and commonly associated with other myopathic conditions. Therefore, using the transgenic Stac3^{NAM} to model MH susceptibility would be valuable. Mouse (Yang et al., 2003) and porcine (Fujii et al., 1991) models of MH susceptibility causing mutations

exist. However, zebrafish are an attractive model since drugs for induction or prevention of MH episodes can be applied externally and skeletal muscle is easy to access and observe. Continuing efforts with Stac3 may illuminate therapeutic agents for both NAM and MH. Furthermore, *STAC3* mutations may be the genetic basis of other unresolved human myopathies.

Putative Role of Stac1 in Neurons

The preliminary findings regarding zebrafish *stac1* allow many possibilities for protein function. However, the similarity of Stac1 to Stac3 allows speculation that the two proteins may serve analogous roles in neurons and skeletal muscle respectively. Perhaps Stac1 also regulates the trafficking of a calcium channel. In the nervous system, different types of calcium channels are implicated in transmitter release, long-term potentiation, and cell survival. Indeed, the *tottering (tg)* mouse, a calcium channel α1A subunit mutant, exhibits ataxia and dystonic episodes (Campbell and Hess, 1999). Furthermore, the *lethargic (lh)* mouse, a calcium channel β4 subunit mutant (Burgess et al., 1997), reshuffles α subunit types in the brain resulting in epilepsy-like phenotypes and ataxia (Burgess et al., 1999). These studies demonstrate the importance of the presence or type of calcium channel in neurons. Therefore, Stac1 regulation of the targeting or activity of neural calcium channels could prove physiologically significant.

Unfortunately, we do not know the calcium channel make-up of either motorneurons or KA interneurons in vertebrates, which comprise the two likely neuron type candidates from the stac1 in-situ from embryonic zebrafish. However, we do know that mouse *STAC1* is expressed in DRG neurons (Legha et al., 2010) as well as various

locations in the adult mouse brain (http://mouse.brain-map.org). Even with this information, we do not have one particular calcium channel type which to focus attention. Despite the current lack of data concerning Stac1 function, the potential for this novel protein is high. Continuing experiments will potentially demonstrate a novel mechanism, in neurons, for Stac1 mediated regulation of calcium channel(s).

What Does it Mean to be STACed?

If future investigations show the STAC protein family share analogous roles in different cell types, then we may be able to ask a broader biologic question. Why do certain neurons or muscle types have a STAC protein while others do not, despite expressing calcium channels? Two possible mechanisms of STAC proteins are that they 1) perform an analogous role of another protein in non-STAC expressing cells or 2) contribute an additional level of regulation.

The paradigm is easily observed be comparing skeletal muscle verse cardiac muscle. Both are striated muscle types dependent on L-type calcium channels for contraction. However, cardiac muscle does not express *stac1* or *stac3* (Horstick et al unpublished). The obvious question then is what is STAC3 doing in skeletal muscle that is not required in cardiac muscle. Indeed, this question would be substantially easier to probe if we knew a direct binding partner for the STAC proteins. If we knew what protein domain or motif STAC proteins bound, then we could determine if this sequence is conserved in STAC interacting proteins and absent in the analogous protein in a non-STAC expressing tissue. Ideally, with continued experiments we can discover the answer

to some of these questions and advance the understanding of regulatory mechanisms across different cell types.

APPENDIX

ACUTE ELEVATION OF SELECTIVE DIVALENT CATIONS RESCUES TOUCH RESPONSE IN THE ZEBRAFISH MUTANT *TOUCHDOWN*

[Published as Low, S.E., Amburgey, K., Horstick, E., Linsley, J., Sprague, S.M., Cui, W.W., Zhou, W., Hirata, H., Saint-Amant, L., Hume, R.I*., et al.* (2011). TRPM7 is required within zebrafish sensory neurons for the activation of touch-evoked escape behaviors. J Neurosci *31*, 11633-11644.]

Abstract

TRPM7 is a member of the superfamily of transient receptor potential (TRP) cation channels. Mutations in zebrafish TRPM7 are responsible for the touch unresponsive *touchdown* mutant. Here we investigate the *mi174* allele of *touchdown* isolated from a mutagenesis screen. Touch response can be rescued in *mi174* by selective rescue within sensory neurons. In addition, acute elevation of selective divalent cations can rescue the touch responsiveness of *mi174*. This data suggests TRPM7 may be required for transmitter release at central synapses.

Introduction

TRPM7 is a member of the cation channel superfamily. This channel is only one of two known ion channels to also possess a catalytically active kinase domain (Montell, 2005). Not surprisingly, numerous studies have attempted to elucidate the in-vivo role of TRPM7. However, progress is impeded by the lack of specific antagonists and that *trpm7* knockdown in mice is embryonic lethal (Jin et al., 2008). Despite these obstacles, TRPM7 is implicated in mechanotransduction (Numata et al., 2007a, b), transmitter

release (Krapivinsky et al., 2006), and cell survival (Nadler et al., 2001). Activity of the kinase domain is also linked to phosphorylation of particular intracellular targets (Clark et al., 2006; Dorovkov and Ryazanov, 2004). From this, we can see many possible avenues of TRPM7 function as either a channel or a kinase. Therefore, the viable *trpm7* zebrafish mutant may yield new understanding to TRPM7 function in-vivo.

Materials and Methods

Animals, Behavioral Analysis and Statistical Analysis

Zebrafish were bred and maintained according to approved guidelines of the University Committee on Use and Care of Animals at the University of Michigan. The *tdo*^{mi174} mutation was isolated from a mutagenesis screen using procedures previously reported (Driever et al., 1996; Haffter et al., 1996). Embryonic behaviors were video-recorded using a Point Grey Firefly MV USB camera mounted on a stereomicroscope.

Ion Elevation

Extracellular solutions and embryo peel preps were as previously described (Buss and Drapeau, 2000), with the following exceptions. Embryos were only pinned through the heart as not to disrupt the muscle. Using a sharp electrode skin was removed from approximately half of one side of the embryo. All embryos were allowed to recovery in normal Evans solutions. Only *tdo*^{174} embryos exhibiting normal swimming in response to pinch were used for further analysis. Embryos were then placed in either Evans solutions with Evans containing 5mM, normal is 2mM, Ca^{2+}, Ba^{2+}, Sr^{2+}, or Mg^{2+}. After 5 minutes, touch response was video recorded.

Results

In mammals, TRPM7 is responsible for facilitating transmitter release at the neuromuscular junction (Brauchi et al., 2008; Krapivinsky et al., 2006). However, in zebrafish we can rule out this model since sensory neuron specific rescue can restore touch response (Low et al., 2011). Despite this difference, a similar mechanism for TRPM7 may exist for different neuron types. Therefore, enhancing transmitter release should rescue the touch defect in *tdo*. To investigate this idea, we placed skin peeled and unpeeled embryos in extracellular solution with Ca^{2+} increased from 2mM to 5mM. Only skin peeled embryos, which allow rapid diffusion of ions into the spinal cord, resulted in proficient rescue of touch response (Figure A.1A). Other divalent ions such as strontium and to a lesser extend barium can enhance vesicle fusion in fish (Neves et al., 2001). Indeed, treating peeled *tdo* mutants with elevated Ca^{2+}, Ba^{2+}, and Sr^{2+} restored touch response. Magnesium, which does not assist in transmitter release, failed to restore any touch response in mutants (Figure A.1B).

Discussion

These findings support a role of TRPM7 in transmitter release of central synapses. However, increasing extracellular ions does not definitively prove this hypothesis. Further work is required to demonstrate TRPM7 is required for normal transmitter release from sensory neurons. An interesting experiment is to find a post-synaptic neuron from zebrafish sensory neurons and record mini-EPSPs in *tdo* compared to wildtype siblings. If mutants show reduced amplitude or frequency of mini-EPSPs, then this would strongly support a TRPM7 based mechanism of transmitter release. In

either case, this current study provides a putative in-vivo model for TRPM7 function in zebrafish central neurons.

Figure A.1

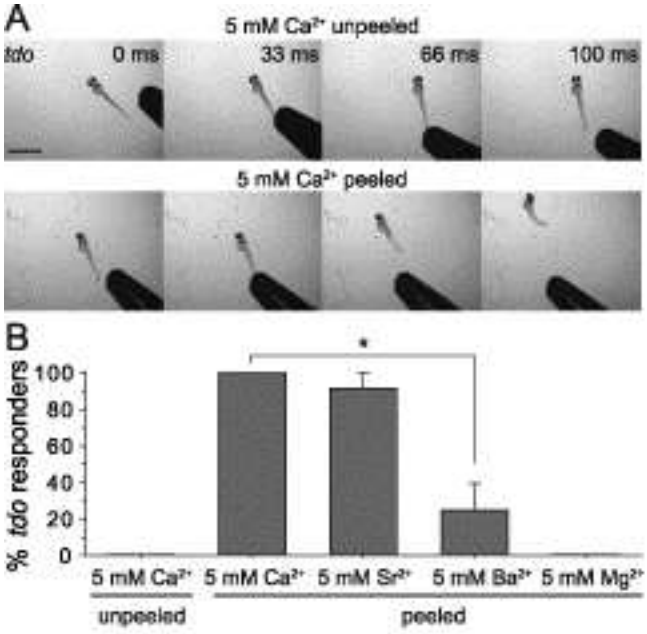

Figure A.1: Elevation of extracellular divalent cations rescues touch responsiveness in *touchdown* mutants. A) Video images of 55 hpf tdo mutants in 5mM Ca^{2+} showing no response to touch with skin intact (top), and exhibiting swimming in response to touch when the skin is removed (bottom). Scale bar 1 mm. B) Average responsiveness of unpeeled embryos in the presence of 5mM Ca^{2+} to touch compared with peeled mutant embryos in the presence of Ca^{2+}, Sr^{2+}, Ba^{2+}, and Mg^{2+} (n=15 from three clutches). *$p<0.05$ t-test.

REFERENCES

Agrawal, V., and Kishan, K.V. (2002). Promiscuous binding nature of SH3 domains to their target proteins. Protein Pept Lett *9*, 185-193.

Ahern, C.A., Powers, P.A., Biddlecome, G.H., Roethe, L., Vallejo, P., Mortenson, L., Strube, C., Campbell, K.P., Coronado, R., and Gregg, R.G. (2001). Modulation of L-type Ca2+ current but not activation of Ca2+ release by the gamma1 subunit of the dihydropyridine receptor of skeletal muscle. BMC Physiol *1*, 8.

Ahern, G.P., Junankar, P.R., and Dulhunty, A.F. (1997). Subconductance states in single-channel activity of skeletal muscle ryanodine receptors after removal of FKBP12. Biophys J *72*, 146-162.

Altier, C., Garcia-Caballero, A., Simms, B., You, H., Chen, L., Walcher, J., Tedford, H.W., Hermosilla, T., and Zamponi, G.W. (2011). The Cavbeta subunit prevents RFP2-mediated ubiquitination and proteasomal degradation of L-type channels. Nat Neurosci *14*, 173-180.

Arikkath, J., Chen, C.C., Ahern, C., Allamand, V., Flanagan, J.D., Coronado, R., Gregg, R.G., and Campbell, K.P. (2003). Gamma 1 subunit interactions within the skeletal muscle L-type voltage-gated calcium channels. J Biol Chem *278*, 1212-1219.

Avila, G., and Dirksen, R.T. (2000). Functional impact of the ryanodine receptor on the skeletal muscle L-type Ca(2+) channel. J Gen Physiol *115*, 467-480.

Bailey, A.G., and Bloch, E.C. (1987). Malignant hyperthermia in a three-month-old American Indian infant. Anesth Analg *66*, 1043-1045.

Bannister, R.A. (2007). Bridging the myoplasmic gap: recent developments in skeletal muscle excitation-contraction coupling. J Muscle Res Cell Motil *28*, 275-283.

Bannister, R.A., Colecraft, H.M., and Beam, K.G. (2008a). Rem inhibits skeletal muscle EC coupling by reducing the number of functional L-type Ca2+ channels. Biophys J *94*, 2631-2638.

Bannister, R.A., Grabner, M., and Beam, K.G. (2008b). The alpha(1S) III-IV loop influences 1,4-dihydropyridine receptor gating but is not directly involved in excitation-contraction coupling interactions with the type 1 ryanodine receptor. J Biol Chem *283*, 23217-23223.

Bannister, R.A., Pessah, I.N., and Beam, K.G. (2009). The skeletal L-type Ca(2+) current is a major contributor to excitation-coupled Ca(2+) entry. J Gen Physiol *133*, 79-91.

Barclay, J., Balaguero, N., Mione, M., Ackerman, S.L., Letts, V.A., Brodbeck, J., Canti, C., Meir, A., Page, K.M., Kusumi, K*., et al.* (2001). Ducky mouse phenotype of epilepsy and ataxia is associated with mutations in the Cacna2d2 gene and decreased calcium channel current in cerebellar Purkinje cells. J Neurosci *21*, 6095-6104.

Bean, B.P. (1989). Multiple types of calcium channels in heart muscle and neurons. Modulation by drugs and neurotransmitters. Ann N Y Acad Sci *560*, 334-345.

Beard, N.A., Laver, D.R., and Dulhunty, A.F. (2004). Calsequestrin and the calcium release channel of skeletal and cardiac muscle. Prog Biophys Mol Biol *85*, 33-69.

Beard, N.A., Wei, L., and Dulhunty, A.F. (2009). Ca(2+) signaling in striated muscle: the elusive roles of triadin, junctin, and calsequestrin. Eur Biophys J *39*, 27-36.

Beguin, P., Mahalakshmi, R.N., Nagashima, K., Cher, D.H., Ikeda, H., Yamada, Y., Seino, Y., and Hunziker, W. (2006). Nuclear sequestration of beta-subunits by Rad and Rem is controlled by 14-3-3 and calmodulin and reveals a novel mechanism for Ca2+ channel regulation. J Mol Biol *355*, 34-46.

Beguin, P., Mahalakshmi, R.N., Nagashima, K., Cher, D.H., Kuwamura, N., Yamada, Y., Seino, Y., and Hunziker, W. (2005a). Roles of 14-3-3 and calmodulin binding in subcellular localization and function of the small G-protein Rem2. Biochem J *390*, 67-75.

Beguin, P., Mahalakshmi, R.N., Nagashima, K., Cher, D.H., Takahashi, A., Yamada, Y., Seino, Y., and Hunziker, W. (2005b). 14-3-3 and calmodulin control subcellular distribution of Kir/Gem and its regulation of cell shape and calcium channel activity. J Cell Sci *118*, 1923-1934.

Beguin, P., Ng, Y.J., Krause, C., Mahalakshmi, R.N., Ng, M.Y., and Hunziker, W. (2007). RGK small GTP-binding proteins interact with the nucleotide kinase domain of Ca2+-channel beta-subunits via an uncommon effector binding domain. J Biol Chem *282*, 11509-11520.

Bernhardt, R.R., Chitnis, A.B., Lindamer, L., and Kuwada, J.Y. (1990). Identification of spinal neurons in the embryonic and larval zebrafish. J Comp Neurol *302*, 603-616.

Bernhardt, R.R., Patel, C.K., Wilson, S.W., and Kuwada, J.Y. (1992). Axonal trajectories and distribution of GABAergic spinal neurons in wildtype and mutant zebrafish lacking floor plate cells. J Comp Neurol *326*, 263-272.

Biel, M., Hullin, R., Freundner, S., Singer, D., Dascal, N., Flockerzi, V., and Hofmann, F. (1991). Tissue-specific expression of high-voltage-activated dihydropyridine-sensitive L-type calcium channels. Eur J Biochem *200*, 81-88.

Biral, D., Volpe, P., Damiani, E., and Margreth, A. (1992). Coexistence of two calsequestrin isoforms in rabbit slow-twitch skeletal muscle fibers. FEBS Lett *299*, 175-178.

Birnbaumer, L., Qin, N., Olcese, R., Tareilus, E., Platano, D., Costantin, J., and Stefani, E. (1998). Structures and functions of calcium channel beta subunits. J Bioenerg Biomembr *30*, 357-375.

Block, B.A., Imagawa, T., Campbell, K.P., and Franzini-Armstrong, C. (1988). Structural evidence for direct interaction between the molecular components of the transverse tubule/sarcoplasmic reticulum junction in skeletal muscle. J Cell Biol *107*, 2587-2600.

Bradley, W.G., Taylor, R., Rice, D.R., Hausmanowa-Petruzewicz, I., Adelman, L.S., Jenkison, M., Jedrzejowska, H., Drac, H., and Pendlebury, W.W. (1990). Progressive myopathy in hyperkalemic periodic paralysis. Arch Neurol *47*, 1013-1017.

Brauchi, S., Krapivinsky, G., Krapivinsky, L., and Clapham, D.E. (2008). TRPM7 facilitates cholinergic vesicle fusion with the plasma membrane. Proc Natl Acad Sci U S A *105*, 8304-8308.

Brenner, S. (1974). The genetics of Caenorhabditis elegans. Genetics *77*, 71-94.

Brill, J., Klocke, R., Paul, D., Boison, D., Gouder, N., Klugbauer, N., Hofmann, F., Becker, C.M., and Becker, K. (2004). entla, a novel epileptic and ataxic Cacna2d2 mutant of the mouse. J Biol Chem *279*, 7322-7330.

Brillantes, A.B., Ondrias, K., Scott, A., Kobrinsky, E., Ondriasova, E., Moschella, M.C., Jayaraman, T., Landers, M., Ehrlich, B.E., and Marks, A.R. (1994). Stabilization of calcium release channel (ryanodine receptor) function by FK506-binding protein. Cell *77*, 513-523.

Brodbeck, J., Davies, A., Courtney, J.M., Meir, A., Balaguero, N., Canti, C., Moss, F.J., Page, K.M., Pratt, W.S., Hunt, S.P., *et al.* (2002). The ducky mutation in Cacna2d2 results in altered Purkinje cell morphology and is associated with the expression of a truncated alpha 2 delta-2 protein with abnormal function. J Biol Chem *277*, 7684-7693.

Bryant, A., Jr., and LaFromboise, T.D. (2005). The racial identity and cultural orientation of Lumbee American Indian high school students. Cultur Divers Ethnic Minor Psychol *11*, 82-89.

Buck, E.D., Nguyen, H.T., Pessah, I.N., and Allen, P.D. (1997). Dyspedic mouse skeletal muscle expresses major elements of the triadic junction but lacks detectable ryanodine receptor protein and function. J Biol Chem *272*, 7360-7367.

Burgess, D.L., Biddlecome, G.H., McDonough, S.I., Diaz, M.E., Zilinski, C.A., Bean, B.P., Campbell, K.P., and Noebels, J.L. (1999). beta subunit reshuffling modifies N- and P/Q-type Ca2+ channel subunit compositions in lethargic mouse brain. Mol Cell Neurosci *13*, 293-311.

Burgess, D.L., Jones, J.M., Meisler, M.H., and Noebels, J.L. (1997). Mutation of the Ca2+ channel beta subunit gene Cchb4 is associated with ataxia and seizures in the lethargic (lh) mouse. Cell *88*, 385-392.

Buss, R.R., and Drapeau, P. (2000). Physiological properties of zebrafish embryonic red and white muscle fibers during early development. J Neurophysiol *84*, 1545-1557.

Campbell, D.B., and Hess, E.J. (1999). L-type calcium channels contribute to the tottering mouse dystonic episodes. Mol Pharmacol *55*, 23-31.

Campbell, D.B., North, J.B., and Hess, E.J. (1999). Tottering mouse motor dysfunction is abolished on the Purkinje cell degeneration (pcd) mutant background. Exp Neurol *160*, 268-278.

Cannon, S.C. (2010). Voltage-sensor mutations in channelopathies of skeletal muscle. J Physiol *588*, 1887-1895.

Catterall, W.A., Perez-Reyes, E., Snutch, T.P., and Striessnig, J. (2005). International Union of Pharmacology. XLVIII. Nomenclature and structure-function relationships of voltage-gated calcium channels. Pharmacol Rev *57*, 411-425.

Chakrabarti, S., Streisinger, G., Singer, F., and Walker, C. (1983). Frequency of gamma-Ray Induced Specific Locus and Recessive Lethal Mutations in Mature Germ Cells of the Zebrafish, BRACHYDANIO RERIO. Genetics *103*, 109-123.

Chelu, M.G., Danila, C.I., Gilman, C.P., and Hamilton, S.L. (2004). Regulation of ryanodine receptors by FK506 binding proteins. Trends Cardiovasc Med *14*, 227-234.

Chen, H., Puhl, H.L., 3rd, Niu, S.L., Mitchell, D.C., and Ikeda, S.R. (2005). Expression of Rem2, an RGK family small GTPase, reduces N-type calcium current without affecting channel surface density. J Neurosci *25*, 9762-9772.

Chen, Y.H., Li, M.H., Zhang, Y., He, L.L., Yamada, Y., Fitzmaurice, A., Shen, Y., Zhang, H., Tong, L., and Yang, J. (2004). Structural basis of the alpha1-beta subunit interaction of voltage-gated Ca2+ channels. Nature *429*, 675-680.

Cheng, W., Altafaj, X., Ronjat, M., and Coronado, R. (2005). Interaction between the dihydropyridine receptor Ca2+ channel beta-subunit and ryanodine receptor type 1 strengthens excitation-contraction coupling. Proc Natl Acad Sci U S A *102*, 19225-19230.

Chopra, N., Yang, T., Asghari, P., Moore, E.D., Huke, S., Akin, B., Cattolica, R.A., Perez, C.F., Hlaing, T., Knollmann-Ritschel, B.E.*, et al.* (2009). Ablation of triadin causes loss of cardiac Ca2+ release units, impaired excitation-contraction coupling, and cardiac arrhythmias. Proc Natl Acad Sci U S A *106*, 7636-7641.

Chu, A., Diaz-Munoz, M., Hawkes, M.J., Brush, K., and Hamilton, S.L. (1990). Ryanodine as a probe for the functional state of the skeletal muscle sarcoplasmic reticulum calcium release channel. Mol Pharmacol *37*, 735-741.

Clark, K., Langeslag, M., van Leeuwen, B., Ran, L., Ryazanov, A.G., Figdor, C.G., Moolenaar, W.H., Jalink, K., and van Leeuwen, F.N. (2006). TRPM7, a novel regulator of actomyosin contractility and cell adhesion. EMBO J *25*, 290-301.

Colon-Gonzalez, F., and Kazanietz, M.G. (2006). C1 domains exposed: from diacylglycerol binding to protein-protein interactions. Biochim Biophys Acta *1761*, 827-837.

Crump, S.M., Correll, R.N., Schroder, E.A., Lester, W.C., Finlin, B.S., Andres, D.A., and Satin, J. (2006). L-type calcium channel alpha-subunit and protein kinase inhibitors modulate Rem-mediated regulation of current. Am J Physiol Heart Circ Physiol *291*, H1959-1971.

Cui, W.W., Low, S.E., Hirata, H., Saint-Amant, L., Geisler, R., Hume, R.I., and Kuwada, J.Y. (2005). The zebrafish shocked gene encodes a glycine transporter and is essential for the function of early neural circuits in the CNS. J Neurosci *25*, 6610-6620.

Curtis, B.M., and Catterall, W.A. (1984). Purification of the calcium antagonist receptor of the voltage-sensitive calcium channel from skeletal muscle transverse tubules. Biochemistry *23*, 2113-2118.

Damiani, E., and Margreth, A. (1994). Characterization study of the ryanodine receptor and of calsequestrin isoforms of mammalian skeletal muscles in relation to fibre types. J Muscle Res Cell Motil *15*, 86-101.

Detrich, H.W., 3rd, Westerfield, M., and Zon, L.I. (1999). Overview of the Zebrafish system. Methods Cell Biol *59*, 3-10.

Di Biase, V., and Franzini-Armstrong, C. (2005). Evolution of skeletal type e-c coupling: a novel means of controlling calcium delivery. J Cell Biol *171*, 695-704.

Dirksen, R.T., and Beam, K.G. (1999). Role of calcium permeation in dihydropyridine receptor function. Insights into channel gating and excitation-contraction coupling. J Gen Physiol *114*, 393-403.

Dolphin, A.C. (2003). Beta subunits of voltage-gated calcium channels. J Bioenerg Biomembr *35*, 599-620.

Donato, R., Page, K.M., Koch, D., Nieto-Rostro, M., Foucault, I., Davies, A., Wilkinson, T., Rees, M., Edwards, F.A., and Dolphin, A.C. (2006). The ducky(2J) mutation in Cacna2d2 results in reduced spontaneous Purkinje cell activity and altered gene expression. J Neurosci *26*, 12576-12586.

Dorovkov, M.V., and Ryazanov, A.G. (2004). Phosphorylation of annexin I by TRPM7 channel-kinase. J Biol Chem *279*, 50643-50646.

Dowling, J.J., Lillis, S., Amburgey, K., Zhou, H., Al-Sarraj, S., Buk, S.J., Wraige, E., Chow, G., Abbs, S., Leber, S.*, et al.* (2011). King-Denborough syndrome with and without mutations in the skeletal muscle ryanodine receptor (RYR1) gene. Neuromuscul Disord *21*, 420-427.

Dowling, J.J., Vreede, A.P., Low, S.E., Gibbs, E.M., Kuwada, J.Y., Bonnemann, C.G., and Feldman, E.L. (2009). Loss of myotubularin function results in T-tubule disorganization in zebrafish and human myotubular myopathy. PLoS Genet *5*, e1000372.

Driever, W., Solnica-Krezel, L., Schier, A.F., Neuhauss, S.C., Malicki, J., Stemple, D.L., Stainier, D.Y., Zwartkruis, F., Abdelilah, S., Rangini, Z.*, et al.* (1996). A genetic screen for mutations affecting embryogenesis in zebrafish. Development *123*, 37-46.

Du, G.G., Oyamada, H., Khanna, V.K., and MacLennan, D.H. (2001). Mutations to Gly2370, Gly2373 or Gly2375 in malignant hyperthermia domain 2 decrease caffeine and cresol sensitivity of the rabbit skeletal-muscle Ca2+-release channel (ryanodine receptor isoform 1). Biochem J *360*, 97-105.

Dyken, M., Zeman, W., and Rusche, T. (1969). Hypokalemic periodic paralysis. Children with permanent myopathic weakness. Neurology *19*, 691-699.

Ekker, M., Speevak, M.D., Martin, C.C., Joly, L., Giroux, G., and Chevrette, M. (1996). Stable transfer of zebrafish chromosome segments into mouse cells. Genomics *33*, 57-64.

Erickson, M.G., Liang, H., Mori, M.X., and Yue, D.T. (2003). FRET two-hybrid mapping reveals function and location of L-type Ca2+ channel CaM preassociation. Neuron *39*, 97-107.

Felder, E., and Franzini-Armstrong, C. (2002). Type 3 ryanodine receptors of skeletal muscle are segregated in a parajunctional position. Proc Natl Acad Sci U S A *99*, 1695-1700.

Felder, E., Protasi, F., Hirsch, R., Franzini-Armstrong, C., and Allen, P.D. (2002). Morphology and molecular composition of sarcoplasmic reticulum surface junctions in the absence of DHPR and RyR in mouse skeletal muscle. Biophys J *82*, 3144-3149.

Ferreiro, A., Quijano-Roy, S., Pichereau, C., Moghadaszadeh, B., Goemans, N., Bonnemann, C., Jungbluth, H., Straub, V., Villanova, M., Leroy, J.P.*, et al.* (2002). Mutations of the selenoprotein N gene, which is implicated in rigid spine muscular dystrophy, cause the classical phenotype of multiminicore disease: reassessing the nosology of early-onset myopathies. Am J Hum Genet *71*, 739-749.

Finlin, B.S., Correll, R.N., Pang, C., Crump, S.M., Satin, J., and Andres, D.A. (2006). Analysis of the complex between Ca2+ channel beta-subunit and the Rem GTPase. J Biol Chem *281*, 23557-23566.

Finlin, B.S., Crump, S.M., Satin, J., and Andres, D.A. (2003). Regulation of voltage-gated calcium channel activity by the Rem and Rad GTPases. Proc Natl Acad Sci U S A *100*, 14469-14474.

Finlin, B.S., Mosley, A.L., Crump, S.M., Correll, R.N., Ozcan, S., Satin, J., and Andres, D.A. (2005). Regulation of L-type Ca2+ channel activity and insulin secretion by the Rem2 GTPase. J Biol Chem *280*, 41864-41871.

Fliegel, L., Newton, E., Burns, K., and Michalak, M. (1990). Molecular cloning of cDNA encoding a 55-kDa multifunctional thyroid hormone binding protein of skeletal muscle sarcoplasmic reticulum. J Biol Chem *265*, 15496-15502.

Flucher, B.E., Andrews, S.B., Fleischer, S., Marks, A.R., Caswell, A., and Powell, J.A. (1993a). Triad formation: organization and function of the sarcoplasmic reticulum calcium release channel and triadin in normal and dysgenic muscle in vitro. J Cell Biol *123*, 1161-1174.

Flucher, B.E., Kasielke, N., and Grabner, M. (2000). The triad targeting signal of the skeletal muscle calcium channel is localized in the COOH terminus of the alpha(1S) subunit. J Cell Biol *151*, 467-478.

Flucher, B.E., Takekura, H., and Franzini-Armstrong, C. (1993b). Development of the excitation-contraction coupling apparatus in skeletal muscle: association of sarcoplasmic reticulum and transverse tubules with myofibrils. Dev Biol *160*, 135-147.

Fontaine, B., Khurana, T.S., Hoffman, E.P., Bruns, G.A., Haines, J.L., Trofatter, J.A., Hanson, M.P., Rich, J., McFarlane, H., Yasek, D.M.*, et al.* (1990). Hyperkalemic periodic paralysis and the adult muscle sodium channel alpha-subunit gene. Science *250*, 1000-1002.

Fontaine, B., Vale-Santos, J., Jurkat-Rott, K., Reboul, J., Plassart, E., Rime, C.S., Elbaz, A., Heine, R., Guimaraes, J., Weissenbach, J.*, et al.* (1994). Mapping of the hypokalaemic periodic paralysis (HypoPP) locus to chromosome 1q31-32 in three European families. Nat Genet *6*, 267-272.

Franzini-Armstrong, C. (1970). STUDIES OF THE TRIAD : I. Structure of the Junction in Frog Twitch Fibers. J Cell Biol *47*, 488-499.

Freise, D., Held, B., Wissenbach, U., Pfeifer, A., Trost, C., Himmerkus, N., Schweig, U., Freichel, M., Biel, M., Hofmann, F.*, et al.* (2000). Absence of the gamma subunit of the skeletal muscle dihydropyridine receptor increases L-type Ca2+ currents and alters channel inactivation properties. J Biol Chem *275*, 14476-14481.

Fruen, B.R., Bardy, J.M., Byrem, T.M., Strasburg, G.M., and Louis, C.F. (2000). Differential Ca(2+) sensitivity of skeletal and cardiac muscle ryanodine receptors in the presence of calmodulin. Am J Physiol Cell Physiol *279*, C724-733.

Fruen, B.R., Black, D.J., Bloomquist, R.A., Bardy, J.M., Johnson, J.D., Louis, C.F., and Balog, E.M. (2003). Regulation of the RYR1 and RYR2 Ca2+ release channel isoforms by Ca2+-insensitive mutants of calmodulin. Biochemistry *42*, 2740-2747.

Fryer, M.W., and Stephenson, D.G. (1996). Total and sarcoplasmic reticulum calcium contents of skinned fibres from rat skeletal muscle. J Physiol *493 (Pt 2)*, 357-370.

Fujii, J., Otsu, K., Zorzato, F., de Leon, S., Khanna, V.K., Weiler, J.E., O'Brien, P.J., and MacLennan, D.H. (1991). Identification of a mutation in porcine ryanodine receptor associated with malignant hyperthermia. Science *253*, 448-451.

Fuller-Bicer, G.A., Varadi, G., Koch, S.E., Ishii, M., Bodi, I., Kadeer, N., Muth, J.N., Mikala, G., Petrashevskaya, N.N., Jordan, M.A.*, et al.* (2009). Targeted disruption of the voltage-dependent calcium channel alpha2/delta-1-subunit. Am J Physiol Heart Circ Physiol *297*, H117-124.

Fureman, B.E., Campbell, D.B., and Hess, E.J. (1999). L-type calcium channel regulation of abnormal tyrosine hydroxylase expression in cerebella of tottering mice. Ann N Y Acad Sci *868*, 217-219.

Gach, M.P., Cherednichenko, G., Haarmann, C., Lopez, J.R., Beam, K.G., Pessah, I.N., Franzini-Armstrong, C., and Allen, P.D. (2008). Alpha2delta1 dihydropyridine receptor subunit is a critical element for excitation-coupled calcium entry but not for formation of tetrads in skeletal myotubes. Biophys J *94*, 3023-3034.

Garcia, J., and Beam, K.G. (1994). Calcium transients associated with the T type calcium current in myotubes. J Gen Physiol *104*, 1113-1128.

Garcia, J., Tanabe, T., and Beam, K.G. (1994). Relationship of calcium transients to calcium currents and charge movements in myotubes expressing skeletal and cardiac dihydropyridine receptors. J Gen Physiol *103*, 125-147.

Geisler, R., Rauch, G.J., Baier, H., van Bebber, F., Bross, L., Dekens, M.P., Finger, K., Fricke, C., Gates, M.A., Geiger, H.*, et al.* (1999). A radiation hybrid map of the zebrafish genome. Nat Genet *23*, 86-89.

Germann, W.J., and Stanfield, C.L. (2005). Principles of human physiology (San Francisco, Pearson Benjamin Cummings), pp. xxxiv, 830 p.

Gonzalez-Gutierrez, G., Miranda-Laferte, E., Neely, A., and Hidalgo, P. (2007). The Src homology 3 domain of the beta-subunit of voltage-gated calcium channels promotes endocytosis via dynamin interaction. J Biol Chem *282*, 2156-2162.

Grabner, M., Dirksen, R.T., and Beam, K.G. (1998). Tagging with green fluorescent protein reveals a distinct subcellular distribution of L-type and non-L-type Ca2+ channels expressed in dysgenic myotubes. Proc Natl Acad Sci U S A *95*, 1903-1908.

Grabner, M., Dirksen, R.T., Suda, N., and Beam, K.G. (1999). The II-III loop of the skeletal muscle dihydropyridine receptor is responsible for the Bi-directional coupling with the ryanodine receptor. J Biol Chem *274*, 21913-21919.

Grabner, M., Wang, Z., Mitterdorfer, J., Rosenthal, F., Charnet, P., Savchenko, A., Hering, S., Ren, D., Hall, L.M., and Glossmann, H. (1994). Cloning and functional expression of a neuronal calcium channel beta subunit from house fly (Musca domestica). J Biol Chem *269*, 23668-23674.

Gregg, R.G., Messing, A., Strube, C., Beurg, M., Moss, R., Behan, M., Sukhareva, M., Haynes, S., Powell, J.A., Coronado, R.*, et al.* (1996). Absence of the beta subunit (cchb1) of the skeletal muscle dihydropyridine receptor alters expression of the alpha 1 subunit and eliminates excitation-contraction coupling. Proc Natl Acad Sci U S A *93*, 13961-13966.

Haffter, P., Granato, M., Brand, M., Mullins, M.C., Hammerschmidt, M., Kane, D.A., Odenthal, J., van Eeden, F.J., Jiang, Y.J., Heisenberg, C.P.*, et al.* (1996). The identification of genes with unique and essential functions in the development of the zebrafish, Danio rerio. Development *123*, 1-36.

Hakamata, Y., Nakai, J., Takeshima, H., and Imoto, K. (1992). Primary structure and distribution of a novel ryanodine receptor/calcium release channel from rabbit brain. FEBS Lett *312*, 229-235.

Halling, D.B., Aracena-Parks, P., and Hamilton, S.L. (2006). Regulation of voltage-gated Ca2+ channels by calmodulin. Sci STKE *2006*, er1.

Halling, D.B., Georgiou, D.K., Black, D.J., Yang, G., Fallon, J.L., Quiocho, F.A., Pedersen, S.E., and Hamilton, S.L. (2009). Determinants in CaV1 channels that regulate the Ca2+ sensitivity of bound calmodulin. J Biol Chem *284*, 20041-20051.

Halloran, M.C., Sato-Maeda, M., Warren, J.T., Su, F., Lele, Z., Krone, P.H., Kuwada, J.Y., and Shoji, W. (2000). Laser-induced gene expression in specific cells of transgenic zebrafish. Development *127*, 1953-1960.

Hanlon, M.R., Berrow, N.S., Dolphin, A.C., and Wallace, B.A. (1999). Modelling of a voltage-dependent Ca2+ channel beta subunit as a basis for understanding its functional properties. FEBS Lett *445*, 366-370.

Higashijima, S., Okamoto, H., Ueno, N., Hotta, Y., and Eguchi, G. (1997). High-frequency generation of transgenic zebrafish which reliably express GFP in whole muscles or the whole body by using promoters of zebrafish origin. Dev Biol *192*, 289-299.

Hille, B. (1992). Ionic channels of excitable membranes, 2nd edn (Sunderland, Mass., Sinauer Associates).

Hirata, H., Saint-Amant, L., Downes, G.B., Cui, W.W., Zhou, W., Granato, M., and Kuwada, J.Y. (2005). Zebrafish bandoneon mutants display behavioral defects due to a mutation in the glycine receptor beta-subunit. Proc Natl Acad Sci U S A *102*, 8345-8350.

Hirata, H., Saint-Amant, L., Waterbury, J., Cui, W., Zhou, W., Li, Q., Goldman, D., Granato, M., and Kuwada, J.Y. (2004). accordion, a zebrafish behavioral mutant, has a muscle relaxation defect due to a mutation in the ATPase Ca2+ pump SERCA1. Development *131*, 5457-5468.

Hirata, H., Watanabe, T., Hatakeyama, J., Sprague, S.M., Saint-Amant, L., Nagashima, A., Cui, W.W., Zhou, W., and Kuwada, J.Y. (2007). Zebrafish relatively relaxed mutants have a ryanodine receptor defect, show slow swimming and provide a model of multi-minicore disease. Development *134*, 2771-2781.

Hosey, M.M., Barhanin, J., Schmid, A., Vandaele, S., Ptasienski, J., O'Callahan, C., Cooper, C., and Lazdunski, M. (1987). Photoaffinity labelling and phosphorylation of a 165 kilodalton peptide associated with dihydropyridine and phenylalkylamine-sensitive calcium channels. Biochem Biophys Res Commun *147*, 1137-1145.

Hukriede, N.A., Joly, L., Tsang, M., Miles, J., Tellis, P., Epstein, J.A., Barbazuk, W.B., Li, F.N., Paw, B., Postlethwait, J.H.*, et al.* (1999). Radiation hybrid mapping of the zebrafish genome. Proc Natl Acad Sci U S A *96*, 9745-9750.

Hullin, R., Singer-Lahat, D., Freichel, M., Biel, M., Dascal, N., Hofmann, F., and Flockerzi, V. (1992). Calcium channel beta subunit heterogeneity: functional expression of cloned cDNA from heart, aorta and brain. EMBO J *11*, 885-890.

Ikemoto, N., Antoniu, B., Kang, J.J., Meszaros, L.G., and Ronjat, M. (1991). Intravesicular calcium transient during calcium release from sarcoplasmic reticulum. Biochemistry *30*, 5230-5237.

Ikemoto, N., Bhatnagar, G.M., Nagy, B., and Gergely, J. (1972). Interaction of divalent cations with the 55,000-dalton protein component of the sarcoplasmic reticulum. Studies of fluorescence and circular dichroism. J Biol Chem *247*, 7835-7837.

Iles, D.E., Lehmann-Horn, F., Scherer, S.W., Tsui, L.C., Olde Weghuis, D., Suijkerbuijk, R.F., Heytens, L., Mikala, G., Schwartz, A., Ellis, F.R.*, et al.* (1994). Localization of the gene encoding the alpha 2/delta-subunits of the L-type voltage-dependent calcium channel to chromosome 7q and analysis of the segregation of flanking markers in malignant hyperthermia susceptible families. Hum Mol Genet *3*, 969-975.

Imagawa, T., Smith, J.S., Coronado, R., and Campbell, K.P. (1987). Purified ryanodine receptor from skeletal muscle sarcoplasmic reticulum is the Ca2+-permeable pore of the calcium release channel. J Biol Chem *262*, 16636-16643.

Inui, M., Saito, A., and Fleischer, S. (1987a). Isolation of the ryanodine receptor from cardiac sarcoplasmic reticulum and identity with the feet structures. J Biol Chem *262*, 15637-15642.

Inui, M., Saito, A., and Fleischer, S. (1987b). Purification of the ryanodine receptor and identity with feet structures of junctional terminal cisternae of sarcoplasmic reticulum from fast skeletal muscle. J Biol Chem *262*, 1740-1747.

Jay, S.D., Ellis, S.B., McCue, A.F., Williams, M.E., Vedvick, T.S., Harpold, M.M., and Campbell, K.P. (1990). Primary structure of the gamma subunit of the DHP-sensitive calcium channel from skeletal muscle. Science *248*, 490-492.

Jay, S.D., Sharp, A.H., Kahl, S.D., Vedvick, T.S., Harpold, M.M., and Campbell, K.P. (1991). Structural characterization of the dihydropyridine-sensitive calcium channel alpha 2-subunit and the associated delta peptides. J Biol Chem *266*, 3287-3293.

Jayaraman, T., Brillantes, A.M., Timerman, A.P., Fleischer, S., Erdjument-Bromage, H., Tempst, P., and Marks, A.R. (1992). FK506 binding protein associated with the calcium release channel (ryanodine receptor). J Biol Chem *267*, 9474-9477.

Jin, J., Desai, B.N., Navarro, B., Donovan, A., Andrews, N.C., and Clapham, D.E. (2008). Deletion of Trpm7 disrupts embryonic development and thymopoiesis without altering Mg2+ homeostasis. Science *322*, 756-760.

Johnson, S.L., Midson, C.N., Ballinger, E.W., and Postlethwait, J.H. (1994). Identification of RAPD primers that reveal extensive polymorphisms between laboratory strains of zebrafish. Genomics *19*, 152-156.

Jones, L.R., Suzuki, Y.J., Wang, W., Kobayashi, Y.M., Ramesh, V., Franzini-Armstrong, C., Cleemann, L., and Morad, M. (1998). Regulation of Ca2+ signaling in transgenic mouse cardiac myocytes overexpressing calsequestrin. J Clin Invest *101*, 1385-1393.

Jungbluth, H. (2007). Central core disease. Orphanet J Rare Dis *2*, 25.

Jungbluth, H., Sewry, C., Brown, S.C., Manzur, A.Y., Mercuri, E., Bushby, K., Rowe, P., Johnson, M.A., Hughes, I., Kelsey, A*., et al.* (2000). Minicore myopathy in children: a clinical and histopathological study of 19 cases. Neuromuscul Disord *10*, 264-273.

Jungbluth, H., Zhou, H., Hartley, L., Halliger-Keller, B., Messina, S., Longman, C., Brockington, M., Robb, S.A., Straub, V., Voit, T*., et al.* (2005). Minicore myopathy with ophthalmoplegia caused by mutations in the ryanodine receptor type 1 gene. Neurology *65*, 1930-1935.

Jurkat-Rott, K., Lehmann-Horn, F., Elbaz, A., Heine, R., Gregg, R.G., Hogan, K., Powers, P.A., Lapie, P., Vale-Santos, J.E., Weissenbach, J*., et al.* (1994). A calcium channel mutation causing hypokalemic periodic paralysis. Hum Mol Genet *3*, 1415-1419.

Jurkat-Rott, K., Uetz, U., Pika-Hartlaub, U., Powell, J., Fontaine, B., Melzer, W., and Lehmann-Horn, F. (1998). Calcium currents and transients of native and heterologously expressed mutant skeletal muscle DHP receptor alpha1 subunits (R528H). FEBS Lett *423*, 198-204.

Jurynec, M.J., Xia, R., Mackrill, J.J., Gunther, D., Crawford, T., Flanigan, K.M., Abramson, J.J., Howard, M.T., and Grunwald, D.J. (2008). Selenoprotein N is required for ryanodine receptor calcium release channel activity in human and zebrafish muscle. Proc Natl Acad Sci U S A *105*, 12485-12490.

Kasielke, N., Obermair, G.J., Kugler, G., Grabner, M., and Flucher, B.E. (2003). Cardiac-type EC-coupling in dysgenic myotubes restored with Ca2+ channel subunit isoforms alpha1C and alpha1D does not correlate with current density. Biophys J *84*, 3816-3828.

Kawai, J., Suzuki, H., Hara, A., Hirose, K., and Watanabe, S. (1998). Human and mouse chromosomal mapping of Stac, a neuron-specific protein with an SH3 domain. Genomics *47*, 140-142.

Klaus, M.M., Scordilis, S.P., Rapalus, J.M., Briggs, R.T., and Powell, J.A. (1983). Evidence for dysfunction in the regulation of cytosolic Ca2+ in excitation-contraction uncoupled dysgenic muscle. Dev Biol *99*, 152-165.

Knollmann, B.C., Chopra, N., Hlaing, T., Akin, B., Yang, T., Ettensohn, K., Knollmann, B.E., Horton, K.D., Weissman, N.J., Holinstat, I.*, et al.* (2006). Casq2 deletion causes sarcoplasmic reticulum volume increase, premature Ca2+ release, and catecholaminergic polymorphic ventricular tachycardia. J Clin Invest *116*, 2510-2520.

Knudson, C.M., Chaudhari, N., Sharp, A.H., Powell, J.A., Beam, K.G., and Campbell, K.P. (1989). Specific absence of the alpha 1 subunit of the dihydropyridine receptor in mice with muscular dysgenesis. J Biol Chem *264*, 1345-1348.

Krapivinsky, G., Mochida, S., Krapivinsky, L., Cibulsky, S.M., and Clapham, D.E. (2006). The TRPM7 ion channel functions in cholinergic synaptic vesicles and affects transmitter release. Neuron *52*, 485-496.

Kugler, G., Weiss, R.G., Flucher, B.E., and Grabner, M. (2004). Structural requirements of the dihydropyridine receptor alpha1S II-III loop for skeletal-type excitation-contraction coupling. J Biol Chem *279*, 4721-4728.

Kuwada, J.Y., Bernhardt, R.R., and Nguyen, N. (1990). Development of spinal neurons and tracts in the zebrafish embryo. J Comp Neurol *302*, 617-628.

Kwok, C., Korn, R.M., Davis, M.E., Burt, D.W., Critcher, R., McCarthy, L., Paw, B.H., Zon, L.I., Goodfellow, P.N., and Schmitt, K. (1998). Characterization of whole genome radiation hybrid mapping resources for non-mammalian vertebrates. Nucleic Acids Res *26*, 3562-3566.

Lai, F.A., Anderson, K., Rousseau, E., Liu, Q.Y., and Meissner, G. (1988). Evidence for a Ca2+ channel within the ryanodine receptor complex from cardiac sarcoplasmic reticulum. Biochem Biophys Res Commun *151*, 441-449.

Lam, E., Martin, M.M., Timerman, A.P., Sabers, C., Fleischer, S., Lukas, T., Abraham, R.T., O'Keefe, S.J., O'Neill, E.A., and Wiederrecht, G.J. (1995). A novel FK506 binding protein can mediate the immunosuppressive effects of FK506 and is associated with the cardiac ryanodine receptor. J Biol Chem *270*, 26511-26522.

Lanner, J.T., Georgiou, D.K., Joshi, A.D., and Hamilton, S.L. (2010). Ryanodine receptors: structure, expression, molecular details, and function in calcium release. Cold Spring Harb Perspect Biol *2*, a003996.

Lapie, P., Goudet, C., Nargeot, J., Fontaine, B., and Lory, P. (1996). Electrophysiological properties of the hypokalaemic periodic paralysis mutation (R528H) of the skeletal muscle alpha 1s subunit as expressed in mouse L cells. FEBS Lett *382*, 244-248.

Lapie, P., Lory, P., and Fontaine, B. (1997). Hypokalemic periodic paralysis: an autosomal dominant muscle disorder caused by mutations in a voltage-gated calcium channel. Neuromuscul Disord *7*, 234-240.

Legha, W., Gaillard, S., Gascon, E., Malapert, P., Hocine, M., Alonso, S., and Moqrich, A. (2010). stac1 and stac2 genes define discrete and distinct subsets of dorsal root ganglia neurons. Gene Expr Patterns *10*, 368-375.

Lehmann-Horn, F., Sipos, I., Jurkat-Rott, K., Heine, R., Brinkmeier, H., Fontaine, B., Kovacs, L., and Melzer, W. (1995). Altered calcium currents in human hypokalemic periodic paralysis myotubes expressing mutant L-type calcium channels. Soc Gen Physiol Ser *50*, 101-113.

Leitch, B., Shevtsova, O., Guevremont, D., and Williams, J. (2009). Loss of calcium channels in the cerebellum of the ataxic and epileptic stargazer mutant mouse. Brain Res *1279*, 156-167.

Leong, P., and MacLennan, D.H. (1998). The cytoplasmic loops between domains II and III and domains III and IV in the skeletal muscle dihydropyridine receptor bind to a contiguous site in the skeletal muscle ryanodine receptor. J Biol Chem *273*, 29958-29964.

Letts, V.A., Felix, R., Biddlecome, G.H., Arikkath, J., Mahaffey, C.L., Valenzuela, A., Bartlett, F.S., 2nd, Mori, Y., Campbell, K.P., and Frankel, W.N. (1998). The mouse stargazer gene encodes a neuronal Ca2+-channel gamma subunit. Nat Genet *19*, 340-347.

Letts, V.A., Valenzuela, A., Kirley, J.P., Sweet, H.O., Davisson, M.T., and Frankel, W.N. (1997). Genetic and physical maps of the stargazer locus on mouse chromosome 15. Genomics *43*, 62-68.

Leuranguer, V., Papadopoulos, S., and Beam, K.G. (2006). Organization of calcium channel beta1a subunits in triad junctions in skeletal muscle. J Biol Chem *281*, 3521-3527.

Li, Q., Shirabe, K., and Kuwada, J.Y. (2004). Chemokine signaling regulates sensory cell migration in zebrafish. Dev Biol *269*, 123-136.

Llinas, R., Sugimori, M., Hillman, D.E., and Cherksey, B. (1992). Distribution and functional significance of the P-type, voltage-dependent Ca2+ channels in the mammalian central nervous system. Trends Neurosci *15*, 351-355.

Low, S.E., Amburgey, K., Horstick, E., Linsley, J., Sprague, S.M., Cui, W.W., Zhou, W., Hirata, H., Saint-Amant, L., Hume, R.I.*, et al.* (2011). TRPM7 is required within zebrafish sensory neurons for the activation of touch-evoked escape behaviors. J Neurosci *31*, 11633-11644.

Lynch, P.J., Tong, J., Lehane, M., Mallet, A., Giblin, L., Heffron, J.J., Vaughan, P., Zafra, G., MacLennan, D.H., and McCarthy, T.V. (1999). A mutation in the transmembrane/luminal domain of the ryanodine receptor is associated with abnormal Ca2+ release channel function and severe central core disease. Proc Natl Acad Sci U S A *96*, 4164-4169.

MacLennan, D.H., Duff, C., Zorzato, F., Fujii, J., Phillips, M., Korneluk, R.G., Frodis, W., Britt, B.A., and Worton, R.G. (1990). Ryanodine receptor gene is a candidate for predisposition to malignant hyperthermia. Nature *343*, 559-561.

Magee, K.R., and Shy, G.M. (1956). A new congenital non-progressive myopathy. Brain *79*, 610-621.

Maljevic, S., Naros, G., Yalcin, O., Blazevic, D., Loeffler, H., Caglayan, H., Steinlein, O.K., and Lerche, H. (2011). Temperature and pharmacological rescue of a folding-defective, dominant-negative KV 7.2 mutation associated with neonatal seizures. Hum Mutat *32*, E2283-2293.

Marx, S.O., Gaburjakova, J., Gaburjakova, M., Henrikson, C., Ondrias, K., and Marks, A.R. (2001). Coupled gating between cardiac calcium release channels (ryanodine receptors). Circ Res *88*, 1151-1158.

Marx, S.O., Ondrias, K., and Marks, A.R. (1998). Coupled gating between individual skeletal muscle Ca2+ release channels (ryanodine receptors). Science *281*, 818-821.

Matthews, E., Labrum, R., Sweeney, M.G., Sud, R., Haworth, A., Chinnery, P.F., Meola, G., Schorge, S., Kullmann, D.M., Davis, M.B.*, et al.* (2009). Voltage sensor charge loss accounts for most cases of hypokalemic periodic paralysis. Neurology *72*, 1544-1547.

McCall, E., Li, L., Satoh, H., Shannon, T.R., Blatter, L.A., and Bers, D.M. (1996). Effects of FK-506 on contraction and Ca2+ transients in rat cardiac myocytes. Circ Res *79*, 1110-1121.

McClatchey, A.I., Van den Bergh, P., Pericak-Vance, M.A., Raskind, W., Verellen, C., McKenna-Yasek, D., Rao, K., Haines, J.L., Bird, T., Brown, R.H., Jr.*, et al.* (1992). Temperature-sensitive mutations in the III-IV cytoplasmic loop region of the skeletal muscle sodium channel gene in paramyotonia congenita. Cell *68*, 769-774.

McMahon, H.T., and Boucrot, E. (2011). Molecular mechanism and physiological functions of clathrin-mediated endocytosis. Nat Rev Mol Cell Biol *12*, 517-533.

Meluch, A.M., Sibert, K.S., and Bloch, E.C. (1989). Malignant hyperthermia following isoflurane anesthesia in an American Lumbee Indian. N C Med J *50*, 485-487.

Mickelson, J.R., and Louis, C.F. (1996). Malignant hyperthermia: excitation-contraction coupling, Ca2+ release channel, and cell Ca2+ regulation defects. Physiol Rev *76*, 537-592.

Miranda-Laferte, E., Gonzalez-Gutierrez, G., Schmidt, S., Zeug, A., Ponimaskin, E.G., Neely, A., and Hidalgo, P. (2011). Homodimerization of the Src homology 3 domain of the calcium channel beta-subunit drives dynamin-dependent endocytosis. J Biol Chem *286*, 22203-22210.

Moghadaszadeh, B., Petit, N., Jaillard, C., Brockington, M., Roy, S.Q., Merlini, L., Romero, N., Estournet, B., Desguerre, I., Chaigne, D.*, et al.* (2001). Mutations in SEPN1 cause congenital muscular dystrophy with spinal rigidity and restrictive respiratory syndrome. Nat Genet *29*, 17-18.

Monnier, N., Ferreiro, A., Marty, I., Labarre-Vila, A., Mezin, P., and Lunardi, J. (2003). A homozygous splicing mutation causing a depletion of skeletal muscle RYR1 is associated with multi-minicore disease congenital myopathy with ophthalmoplegia. Hum Mol Genet *12*, 1171-1178.

Monnier, N., Procaccio, V., Stieglitz, P., and Lunardi, J. (1997). Malignant-hyperthermia susceptibility is associated with a mutation of the alpha 1-subunit of the human dihydropyridine-sensitive L-type voltage-dependent calcium-channel receptor in skeletal muscle. Am J Hum Genet *60*, 1316-1325.

Monnier, N., Romero, N.B., Lerale, J., Nivoche, Y., Qi, D., MacLennan, D.H., Fardeau, M., and Lunardi, J. (2000). An autosomal dominant congenital myopathy with cores and rods is associated with a neomutation in the RYR1 gene encoding the skeletal muscle ryanodine receptor. Hum Mol Genet *9*, 2599-2608.

Montell, C. (2005). The TRP superfamily of cation channels. Sci STKE *2005*, re3.

Moore, C.P., Rodney, G., Zhang, J.Z., Santacruz-Toloza, L., Strasburg, G., and Hamilton, S.L. (1999). Apocalmodulin and Ca2+ calmodulin bind to the same region on the skeletal muscle Ca2+ release channel. Biochemistry *38*, 8532-8537.

Moore, E.D., Voigt, T., Kobayashi, Y.M., Isenberg, G., Fay, F.S., Gallitelli, M.F., and Franzini-Armstrong, C. (2004). Organization of Ca2+ release units in excitable smooth muscle of the guinea-pig urinary bladder. Biophys J *87*, 1836-1847.

Mullins, M.C., Hammerschmidt, M., Haffter, P., and Nusslein-Volhard, C. (1994). Large-scale mutagenesis in the zebrafish: in search of genes controlling development in a vertebrate. Curr Biol *4*, 189-202.

Murata, M., Cingolani, E., McDonald, A.D., Donahue, J.K., and Marban, E. (2004). Creation of a genetic calcium channel blocker by targeted gem gene transfer in the heart. Circ Res *95*, 398-405.

Myers, P.Z. (1985). Spinal motoneurons of the larval zebrafish. J Comp Neurol *236*, 555-561.

Nadler, M.J., Hermosura, M.C., Inabe, K., Perraud, A.L., Zhu, Q., Stokes, A.J., Kurosaki, T., Kinet, J.P., Penner, R., Scharenberg, A.M*., et al.* (2001). LTRPC7 is a Mg.ATP-regulated divalent cation channel required for cell viability. Nature *411*, 590-595.

Naganawa, Y., and Hirata, H. (2011). Developmental transition of touch response from slow muscle-mediated coilings to fast muscle-mediated burst swimming in zebrafish. Dev Biol *355*, 194-204.

Nakai, J., Dirksen, R.T., Nguyen, H.T., Pessah, I.N., Beam, K.G., and Allen, P.D. (1996). Enhanced dihydropyridine receptor channel activity in the presence of ryanodine receptor. Nature *380*, 72-75.

Nakai, J., Imagawa, T., Hakamat, Y., Shigekawa, M., Takeshima, H., and Numa, S. (1990). Primary structure and functional expression from cDNA of the cardiac ryanodine receptor/calcium release channel. FEBS Lett *271*, 169-177.

Nakai, J., Sekiguchi, N., Rando, T.A., Allen, P.D., and Beam, K.G. (1998a). Two regions of the ryanodine receptor involved in coupling with L-type Ca2+ channels. J Biol Chem *273*, 13403-13406.

Nakai, J., Tanabe, T., Konno, T., Adams, B., and Beam, K.G. (1998b). Localization in the II-III loop of the dihydropyridine receptor of a sequence critical for excitation-contraction coupling. J Biol Chem *273*, 24983-24986.

Nelson, T.E., Bedell, D.M., and Jones, E.W. (1975). Porcine malignant hyperthermia: effects of temperature and extracellular calcium concentration on halothane-induced contracture of susceptible skeletal muscle. Anesthesiology *42*, 301-306.

Neves, G., Neef, A., and Lagnado, L. (2001). The actions of barium and strontium on exocytosis and endocytosis in the synaptic terminal of goldfish bipolar cells. J Physiol *535*, 809-824.

Noebels, J.L., Qiao, X., Bronson, R.T., Spencer, C., and Davisson, M.T. (1990). Stargazer: a new neurological mutant on chromosome 15 in the mouse with prolonged cortical seizures. Epilepsy Res *7*, 129-135.

Nowycky, M.C., Fox, A.P., and Tsien, R.W. (1985a). Long-opening mode of gating of neuronal calcium channels and its promotion by the dihydropyridine calcium agonist Bay K 8644. Proc Natl Acad Sci U S A *82*, 2178-2182.

Nowycky, M.C., Fox, A.P., and Tsien, R.W. (1985b). Three types of neuronal calcium channel with different calcium agonist sensitivity. Nature *316*, 440-443.

Numata, T., Shimizu, T., and Okada, Y. (2007a). Direct mechano-stress sensitivity of TRPM7 channel. Cell Physiol Biochem *19*, 1-8.

Numata, T., Shimizu, T., and Okada, Y. (2007b). TRPM7 is a stretch- and swelling-activated cation channel involved in volume regulation in human epithelial cells. Am J Physiol Cell Physiol *292*, C460-467.

Nusslein-Volhard, C., and Wieschaus, E. (1980). Mutations affecting segment number and polarity in Drosophila. Nature *287*, 795-801.

Obermair, G.J., Kugler, G., Baumgartner, S., Tuluc, P., Grabner, M., and Flucher, B.E. (2005). The Ca2+ channel alpha2delta-1 subunit determines Ca2+ current kinetics in skeletal muscle but not targeting of alpha1S or excitation-contraction coupling. J Biol Chem *280*, 2229-2237.

Ohrtman, J., Ritter, B., Polster, A., Beam, K.G., and Papadopoulos, S. (2008). Sequence differences in the IQ motifs of CaV1.1 and CaV1.2 strongly impact calmodulin binding and calcium-dependent inactivation. J Biol Chem *283*, 29301-29311.

Ondrias, K., Marx, S.O., Gaburjakova, M., and Marks, A.R. (1998). FKBP12 modulates gating of the ryanodine receptor/calcium release channel. Ann N Y Acad Sci *853*, 149-156.

Opatowsky, Y., Chen, C.C., Campbell, K.P., and Hirsch, J.A. (2004). Structural analysis of the voltage-dependent calcium channel beta subunit functional core and its complex with the alpha 1 interaction domain. Neuron *42*, 387-399.

Ottini, L., Marziali, G., Conti, A., Charlesworth, A., and Sorrentino, V. (1996). Alpha and beta isoforms of ryanodine receptor from chicken skeletal muscle are the homologues of mammalian RyR1 and RyR3. Biochem J *315 (Pt 1)*, 207-216.

Oyamada, H., Murayama, T., Takagi, T., Iino, M., Iwabe, N., Miyata, T., Ogawa, Y., and Endo, M. (1994). Primary structure and distribution of ryanodine-binding protein isoforms of the bullfrog skeletal muscle. J Biol Chem *269*, 17206-17214.

Ozawa, T. (2010). Modulation of ryanodine receptor Ca2+ channels (Review). Mol Med Report *3*, 199-204.

Paolini, C., Fessenden, J.D., Pessah, I.N., and Franzini-Armstrong, C. (2004a). Evidence for conformational coupling between two calcium channels. Proc Natl Acad Sci U S A *101*, 12748-12752.

Paolini, C., Protasi, F., and Franzini-Armstrong, C. (2004b). The relative position of RyR feet and DHPR tetrads in skeletal muscle. J Mol Biol *342*, 145-153.

Paolini, C., Quarta, M., Nori, A., Boncompagni, S., Canato, M., Volpe, P., Allen, P.D., Reggiani, C., and Protasi, F. (2007). Reorganized stores and impaired calcium handling in skeletal muscle of mice lacking calsequestrin-1. J Physiol *583*, 767-784.

Papadopoulos, S., Leuranguer, V., Bannister, R.A., and Beam, K.G. (2004). Mapping sites of potential proximity between the dihydropyridine receptor and RyR1 in muscle using a cyan fluorescent protein-yellow fluorescent protein tandem as a fluorescence resonance energy transfer probe. J Biol Chem *279*, 44046-44056.

Pate, P., Mochca-Morales, J., Wu, Y., Zhang, J.Z., Rodney, G.G., Serysheva, II, Williams, B.Y., Anderson, M.E., and Hamilton, S.L. (2000). Determinants for calmodulin binding on voltage-dependent Ca2+ channels. J Biol Chem *275*, 39786-39792.

Perez-Reyes, E., Kim, H.S., Lacerda, A.E., Horne, W., Wei, X.Y., Rampe, D., Campbell, K.P., Brown, A.M., and Birnbaumer, L. (1989). Induction of calcium currents by the expression of the alpha 1-subunit of the dihydropyridine receptor from skeletal muscle. Nature *340*, 233-236.

Peterson, B.Z., DeMaria, C.D., Adelman, J.P., and Yue, D.T. (1999). Calmodulin is the Ca2+ sensor for Ca2+ -dependent inactivation of L-type calcium channels. Neuron *22*, 549-558.

Pirone, A., Schredelseker, J., Tuluc, P., Gravino, E., Fortunato, G., Flucher, B.E., Carsana, A., Salvatore, F., and Grabner, M. (2010). Identification and functional characterization of malignant hyperthermia mutation T1354S in the outer pore of the Cavalpha1S-subunit. Am J Physiol Cell Physiol *299*, C1345-1354.

Postlethwait, J.H., Johnson, S.L., Midson, C.N., Talbot, W.S., Gates, M., Ballinger, E.W., Africa, D., Andrews, R., Carl, T., Eisen, J.S*., et al.* (1994). A genetic linkage map for the zebrafish. Science *264*, 699-703.

Proenza, C., O'Brien, J., Nakai, J., Mukherjee, S., Allen, P.D., and Beam, K.G. (2002). Identification of a region of RyR1 that participates in allosteric coupling with the alpha(1S) (Ca(V)1.1) II-III loop. J Biol Chem *277*, 6530-6535.

Prosser, B.L., Wright, N.T., Hernandez-Ochoa, E.O., Varney, K.M., Liu, Y., Olojo, R.O., Zimmer, D.B., Weber, D.J., and Schneider, M.F. (2008). S100A1 binds to the calmodulin-binding site of ryanodine receptor and modulates skeletal muscle excitation-contraction coupling. J Biol Chem *283*, 5046-5057.

Protasi, F. (2002). Structural interaction between RYRs and DHPRs in calcium release units of cardiac and skeletal muscle cells. Front Biosci *7*, d650-658.

Protasi, F., Franzini-Armstrong, C., and Allen, P.D. (1998). Role of ryanodine receptors in the assembly of calcium release units in skeletal muscle. J Cell Biol *140*, 831-842.

Protasi, F., Paolini, C., Nakai, J., Beam, K.G., Franzini-Armstrong, C., and Allen, P.D. (2002). Multiple regions of RyR1 mediate functional and structural interactions with alpha(1S)-dihydropyridine receptors in skeletal muscle. Biophys J *83*, 3230-3244.

Protasi, F., Sun, X.H., and Franzini-Armstrong, C. (1996). Formation and maturation of the calcium release apparatus in developing and adult avian myocardium. Dev Biol *173*, 265-278.

Protasi, F., Takekura, H., Wang, Y., Chen, S.R., Meissner, G., Allen, P.D., and Franzini-Armstrong, C. (2000). RYR1 and RYR3 have different roles in the assembly of calcium release units of skeletal muscle. Biophys J *79*, 2494-2508.

Ptacek, L.J., George, A.L., Jr., Barchi, R.L., Griggs, R.C., Riggs, J.E., Robertson, M., and Leppert, M.F. (1992). Mutations in an S4 segment of the adult skeletal muscle sodium channel cause paramyotonia congenita. Neuron *8*, 891-897.

Ptacek, L.J., Tawil, R., Griggs, R.C., Engel, A.G., Layzer, R.B., Kwiecinski, H., McManis, P.G., Santiago, L., Moore, M., Fouad, G*., et al.* (1994). Dihydropyridine receptor mutations cause hypokalemic periodic paralysis. Cell *77*, 863-868.

Rainier, S., Sher, C., Reish, O., Thomas, D., and Fink, J.K. (2006). De novo occurrence of novel SPG3A/atlastin mutation presenting as cerebral palsy. Arch Neurol *63*, 445-447.

Ren, D., and Hall, L.M. (1997). Functional expression and characterization of skeletal muscle dihydropyridine receptors in Xenopus oocytes. J Biol Chem *272*, 22393-22396.

Reuter, H. (1983). Calcium channel modulation by neurotransmitters, enzymes and drugs. Nature *301*, 569-574.

Robinson, R., Carpenter, D., Shaw, M.A., Halsall, J., and Hopkins, P. (2006). Mutations in RYR1 in malignant hyperthermia and central core disease. Hum Mutat *27*, 977-989.

Robinson, R.L., Brooks, C., Brown, S.L., Ellis, F.R., Halsall, P.J., Quinnell, R.J., Shaw, M.A., and Hopkins, P.M. (2002). RYR1 mutations causing central core disease are associated with more severe malignant hyperthermia in vitro contracture test phenotypes. Hum Mutat *20*, 88-97.

Rodney, G.G., Williams, B.Y., Strasburg, G.M., Beckingham, K., and Hamilton, S.L. (2000). Regulation of RYR1 activity by Ca(2+) and calmodulin. Biochemistry *39*, 7807-7812.

Rusconi, R., Scalmani, P., Cassulini, R.R., Giunti, G., Gambardella, A., Franceschetti, S., Annesi, G., Wanke, E., and Mantegazza, M. (2007). Modulatory proteins can rescue a trafficking defective epileptogenic Nav1.1 Na+ channel mutant. J Neurosci *27*, 11037-11046.

Russ, D.W., Grandy, J.S., Toma, K., and Ward, C.W. (2011). Ageing, but not yet senescent, rats exhibit reduced muscle quality and sarcoplasmic reticulum function. Acta Physiol (Oxf) *201*, 391-403.

Russell, W.L., Kelly, E.M., Hunsicker, P.R., Bangham, J.W., Maddux, S.C., and Phipps, E.L. (1979). Specific-locus test shows ethylnitrosourea to be the most potent mutagen in the mouse. Proc Natl Acad Sci U S A *76*, 5818-5819.

Ruth, P., Rohrkasten, A., Biel, M., Bosse, E., Regulla, S., Meyer, H.E., Flockerzi, V., and Hofmann, F. (1989). Primary structure of the beta subunit of the DHP-sensitive calcium channel from skeletal muscle. Science *245*, 1115-1118.

Saint-Amant, L., and Drapeau, P. (1998). Time course of the development of motor behaviors in the zebrafish embryo. J Neurobiol *37*, 622-632.

Saito, A., Seiler, S., Chu, A., and Fleischer, S. (1984). Preparation and morphology of sarcoplasmic reticulum terminal cisternae from rabbit skeletal muscle. J Cell Biol *99*, 875-885.

Samso, M., and Wagenknecht, T. (2002). Apocalmodulin and Ca2+-calmodulin bind to neighboring locations on the ryanodine receptor. J Biol Chem *277*, 1349-1353.

Sasaki, T., Shibasaki, T., Beguin, P., Nagashima, K., Miyazaki, M., and Seino, S. (2005). Direct inhibition of the interaction between alpha-interaction domain and beta-interaction domain of voltage-dependent Ca2+ channels by Gem. J Biol Chem *280*, 9308-9312.

Sato, Y., Ferguson, D.G., Sako, H., Dorn, G.W., 2nd, Kadambi, V.J., Yatani, A., Hoit, B.D., Walsh, R.A., and Kranias, E.G. (1998). Cardiac-specific overexpression of mouse cardiac calsequestrin is associated with depressed cardiovascular function and hypertrophy in transgenic mice. J Biol Chem *273*, 28470-28477.

Schredelseker, J., Dayal, A., Schwerte, T., Franzini-Armstrong, C., and Grabner, M. (2009). Proper restoration of excitation-contraction coupling in the dihydropyridine receptor beta1-null zebrafish relaxed is an exclusive function of the beta1a subunit. J Biol Chem *284*, 1242-1251.

Schredelseker, J., Di Biase, V., Obermair, G.J., Felder, E.T., Flucher, B.E., Franzini-Armstrong, C., and Grabner, M. (2005). The beta 1a subunit is essential for the assembly of dihydropyridine-receptor arrays in skeletal muscle. Proc Natl Acad Sci U S A *102*, 17219-17224.

Schredelseker, J., Shrivastav, M., Dayal, A., and Grabner, M. (2010). Non-Ca2+-conducting Ca2+ channels in fish skeletal muscle excitation-contraction coupling. Proc Natl Acad Sci U S A *107*, 5658-5663.

Schulte-Merker, S., Hammerschmidt, M., Beuchle, D., Cho, K.W., De Robertis, E.M., and Nusslein-Volhard, C. (1994a). Expression of zebrafish goosecoid and no tail gene products in wild-type and mutant no tail embryos. Development *120*, 843-852.

Schulte-Merker, S., van Eeden, F.J., Halpern, M.E., Kimmel, C.B., and Nusslein-Volhard, C. (1994b). no tail (ntl) is the zebrafish homologue of the mouse T (Brachyury) gene. Development *120*, 1009-1015.

Scott, B.T., Simmerman, H.K., Collins, J.H., Nadal-Ginard, B., and Jones, L.R. (1988). Complete amino acid sequence of canine cardiac calsequestrin deduced by cDNA cloning. J Biol Chem *263*, 8958-8964.

Serysheva, II, Ludtke, S.J., Baker, M.L., Cong, Y., Topf, M., Eramian, D., Sali, A., Hamilton, S.L., and Chiu, W. (2008). Subnanometer-resolution electron cryomicroscopy-based domain models for the cytoplasmic region of skeletal muscle RyR channel. Proc Natl Acad Sci U S A *105*, 9610-9615.

Seu, L., and Pitt, G.S. (2006). Dose-dependent and isoform-specific modulation of Ca2+ channels by RGK GTPases. J Gen Physiol *128*, 605-613.

Sharkey, L.M., Cheng, X., Drews, V., Buchner, D.A., Jones, J.M., Justice, M.J., Waxman, S.G., Dib-Hajj, S.D., and Meisler, M.H. (2009). The ataxia3 mutation in the N-terminal cytoplasmic domain of sodium channel Na(v)1.6 disrupts intracellular trafficking. J Neurosci *29*, 2733-2741.

Sharp, A.H., Black, J.L., 3rd, Dubel, S.J., Sundarraj, S., Shen, J.P., Yunker, A.M., Copeland, T.D., and McEnery, M.W. (2001). Biochemical and anatomical evidence for specialized voltage-dependent calcium channel gamma isoform expression in the epileptic and ataxic mouse, stargazer. Neuroscience *105*, 599-617.

Shimoda, N., Knapik, E.W., Ziniti, J., Sim, C., Yamada, E., Kaplan, S., Jackson, D., de Sauvage, F., Jacob, H., and Fishman, M.C. (1999). Zebrafish genetic map with 2000 microsatellite markers. Genomics *58*, 219-232.

Shin, D.W., Pan, Z., Kim, E.K., Lee, J.M., Bhat, M.B., Parness, J., Kim, D.H., and Ma, J. (2003). A retrograde signal from calsequestrin for the regulation of store-operated Ca2+ entry in skeletal muscle. J Biol Chem *278*, 3286-3292.

Shou, W., Aghdasi, B., Armstrong, D.L., Guo, Q., Bao, S., Charng, M.J., Mathews, L.M., Schneider, M.D., Hamilton, S.L., and Matzuk, M.M. (1998). Cardiac defects and altered ryanodine receptor function in mice lacking FKBP12. Nature *391*, 489-492.

Shuaib, A., Paasuke, R.T., and Brownell, K.W. (1987). Central core disease. Clinical features in 13 patients. Medicine (Baltimore) *66*, 389-396.

Sipos, I., Jurkat-Rott, K., Harasztosi, C., Fontaine, B., Kovacs, L., Melzer, W., and Lehmann-Horn, F. (1995). Skeletal muscle DHP receptor mutations alter calcium currents in human hypokalaemic periodic paralysis myotubes. J Physiol *483 (Pt 2)*, 299-306.

Smith, J.S., Imagawa, T., Ma, J., Fill, M., Campbell, K.P., and Coronado, R. (1988). Purified ryanodine receptor from rabbit skeletal muscle is the calcium-release channel of sarcoplasmic reticulum. J Gen Physiol *92*, 1-26.

Stamm, D.S., Aylsworth, A.S., Stajich, J.M., Kahler, S.G., Thorne, L.B., Speer, M.C., and Powell, C.M. (2008a). Native American myopathy: congenital myopathy with cleft palate, skeletal anomalies, and susceptibility to malignant hyperthermia. Am J Med Genet A *146A*, 1832-1841.

Stamm, D.S., Powell, C.M., Stajich, J.M., Zismann, V.L., Stephan, D.A., Chesnut, B., Aylsworth, A.S., Kahler, S.G., Deak, K.L., Gilbert, J.R.*, et al.* (2008b). Novel congenital myopathy locus identified in Native American Indians at 12q13.13-14.1. Neurology *71*, 1764-1769.

Stewart, C.R., Kahler, S.G., and Gilchrist, J.M. (1988). Congenital myopathy with cleft palate and increased susceptibility to malignant hyperthermia: King syndrome? Pediatr Neurol *4*, 371-374.

Stewart, S.L., Hogan, K., Rosenberg, H., and Fletcher, J.E. (2001). Identification of the Arg1086His mutation in the alpha subunit of the voltage-dependent calcium channel (CACNA1S) in a North American family with malignant hyperthermia. Clin Genet *59*, 178-184.

Streisinger, G. (1983). Extrapolations from species to species and from various cell types in assessing risks from chemical mutagens. Mutat Res *114*, 93-105.

Streisinger, G., Singer, F., Walker, C., Knauber, D., and Dower, N. (1986). Segregation analyses and gene-centromere distances in zebrafish. Genetics *112*, 311-319.

Stroffekova, K. (2008). Ca2+/CaM-dependent inactivation of the skeletal muscle L-type Ca2+ channel (Cav1.1). Pflugers Arch *455*, 873-884.

Strube, C., Beurg, M., Powers, P.A., Gregg, R.G., and Coronado, R. (1996). Reduced Ca2+ current, charge movement, and absence of Ca2+ transients in skeletal muscle deficient in dihydropyridine receptor beta 1 subunit. Biophys J *71*, 2531-2543.

Struyk, A.F., and Cannon, S.C. (2007). A Na+ channel mutation linked to hypokalemic periodic paralysis exposes a proton-selective gating pore. J Gen Physiol *130*, 11-20.

Sudbrak, R., Golla, A., Hogan, K., Powers, P., Gregg, R., Du Chesne, I., Lehmann-Horn, F., and Deufel, T. (1993). Exclusion of malignant hyperthermia susceptibility (MHS) from a putative MHS2 locus on chromosome 17q and of the alpha 1, beta 1, and gamma subunits of the dihydropyridine receptor calcium channel as candidates for the molecular defect. Hum Mol Genet *2*, 857-862.

Suzuki, H., Kawai, J., Taga, C., Yaoi, T., Hara, A., Hirose, K., Hayashizaki, Y., and Watanabe, S. (1996). Stac, a novel neuron-specific protein with cysteine-rich and SH3 domains. Biochem Biophys Res Commun *229*, 902-909.

Takahashi, M., Seagar, M.J., Jones, J.F., Reber, B.F., and Catterall, W.A. (1987). Subunit structure of dihydropyridine-sensitive calcium channels from skeletal muscle. Proc Natl Acad Sci U S A *84*, 5478-5482.

Takei, K., Yoshida, Y., and Yamada, H. (2005). Regulatory mechanisms of dynamin-dependent endocytosis. J Biochem *137*, 243-247.

Takekura, H., and Franzini-Armstrong, C. (1999). Correct targeting of dihydropyridine receptors and triadin in dyspedic mouse skeletal muscle in vivo. Dev Dyn *214*, 372-380.

Takekura, H., and Franzini-Armstrong, C. (2002). The structure of Ca(2+) release units in arthropod body muscle indicates an indirect mechanism for excitation-contraction coupling. Biophys J *83*, 2742-2753.

Takekura, H., Nishi, M., Noda, T., Takeshima, H., and Franzini-Armstrong, C. (1995). Abnormal junctions between surface membrane and sarcoplasmic reticulum in skeletal muscle with a mutation targeted to the ryanodine receptor. Proc Natl Acad Sci U S A *92*, 3381-3385.

Takeshima, H., Nishimura, S., Matsumoto, T., Ishida, H., Kangawa, K., Minamino, N., Matsuo, H., Ueda, M., Hanaoka, M., Hirose, T.*, et al.* (1989). Primary structure and expression from complementary DNA of skeletal muscle ryanodine receptor. Nature *339*, 439-445.

Tanabe, T., Beam, K.G., Adams, B.A., Niidome, T., and Numa, S. (1990). Regions of the skeletal muscle dihydropyridine receptor critical for excitation-contraction coupling. Nature *346*, 567-569.

Tanabe, T., Beam, K.G., Powell, J.A., and Numa, S. (1988). Restoration of excitation-contraction coupling and slow calcium current in dysgenic muscle by dihydropyridine receptor complementary DNA. Nature *336*, 134-139.

Tanabe, T., Takeshima, H., Mikami, A., Flockerzi, V., Takahashi, H., Kangawa, K., Kojima, M., Matsuo, H., Hirose, T., and Numa, S. (1987). Primary structure of the receptor for calcium channel blockers from skeletal muscle. Nature *328*, 313-318.

Tang, W., Halling, D.B., Black, D.J., Pate, P., Zhang, J.Z., Pedersen, S., Altschuld, R.A., and Hamilton, S.L. (2003). Apocalmodulin and Ca2+ calmodulin-binding sites on the CaV1.2 channel. Biophys J *85*, 1538-1547.

Tang, W., Ingalls, C.P., Durham, W.J., Snider, J., Reid, M.B., Wu, G., Matzuk, M.M., and Hamilton, S.L. (2004). Altered excitation-contraction coupling with skeletal muscle specific FKBP12 deficiency. FASEB J *18*, 1597-1599.

Tang, W., Sencer, S., and Hamilton, S.L. (2002). Calmodulin modulation of proteins involved in excitation-contraction coupling. Front Biosci *7*, d1583-1589.

Tian, L., Hires, S.A., Mao, T., Huber, D., Chiappe, M.E., Chalasani, S.H., Petreanu, L., Akerboom, J., McKinney, S.A., Schreiter, E.R.*, et al.* (2009). Imaging neural activity in worms, flies and mice with improved GCaMP calcium indicators. Nat Methods *6*, 875-881.

Tijskens, P., Meissner, G., and Franzini-Armstrong, C. (2003). Location of ryanodine and dihydropyridine receptors in frog myocardium. Biophys J *84*, 1079-1092.

Tilgen, N., Zorzato, F., Halliger-Keller, B., Muntoni, F., Sewry, C., Palmucci, L.M., Schneider, C., Hauser, E., Lehmann-Horn, F., Muller, C.R.*, et al.* (2001). Identification of four novel mutations in the C-terminal membrane spanning domain of the ryanodine receptor 1: association with central core disease and alteration of calcium homeostasis. Hum Mol Genet *10*, 2879-2887.

Timerman, A.P., Ogunbumni, E., Freund, E., Wiederrecht, G., Marks, A.R., and Fleischer, S. (1993). The calcium release channel of sarcoplasmic reticulum is modulated by FK-506-binding protein. Dissociation and reconstitution of FKBP-12 to the calcium release channel of skeletal muscle sarcoplasmic reticulum. J Biol Chem *268*, 22992-22999.

Tong, J., Oyamada, H., Demaurex, N., Grinstein, S., McCarthy, T.V., and MacLennan, D.H. (1997). Caffeine and halothane sensitivity of intracellular Ca2+ release is altered by 15 calcium release channel (ryanodine receptor) mutations associated with malignant hyperthermia and/or central core disease. J Biol Chem *272*, 26332-26339.

Tripathy, A., Xu, L., Mann, G., and Meissner, G. (1995). Calmodulin activation and inhibition of skeletal muscle Ca2+ release channel (ryanodine receptor). Biophys J *69*, 106-119.

Tsien, R.W., Lipscombe, D., Madison, D.V., Bley, K.R., and Fox, A.P. (1988). Multiple types of neuronal calcium channels and their selective modulation. Trends Neurosci *11*, 431-438.

Ursu, D., Sebille, S., Dietze, B., Freise, D., Flockerzi, V., and Melzer, W. (2001). Excitation-contraction coupling in skeletal muscle of a mouse lacking the dihydropyridine receptor subunit gamma1. J Physiol *533*, 367-377.

Van Petegem, F., Clark, K.A., Chatelain, F.C., and Minor, D.L., Jr. (2004). Structure of a complex between a voltage-gated calcium channel beta-subunit and an alpha-subunit domain. Nature *429*, 671-675.

Wagenknecht, T., Berkowitz, J., Grassucci, R., Timerman, A.P., and Fleischer, S. (1994). Localization of calmodulin binding sites on the ryanodine receptor from skeletal muscle by electron microscopy. Biophys J *67*, 2286-2295.

Wagenknecht, T., Radermacher, M., Grassucci, R., Berkowitz, J., Xin, H.B., and Fleischer, S. (1997). Locations of calmodulin and FK506-binding protein on the three-dimensional architecture of the skeletal muscle ryanodine receptor. J Biol Chem *272*, 32463-32471.

Walker, C., and Streisinger, G. (1983). Induction of Mutations by gamma-Rays in Pregonial Germ Cells of Zebrafish Embryos. Genetics *103*, 125-136.

Wang, S., Trumble, W.R., Liao, H., Wesson, C.R., Dunker, A.K., and Kang, C.H. (1998). Crystal structure of calsequestrin from rabbit skeletal muscle sarcoplasmic reticulum. Nat Struct Biol *5*, 476-483.

Wehner, M., Rueffert, H., Koenig, F., Neuhaus, J., and Olthoff, D. (2002). Increased sensitivity to 4-chloro-m-cresol and caffeine in primary myotubes from malignant hyperthermia susceptible individuals carrying the ryanodine receptor 1 Thr2206Met (C6617T) mutation. Clin Genet *62*, 135-146.

Wei, L., Hanna, A.D., Beard, N.A., and Dulhunty, A.F. (2009). Unique isoform-specific properties of calsequestrin in the heart and skeletal muscle. Cell Calcium *45*, 474-484.

Weiss, R.G., O'Connell, K.M., Flucher, B.E., Allen, P.D., Grabner, M., and Dirksen, R.T. (2004). Functional analysis of the R1086H malignant hyperthermia mutation in the DHPR reveals an unexpected influence of the III-IV loop on skeletal muscle EC coupling. Am J Physiol Cell Physiol *287*, C1094-1102.

Wilkens, C.M., and Beam, K.G. (2003). Insertion of alpha1S II-III loop and C terminal sequences into alpha1H fails to restore excitation-contraction coupling in dysgenic myotubes. J Muscle Res Cell Motil *24*, 99-109.

Wright, N.T., Prosser, B.L., Varney, K.M., Zimmer, D.B., Schneider, M.F., and Weber, D.J. (2008). S100A1 and calmodulin compete for the same binding site on ryanodine receptor. J Biol Chem *283*, 26676-26683.

Wu, S., Ibarra, M.C., Malicdan, M.C., Murayama, K., Ichihara, Y., Kikuchi, H., Nonaka, I., Noguchi, S., Hayashi, Y.K., and Nishino, I. (2006). Central core disease is due to RYR1 mutations in more than 90% of patients. Brain *129*, 1470-1480.

Yada, H., Murata, M., Shimoda, K., Yuasa, S., Kawaguchi, H., Ieda, M., Adachi, T., Ogawa, S., and Fukuda, K. (2007). Dominant negative suppression of Rad leads to QT prolongation and causes ventricular arrhythmias via modulation of L-type Ca2+ channels in the heart. Circ Res *101*, 69-77.

Yang, T., Ta, T.A., Pessah, I.N., and Allen, P.D. (2003). Functional defects in six ryanodine receptor isoform-1 (RyR1) mutations associated with malignant hyperthermia and their impact on skeletal excitation-contraction coupling. J Biol Chem *278*, 25722-25730.

Yang, T., Xu, X., Kernan, T., Wu, V., and Colecraft, H.M. (2010). Rem, a member of the RGK GTPases, inhibits recombinant CaV1.2 channels using multiple mechanisms that require distinct conformations of the GTPase. J Physiol *588*, 1665-1681.

Zhang, L., Kelley, J., Schmeisser, G., Kobayashi, Y.M., and Jones, L.R. (1997). Complex formation between junctin, triadin, calsequestrin, and the ryanodine receptor. Proteins of the cardiac junctional sarcoplasmic reticulum membrane. J Biol Chem *272*, 23389-23397.

Zhang, W., Kuhlers, D.L., and Rempel, W.E. (1992). Halothane gene and swine performance. J Anim Sci *70*, 1307-1313.

Zhang, Y., Chen, H.S., Khanna, V.K., De Leon, S., Phillips, M.S., Schappert, K., Britt, B.A., Browell, A.K., and MacLennan, D.H. (1993). A mutation in the human ryanodine receptor gene associated with central core disease. Nat Genet *5*, 46-50.

Zhou, W., Horstick, E.J., Hirata, H., and Kuwada, J.Y. (2008). Identification and expression of voltage-gated calcium channel beta subunits in Zebrafish. Dev Dyn *237*, 3842-3852.

Zhou, W., Saint-Amant, L., Hirata, H., Cui, W.W., Sprague, S.M., and Kuwada, J.Y. (2006). Non-sense mutations in the dihydropyridine receptor beta1 gene, CACNB1, paralyze zebrafish relaxed mutants. Cell Calcium *39*, 227-236.

Zorzato, F., Fujii, J., Otsu, K., Phillips, M., Green, N.M., Lai, F.A., Meissner, G., and MacLennan, D.H. (1990). Molecular cloning of cDNA encoding human and rabbit forms of the Ca2+ release channel (ryanodine receptor) of skeletal muscle sarcoplasmic reticulum. J Biol Chem *265*, 2244-2256.

Zorzato, F., Jungbluth, H., Zhou, H., Muntoni, F., and Treves, S. (2007). Functional effects of mutations identified in patients with multiminicore disease. IUBMB Life *59*, 14-20.

Zuhlke, R.D., Pitt, G.S., Deisseroth, K., Tsien, R.W., and Reuter, H. (1999). Calmodulin supports both inactivation and facilitation of L-type calcium channels. Nature *399*, 159-162.